INACTIVATION OF COMPETING PATHWAYS AND INCREASED GENE COPIES FOR ENHANCED ISOPRENE PRODUCTION IN *SYNECHOCOCCUS SP*. PCC 7002 CYANOBACTERIA

By Olalekan R. Aremu

Renewable energy resources are necessary for a sustainable environment, energy independence, and national security. Cyanobacteria (blue-green microalgae) hold great potential as sources of sustainable bioproducts because of their ability to convert sunlight and atmospheric carbon-dioxide into energy-rich compounds such as isoprene, a high-value precursor for synthetic rubber and biofuels. Our group has introduced optimized transgenes for an isoprene synthase (IspS) enzyme and a rate-limiting, methyl erythritol phosphate (MEP) pathway isomerase (IDI) from poplar into the fast-growing marine cyanobacterium, *Synechococcus* sp. PCC 7002, and achieved isoprene synthesis at 4 mg L culture^{-1}12 h day^{-1} (~ 40 to 80-fold higher than previously reported for cyanobacteria). To further improve isoprene yields: 1) a competing glycogen biosynthesis pathway was inactivated, 2) the *IspS* and *IDI* genes were targeted to a chromosomal *petJ2* site to improve genetic stability, and 3) a second set of *IspS-IDI* genes was targeted to a high copy plasmid (pAQ1) of *Synechococcus*. I hypothesized that 1) inactivation of glycogen synthesis, a major carbon-storage pathway, will increase carbon flux to isoprene, 2) targeting the *IspS-IDI* genes to the chromosome will increase their stability, and 3) increasing the copy number of the *IpsS* and *IDI* genes, by targeting both the chromosome and plasmid, will further improve isoprene yield.

The *glgA1* and *glgA2* glycogen synthase genes were inactivated. However, isoprene production in these *Synechococcus* strains was only ~ 20% higher than in strains with functional glycogen synthesis. This suggested that carbon previously used for glycogen synthesis was directed to pathways other than the MEP pathway. Integration of the *IspS-IDI* transgenes into the chromosomal *petJ2* site (encoding a c_6-like cytochrome protein) resulted in continuous, stable isoprene production in these strains (*petJ2::IspS-IDI*) compared to strains carrying these genes only on the plasmid (*pAQ1::IspS-IDI*). Inactivation of the *petJ2* gene had no observable impact on growth, thus identifying *petJ2* as a suitable site for transgene integration. Increased copies of the *IspS-IDI* transgenes, achieved by targeting these genes to the plasmid as well as the chromosomal *petJ2* site, resulted in strains (*petJ2::IspS-IDI, pAQ1::IspS-IDI*) that produced ~ 1.5 times more isoprene than strains carrying these genes on plasmid pAQ1 only. Reverse transcriptase quantitative polymerase chain reaction gene-expression experiments showed that *IspS* transcript levels in the *petJ2::IspS-IDI* strains were several hundred fold higher, especially in old, dense cultures, than in strains with the *IspS-IDI* genes on plasmid pAQ1 only. These data demonstrate that improved isoprene yields in the *petJ2::IspS-IDI* strains resulted both from greater stability of the transgenes and increased mRNA transcript levels.

This research demonstrates the utility of the *petJ2* site and chromosomal integration for transgene stability and expression of isoprene synthase (*IspS*) and MEP pathway genes for enhanced isoprene production. The study further shows that *Synechococccus* sp. PCC 7002 is an excellent platform for genetic engineering to achieve improved yields of isoprene and other industrially relevant terpenes or bioproduct-biofuel chemicals.

INACTIVATION OF COMPETING PATHWAYS AND INCREASED GENE COPIES FOR ENHANCED ISOPRENE PRODUCTION IN *SYNECHOCOCCUS sp.* PCC 7002 CYANOBACTERIA

by

Olalekan R. Aremu

A Thesis submitted
In partial fulfillment of the requirements
For the Degree of

Master of Science-Biology
Microbiology

at

The University of Wisconsin Oshkosh
Oshkosh WI 54901-8621

June 2015

COMMITTEE APPROVAL

Advisor

6/16/2015 Date Approved

Member

6/17/15 Date Approved

Member

6/17/15 Date Approved

DEAN OF GRADUATE STUDIES

6/26/2015
Date Approved

FORMAT APPROVAL

6/10/15
Date Approved

To my lovely Mom for always being a source of motivation.

ACKNOWLEDGEMENTS

My profound appreciation to my advisor, Dr. Toivo Kallas for the dedicated mentorship and support he offered during my study at the University of Wisconsin, Oshkosh. I am also thankful for showing belief in my potentials to succeed as a graduate student despite my research inexperience and for providing me the opportunity to be a part of the Bio-Isoprene project in his lab. I will forever be grateful for stimulating my interest in Biofuels research. I also thank my thesis committee members, Dr. Lisa Dorn and Dr. Eric Matson for their valued inputs. An important resource that I was quick to turn to whenever I needed help in the lab especially with experimental protocols was Matthew Nelson; you are awesome! My immense gratitude goes to my lovely parents, for always believing in the power of quality education. Also, special thanks to grandma for her prayers, and my siblings for their support. Lastly, to faculty members, lab mates and colleagues that made my stay at the UW-Oshkosh a memorable and successful experience, I cannot thank you enough!

TABLE OF CONTENTS

Page

LIST OF TABLES vi

LIST OF FIGURES vii

INTRODUCTION 1

Statement of Problem 1
Background 9
Cyanobacteria as Cell Factories for Biofuels Production 16
Isoprene Synthesis in Cyanobacteria 19
Rationale and Objectives of the Study 26

MATERIALS AND METHODS 34

Strains and Culture Conditions 34
Growth and Maintenance of Stock Cultures 36
Optical Density (O.D) Measurements and Analysis of Growth 37
DNA Manipulations and Cloning 38
Quantification of DNA and RNA 39
Polymerase Chain Reaction (PCR) 39
Gel Electrophoresis 40
Construction of Recombinant Plasmids 40
Construction of the *Synechococcus* 7002-IspS-IDI Strain 43
Restriction Enzyme Digestion 45
Glycogen Assay 48
RNA Isolation and Purity Check 50
Complementary DNA (cDNA) Synthesis for Reverse Transcriptase Quantitative PCR (RT-qPCR) 54
Primers and Probes for RT-qPCR 54
Primer-Probe Validation and Efficiency Determination 55
RT-qPCR Gene Expression Studies 56
Isoprene Toxicity Test 57

TABLE OF CONTENTS (Continued)

Page

Isoprene Production Assays 58
Fast Isoprene Sensor (FIS) for Real-Time Isoprene Measurements 59

RESULTS 62

Inactivation of a Competing Glycogen Pathway 62
Construction of the pUC57-glgA2-Em^R Recombinant Plasmid 62
Construction of the Double Glycogen Synthase Null Mutant (7002 ΔGlgA1A2) 68
Impact of *glgA1* and *glgA2* 'Knockouts' on Glycogen Synthesis 71
Impact of *glgA* 'Knockouts' on Growth under Continuous Culture Condition 73
Impact of *glgA* 'Knockouts' on Growth under Closed Culture Condition 75
Impact of Glycogen Inactivation on Isoprene Yield 76
Construction of 7002 ΔGlgA1A2-IspS-IDI Transformant 76
Isoprene Production in 7002 ΔGlgA1A2-IspS-IDI Transformant 79
Isoprene Toxicity Test 82
Chromosomal Integration of *IspS* and *IDI* for Improved Genetic Stability 84
Construction of pUC57-petJ2-IspS-IDI-Sp^R/Sm^R Recombinant Plasmid 84
Construction of a ΔpetJ2 Mutant 88
Chromosomal Integration of *IspS-IDI* Transgenes Increases Gene Stability 89
Increased Copies of Optimized *IspS* and *IDI* for Improved Isoprene Yield 91
Construction of 'Dual IspS-IDI' Strain 91
Impact of Increased Copies of Optimized *IspS and IDI* on Isoprene production 96
RT-qPCR Gene Expression Analysis 98

DISCUSSION 101

CONCLUSION 111

APPENDIXES 112

TABLE OF CONTENTS (Continued)

Page

APPENDIX A: Microbial Media 112
Liquid A (D7) Medium 113
Solid A (D7) Medium 114
D7 Micronutrients 114
S.O.C Medium 115
Luria-Bertani (LB) Broth [pH=7.0] 115
LB Agar 115
APPENDIX B: Buffers and Reagents 116
TBE Buffer (5x) 117
Diethylpyrocarbonate (DEPC) Treated Sterile Milli-Q H_2O 117
DEPC Treated 10T/0.1E (pH=8.0) 117
600 mM Sucrose 117
Sodium Acetate (pH=4.5) 118
0.5 M Sodium EDTA (Disodium Ethylenediaminetetraacetate) [pH=8.0] 118
0.5 M Tris (Tris Hydroxymethylaminomethane) 118
100 mM Tris-HCl (pH=8.2) 118
Equilibrated Phenol 119
10x Metabolic Stop Solution 119
Equilibrated phenol/Chloroform/Isoamylalchohol (25:24:1) 120
Chloroform/Isoamylalchohol (24:1) 120
Vitamin B_{12} (Cobalamin) 120
Antibiotics 120
APPENDIX C: Protocols 122
DNA Extraction Protocol 123
Transformation of *Synechococcus sp*. PCC 7002 123
Preparation of DH5α Electrocompetent *E. coli* cells 125

REFERENCES 126

LIST OF TABLES

Page

Table 1: Examples of Terpenes and Isoprene Units 21

Table 2: *Synechococcus* sp. PCC 7002 Mutant Strains used in this Study 35

Table 3: PCR Primers used in this Study 42

Table 4: Glucose Standard Preparation and Concentrations 49

Table 5: Probe and Primers Designed for RT-qPCR 55

LIST OF FIGURES

page

Figure 1: The Methyl Erythritol Phosphate (MEP) Pathway 2

Figure 2: Photosynthetic and Respiratory Electron Flux Pathways in Thylakoid Membranes of Cyanobacteria 15

Figure 3: Transmission Electron Micrograph of *Synechococcus* sp. PCC 7002 18

Figure 4: Chemical Structure of Isoprene 19

Figure 5: Substrate Flux via the MEP and Mevalonate (MVA) Pathways for Isopentenyl Diphosphate (IPP) and Dimethylallyldiphosphate (DMAPP) Synthesis 25

Figure 6: Isoprene Production in Cyanobacteria via the MEP Pathway and Competing Carbon Pathway for Glycogen Synthesis 26

Figure 7: Illustration of the DNA Construct Carrying Codon-Optimized Isoprene Synthase (*IspS*) and Isopentenyl Diphosphate Isomerase (*IDI*) Transgenes from Poplar Plant 32

Figure 8: Genetic Engineering Strategy for Targeting Codon-Optimized *IspS* and *IDI* Transgenes to Plasmid pAQ1 44

Figure 9: Plasmid pRL409 46

Figure 10: Plasmid pOSH1108 47

Figure 11: Schematic of the Fast Isoprene Sensor (FIS) for Measurement of Isoprene from Culture Head-Spaces 61

Figure 12: GlgA2-Em^R DNA Construct for Glycogen Synthase *glgA2* gene Inactivation 62

Figure 13: Gibson Assembly Reaction DNA Fragments for pUC57-glgA2-Em^R Recombinant Plasmid Construction 64

Figure 14: Recombinant Plasmid pUC57-glgA2-Em^R Carrying the *glgA2*-Em^R Inactivation DNA Construct 65

Figure 15: PCR Tests to Characterize the Recombinant pUC57-glgA2-Em^R Plasmid .. 66

LIST OF FIGURES (Continued)

Page

Figure 16: PCR Analysis to Determine Replacement of the Native *glgA2* with the Inactivated *glgA2*-Em^R Gene Construct in *Synechococcus* ΔGlgA2 Mutants 67

Figure 17: Restriction Analysis of *Synechococcu*s 7002 ΔGlgA2 Mutants..... 68

Figure 18: PCR Analysis to Characterize *Synechococcus* 7002 ΔGlgA1A2 (Glycogen Synthase Null) Mutants 70

Figure 19: Glycogen Content of *Synechococcus* Wild Type and Mutants 71

Figure 20: Growth Rates of *Synechococcus* Glycogen Synthase Mutants..... 74

Figure 21: Impact of Glycogen Synthase Mutations on Growth of Isoprene-Producing Glycogen Mutant Strains in Sealed Bottles 75

Figure 22: PCR Analysis to Characterize 7002 ΔGlgA1A2-IspS-IDI Transformants ... 78

Figure 23: Representative Gas Chromatography-Mass Spectrometry (GC-MS) Chromatogram of Isoprene Production in an Isoprene-Producing *Synechococcus* PCC 7002 Strain (1108, pAQ1::*Isps-IDI*) 79

Figure 24: (GC-MS) Chromatogram of Isoprene Produced by a *Synechococcus* 7002 ΔGlgA1A2 'Knockout' Strain 80

Figure 25: Impact of Isoprene on Growth of *Synechococc*us sp. PCC 7002 82

Figure 26: PetJ2-IspS-IDI-Sp^R/Sm^R DNA Construct for Inserting *IspS-IDI* Genes into the Chromosomal *petJ2* Gene 84

Figure 27: Recombinant Plamid pUC57-petJ2-IspS-IDI-Sp^R/Sm^R Carrying the petJ2-IspS-IDI-Sp^R/Sm^R Construct..... 86

Figure 28: PCR Analysis to Characterize Recombinant Plasmid pUC57-petJ2-IspS-IDI-Sp^R/Sm^R 87

Figure 29: PCR Analysis to Characterize 7002 ΔpetJ2 Mutants 89

LIST OF FIGURES (Continued)

Page

Figure 30: Stable and Continuous Isoprene Production in a 7002 ΔpetJ2 Strain 90

Figure 31: Plasmid pOSH1309 for Targeting *Isps-IDI-Km*^{R} Genes to the Plasmid pAQ1 of *Synechococcus* 92

Figure 32: Illustration of *IspS-IDI* Gene Constructs Targeted to the Chromosomal *petJ2* and Plasmid pAQ1 Sites 93

Figure 33: PCR Analysis of *IspS-IDI* Genes Targeted to Plasmid pAQ1 in the 'Dual IspS-IDI' Strain 95

Figure 34: Real-Time Fast Isoprene Sensor (FIS) Measurements of Isoprene Production in a 'Dual-IspS-IDI' *Synechococcus* 7002 Strain 96

Figure 35: Reverse Transcriptase Quantitative PCR (RT-qPCR) Amplification Plot of *IspS* Transcript Abundance in *Synechococcus* Strains with Chromosomal and Plasmid Targeted *IspS-IDI* Genes 98

Figure 36: Relative *IspS* Transcript Abundance in *Synechococcus* Strains with Chromosomal and Plasmid Targeted *IspS-IDI* Genes 99

INTRODUCTION

Statement of Problem

The development of alternative energy resources is necessary for a sustainable environment, reduced energy cost and national security. Photosynthetic organisms such as cyanobacteria and microalgae hold great potential as sources of sustainable biofuels and bio-products because of their ability to use energy from sunlight to convert atmospheric carbon-dioxide (CO_2) into energy-rich compounds including isoprene and terpenes such as β-pinene, limonene and camphene that can be efficiently converted to jet fuels with high energy density (1, 2). Isoprene is a high-value precursor for thousands of terpene products including synthetic rubber, pharmaceuticals, fragrances, and biofuels. It is produced biologically by many plants such as poplar, kudzu, oak, and in low yields by marine algae (3, 4, 5). Cyanobacteria, despite their methyl erythritol phosphate pathway (MEP) for terpenoids biosynthesis, lack the key isoprene synthase (IspS) enzyme for isoprene biosynthesis, but have been genetically engineered to produce isoprene for possible commercial exploitation (6, 7). The MEP pathway is important as products of CO_2 fixation and sugar intermediates are channeled into this biosynthetic route for the synthesis of essential terpenoids such as chlorophyll, carotenoids, and quinones.

The methyl erythritol phosphate (MEP) biosynthesis pathway (Figure 1) uses pyruvate and glyceraldehyde-3-phosphate (G3P) as substrates. These substrates are condensed to form deoxyxylulose-5-phosphate (DXP). The DXP is then converted into MEP which is subsequently converted by a series of enzymes into

hydroxymethylbutenyldiphosphate (HMBPP). HMBPP is used as a substrate in the formation of isopentenyl diphosphate (IPP) and dimethylallyl diphosphate (DMAPP). The interconversion of DMAPP and IPP is catalyzed by isopentenyl diphosphate isomerase (IDI).

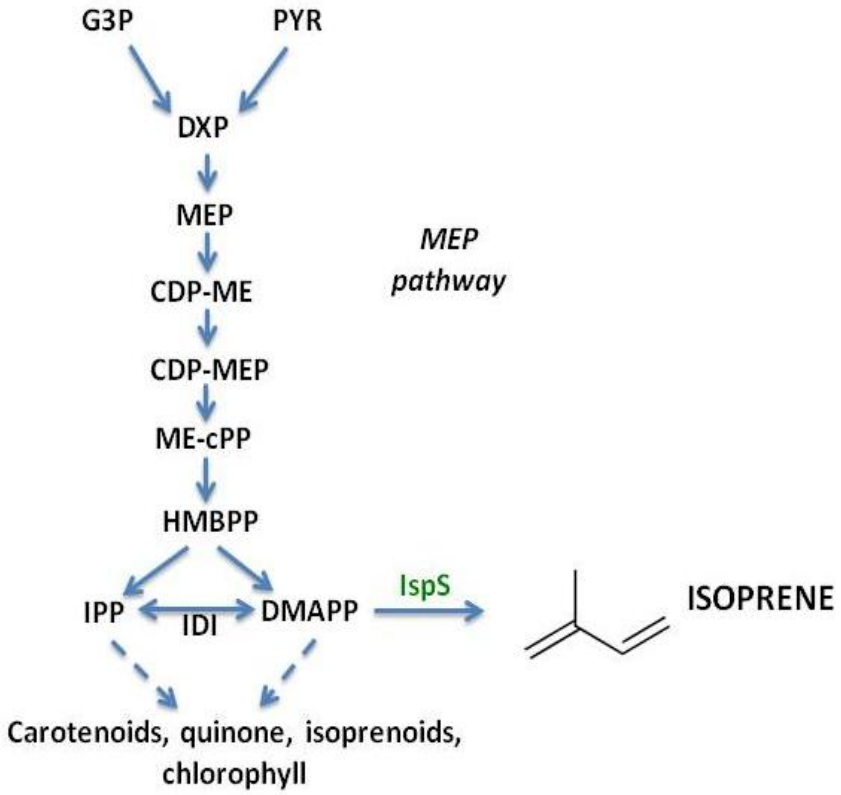

Figure 1. **The Methyl Erythritol Phosphate (MEP) pathway**. Glyceraldehyde-3-phosphate (G3P) and pyruvate (PYR) serve as starting substrates for the MEP pathway. The arrows point in the direction of the products formed at different points in the pathway. DXP, 1-Deoxy-D-xylulose-5-phosphate; MEP, 2-C-methyl-D-erythritol 4-phosphate; CDP-ME, 4-(Cytidine 5'-diphospho)-2-C-methyl-D-erythritol; CDP-MEP, 2-Phospho-4-(Cytidine 5'-diphospho)-2-C-methyl-D-erythritol; ME-Cpp, 2-C-methyl-D-erythritol 2,4-cyclodiphosphate; HMBPP, 1-Hydroxy-2-methyl-2-butenyl-4-diphosphate;IPP, Isopentenyl diphosphate**;** DMAPP, Dimethylallyl diphosphate; IspS, Isoprene synthase.

Although most eukaryotes and some bacteria possess a well characterized type I IDI isomerase (8), Ershov et al. (9) reported that both the *Synechocystis sp.* PCC 6803 and *Synechococcus sp.* PCC 7942 cyanobacteria lack this isomerase activity. However, a functional type-II IDI was later identified from *Synechocystis sp.* PCC 6803 (10), and also in the archaean, *Sulfolobus shibatae* (11), indicating that multiple and unrelated forms of IDI may exist, especially across different cyanobacterial species. Alternatively, IPP can be generated by an independent and non-homologous mevalonic acid pathway (MVA). The MVA pathway had been known as the source of DMAPP and IPP in several different groups of organisms, before the discovery of the MEP pathway in bacteria. The MVA pathway is found in eukaryotes, archaea and some bacteria, but has not been found in cyanobacteria (12). The Isopentenyl diphosphate (IPP) and dimethylallyl diphosphate (DMAPP) serve as two important precursors of isoprenoids/terpenoids with DMAPP being converted into isoprene by the isoprene synthase (IspS) enzyme.

Isoprene production has been successfully demonstrated in *E. coli* with the application of genetic engineering strategies. Although strategies to further improve bio-isoprene yield have produced results, increased efforts are still needed to achieve commercial production levels. The native MEP pathway in *E. coli* has been targeted to increase the DMAPP and IPP pool for enhanced metabolic flux through this pathway, resulting in improved production of carotenoids and other terpenoids (13, 14). Also, a combination of protein and metabolic engineering strategies has been used to improve the catalytic activity of relevant enzymes involved in the MEP pathway and increase the metabolic flux towards terpenoid biosynthesis (15). The overexpression of selected genes

coding for important enzymes in the MEP pathway or expression of heterologous genes coding for enzymes involved in either the MVA or MEP pathway in *E. coli* and *B. subtilis* resulted in improved terpenoid/isoprene yields (16, 17, 18). In another study, the overexpression of enzymes involved in the native MEP pathway as well as expression of a complete suite of heterologous MVA pathway genes was used. The genetically engineered *E. coli* strain expressing both a heterologous kudzu *IspS* (*kIspS*) and an optimized MVA operon carrying *E. coli*- specific ribosomal binding sites (RBS) resulted in a 150-fold increase in isoprene production compared to control strains expressing only a native kIspS enzyme (19). These results demonstrate the importance of genetic engineering strategies as a viable research tool for further improving bio-isoprene production in suitable model organisms.

Isoprene production has also been achieved in cyanobacteria by the introduction of a codon-optimized gene for isoprene synthase (IspS) from kudzu (6). Lindberg et al. (6) reported a 10-fold increase in isoprene production resulting in ~50 µg/g dry cell per day, under ~ 40 µmol photons $m^{-2}s^{-1}$ light intensity in the cyanobacterium, *Synechocystis* sp. 6803. The introduction of a codon-optimized kudzu *IspS* gene transcriptionally fused to a native *PsbA2* promoter increased isoprene yield compared to *Synechocystis* sp. 6803 strain expressing a native kudzu *IspS* (6). Recent studies have successfully demonstrated improved isoprenoids and isoprene production by metabolically engineering the native MEP pathways in cyanobacterial strains (7, 20). Kudoh et al. (20) reported that overexpression of the MEP pathway deoxy-xylulose-5-phosphate synthase enzyme in *Synechocystis* sp. 6803 resulted in the production of 1.5 times more carotenoids

compared to wild type strains. Bentley et al. (7), showed the successful heterologous expression of a complete set of MVA pathway genes of bacterial origin under the control of the photosynthetic *PsbA2* promoter in a *Synechosystis* sp. 6803 strain carrying a codon-optimized *IspS* gene resulting in a 2.5-fold increase in isoprene production compared to strains expressing only the codon-optimized kudzu *IspS* gene.

Also, isoprene production has been achieved in cyanobacteria by the introduction of codon-optimized IspS and IDI isomerase transgenes from poplar (Nelson and Kallas, unpublished). In 2011, Nelson and Kallas introduced codon-optimized poplar transgenes for a rate-limiting, methyl erythritol phosphate (MEP) pathway isomerase (IDI), and an isoprene synthase (IspS) enzyme into the marine cyanobacterium, *Synechococcus* sp. PCC 7002, and produced isoprene at rates ~ 40 to 80-fold higher (i.e. ~ 4 mg gDW^{-1} 12 h day^{-1}) than previously reported for cyanobacteria. The introduction of a codon-optimized, rate-limiting isomerase *IDI* transgene from poplar plant enhanced isoprene yield by ~ 15-fold compared to the original transformant strain that carried only the codon-optimized, poplar *IspS* gene. The result suggested that the introduced heterologous *IDI* further enhanced the MEP pathway for increased isoprene yield. These data show that modifications that increase carbon flow through the MEP pathway to DMAPP can greatly increase isoprene production in *Synechococcus* sp. PCC 7002.

Bio-isoprene production from cyanobacterial species has not yet reached a sufficient level for purposes of commercial exploitation. A major problem that needs to be addressed is the physiological inefficiency of cyanobacteria and microalgae to convert solar energy into biofuels under mass culture conditions (21, 22). Despite the highly

efficient light capturing mechanism as well as higher photosynthetic efficiency exhibited by microalgae and cyanobacteria compared to terrestrial plants, their solar energy conversion efficiency can be further improved. Not all of the usable active radiation (~ 400 nm – 700 nm) reaching the earth from the sun is absorbed by light harvesting pigments associated with photosynthesis (21). Cyanobacteria and microalgae absorb low energy, longer wavelengths (680 nm and 700 nm) light photons to drive photosynthetic reaction center chemistries respectively, in photosystem II and photosystem I. Therefore, shorter wavelengths captured and trapped by the photosynthetic reaction centers are lost as heat or fluorescence (via non-photochemical quenching (23)) which further reduces available incident solar radiation for conversion into chemical energy and biomass (21, 24).

More so, under dense culture conditions, the problems of self-shading by cells prevents light from reaching cells deep in the culture and this can reduce photosynthetic efficiency by 95% due to light limitation (21, 25, 26). Cells at the surface of such dense cultures become saturated with excessive high light leading to photoinhibition (damage to photosynthetic machinery caused by excessive light) which also reduces the photosynthetic efficiency (21), although some cyanobacteria species such as *Synechococcus sp.* PCC 7002 can tolerate twice full sunlight intensity (27). Furthermore, about 30% of fixed carbon is used during respiration, which further reduces the carbon pool available for conversion into biomass and biofuels, though this may vary depending on species of cyanobacteria or microalgae (21).

To improve algal biofuels and bio-products yield, strategies involving optimization of carbon fixation and organic carbon utilization, light capture, energy transfer, and culture conditions (21, 28, 29) will further enhance the photosynthetic efficiency for conversion of light energy into chemical energy in cyanobacteria and microalgae. As shown in the successful truncation of antenna complexes in the alga *Chlamydomonas reinhardtii* (30, 31) which resulted in enhanced availability of light to cells over a large cross-sectional area of a controlled culture condition such as that in a photobioreactor. The enhanced light availability to cells increased photosynthetic activity and energy conversion efficiency under high saturating light and mass culture conditions. Therefore, improved light capture resulting from truncation of light harvesting antenna will be fundamental in generating algal biofuels at commercially significant rates (25, 26). Consequently, our group (Kallas' lab) has proposed the inactivation of selected genes in the phycocyanin cluster in the model organism *Synechococcus sp.* PCC 7002 to reduce the antenna complex for increased isoprene yields under high light conditions.

Recent studies have also involved strategies aimed at improving CO_2 assimilation via the Calvin Benson cycle by overexpression of the ribulose-1, 5-biphosphate carboxylase/oxygenase enzyme (RuBisCO) for increased photosynthetic productivity (32). The overexpression of key enzymes involved in the Calvin Benson cycle for enhanced photosynthetic capacity and bio-products yield is also gaining interest (33). In addition to metabolic engineering of relevant pathways as part of strain optimization, further strategies involving efficient culturing and harvesting practices have been suggested (National Alliance for Advanced Biofuels and Bio-products (NAABB), Final

report 2014, www.energy.gov). These strategies will potentially improve production of bio-products and biofuels yield.

As part of efforts toward improving algal biofuels/bioproducts production, my research involved a carbon partitioning strategy based on the inactivation of a competing carbon pathway for glycogen biosynthesis in *Synechococcus sp.* PCC 7002, so that carbon stored as glycogen will be re-routed to the MEP pathway for increased isoprene synthesis. In addition, the optimized poplar *IspS* and *IDI* genes previously expressed on a high-copy plasmid in *Synechococcus sp.* PCC 7002 were targeted to a chromosomal neutral site to circumvent the problem of decreased isoprene yield over time, possibly resulting from loss of transgenes from the plasmid. I expected that the chromosomal integration of these optimized genes would enhance the stability of their messenger RNA (mRNA) transcripts for long-term isoprene production. Once target DNA is stably integrated to the chromosome, such gene(s) of interest are also replicated with the chromosome and therefore not easily lost compared to heterologous genes expressed on plasmids. Therefore, the stability of the *IspS* and *IDI* genes is expected to improve stable gene expression for long-term isoprene production.

To further improve isoprene production, I targeted the *IspS* to a pAQ1 plasmid, in addition to a chromosomal site. The targeting of *IspS* and *IDI* to both a chromosomal and plasmid location was expected to increase their gene copies and thus increase *IspS* and *IDI* expression levels for improved isoprene yield. The research further involved gene expression studies to analyze the link between *IspS* transcript levels and isoprene

production. The result of the experiment is expected to improve our understanding of the effect of increased copies of key MEP pathway genes on isoprene yield. The experimental outcome is also expected to aid the design of future experiments that may involve overexpression of heterologous MEP pathway enzymes in *Synechococcus sp.* PCC 7002.

The field of algal biofuels will have to overcome the current production hurdles by developing appropriate and desirable carbon partitioning strategies that will ensure that the carbon requirements and priorities for cell biomass are compatible with the carbon flux available or channeled towards the synthesis of useful products (34, 35) such as isoprene and terpenoids. Also, the development of efficient strategies that will improve culture conditions for increased photosynthetic activities will be necessary to achieve commercial-scale biofuels production.

Background

Recently, scientists have found photoautotrophic organisms such as cyanobacteria, microalgae and some algal species, to be excellent model organisms for genetic engineering and production of bioproducts and biofuels because of their genetic plasticity comparable to *E. coli* and yeast (36). For about 2.5 billion years during earth's history, cyanobacteria have played an important role as a source of atmospheric oxygen (37). They are also important players in the earth's carbon and nitrogen energy cycling (38). Cyanobacteria comprise a large and morphologically diverse group of photosynthetic bacteria (39) which can vary from 1 µm to 65 µm in width (as in *Lyngbya wollei*) (40).

Cyanobacteria, (formerly described as blue-green algae) are unicellular or filamentous organisms sometimes mistaken for microalgae but differ from algae because of their lack of defined organelles such as nucleus, chloroplast and mitochondria – i.e. because of their prokaryotic cellular organization (41). Cyanobacteria are gram-negative (42), but possess photosystem I and II (PSI and PSII) and cholorophyll a pigments. A characteristic morphological feature of the cyanobacterial cell is an envelope structure comprising an external surface structure, outermembrane, polypeptidoglycan layer and a cytoplasmic membrane typical of gram negative membrane structures. However, the cyanobacterial peptidoglycan layer is thicker and more highly cross-linked than most gram negative cells (43). In addition to their cytoplasmic membrane, cyanobacteria possess uniform sheet-like thylakoid membranes (44) containing the components of their photosynthetic electron transfer chain. Cyanobacteria can be found in different environments such as land, fresh water, and marine habitats (45).

Cyanobacteria carry out oxygenic photosynthesis using photosynthetic pigments such as phycobilisomes, chlorophyll *a*, and chlorophyll *b* (found only in a few cyanobacteria), and electron transport chain components located in the thylakoid membrane (46), allowing them survive a broad range of environmental conditions. The phycobilisomes contain phycobilin pigments composed of bilin proteins involved in transfer of light energy to PSII which in turn transduces the excitation energy into chemical energy. Phycobilisomes are light harvesting proteins that absorb light of wavelength between 500 - 670 nm (47) in the visible spectrum, largely outside the range of chlorophyll a (48). Bilin proteins can be classified majorly into allophycocyanins (AP),

phycocyanins (PC), and phycoerythrins (PE) with peak absorbances of ~ 650 nm, ~ 620 nm, and ~ 560 nm respectively (49).

Cyanobacteria fix CO_2 via the Calvin Benson cycle by means of enzymes such as RuBisCO (ribulose-1, 5-biphosphate carboxylase/oxygenase) and carboxysomal carbonic anhydrase (CA) (50) located in microcompartments called carboxysomes. Photosynthetic aquatic prokaryotes such as cyanobacteria have evolved a carbon concentrating mechanism (CCM) to help them deal with the fluctuations of CO_2 in their habitats and overcome the inefficient process of CO_2 fixation mediated by the cyanobacterial RuBisCO enzyme (51). The RuBisCO in cyanobacterial cells is less efficient compared to that in terrestrial plants and other algal cells. This can be attributed to the significantly lower CO_2 diffusion rate in aquatic cyanobacterial species due to the slow equilibration of CO_2 in water compared to air (52).

In addition to the slow chemical equilibrium between bicarbonate (HCO_3^-) and CO_2, the less abundant inorganic carbon available for cyanobacteria in acidic environments, contribute to a less efficient RuBisCO (52). The CCM therefore increases RuBisCO efficiency by elevating CO_2 levels around the active sites of the RuBisCO enzyme and thus, allows the accumulation of bicarbonate via the operation of some active CO_2 and bicarbonate transporters found in both the thylakoid and plasma membranes (51). Consequently, the pooled cytosolic bicarbonate is then converted by CA into CO_2 within the carboxysomes.

Carbon fixation in cyanobacteria results in the generation of sugars or polysaccharides, which are stored majorly as glycogen reserves. In addition to glycogen, some cyanobacteria store nitrogen in cyanophycin granules, which are polymers of arginine and aspartic acid (38). The polysaccharides or sugars generated from carbon assimilation are broken down through glycolysis to generate intermediates that serve as substrates for the tricarboxylic acid cycle (TCA), thus, generating useful respiratory intermediates for adenosine-triphopshate (ATP) synthesis. Until now, it was thought that cyanobacteria lacked a functional citric acid cycle because of the absence of an α-ketoglutarate dehydrogenase. The absence of a 2-oxoglutarate dehydrogenase had been the premise for the incomplete TCA cycle described in cyanobacteria over the decades. Also, this incomplete citric acid cycle had been described as the reason why majority of cyanobacteria are obligate photoauthotrophs (53). Although many cyanobacteria are obligate photolithoautotrophs (e.g. *Synechococcus sp.* PCC 7002 which can also grow photoheterotrophically on glycerol (54)), some cyanobacteria can grow chemoheterotrophically (e.g. *Anabaena sp*.) in the dark by oxidizing glucose or other sugars.

However, in a recent study by Zhang and Bryant (55), it was shown that genes encoding 2-oxoglutarate decarboxylase and succinic semialdehyde dehydrogenase in *Synechococcus sp*. PCC 7002 could convert 2-oxoglutarate to succinate and therefore acted as functional replacements for 2-oxoglutarate dehydrogenase and succinyl-CoA synthetase, respectively. This variant of the TCA cycle as described in *Synechococcus sp*.

PCC 7002, by Zhang and Bryant may be responsible for the metabolic adaptation of cyanobacteria to different physiological and ecological requirements (53).

In most cyanobacteria, photosynthetic electron transport occurs in the thylakoids while respiratory electron transport occurs in both the cytoplasmic membranes and thylakoids. The photosynthetic electron transport chain is triggered by light energy from the sun. PSII uses this energy as a catalyst for splitting water molecules and electrons generated are subsequently used to reduce plastoquinone (PQ). These electrons then move from the PQ pool to the cytochrome b_6f complex and from there to a soluble electron carrier such as plastocyanin (found in many cyanobacteria under copper replete conditions) or cytochrome c_6 (as found in *Synechococcus sp*. PCC 7002) (46). Cytochrome c_6, or plastocyanin, which carry one electron at a time reduce the oxidized PSI reaction center chlorophyll, $P700^+$. The Oxidation of P700 reaction center results from the transfer of electron from PSI to ferredoxin and then back to $NADP^+$. This process uses light energy from the sun. The protons generated during the splitting of water and oxidation of the PQ pool by the cytochrome b_6f complex flow into the lumen to generate a proton gradient across the thylakoid membrane, which is used for ATP synthesis by the thylakoid-membrane ATP synthase (Figure 2). This photosynthetic electron flow route is described as linear electron flow.

In addition to the above mentioned linear electron flow pathway, a cyclic electron transport also occurs. This pathway involves the ferredoxin, that was reduced by PSI, transferring its electron either via an NADPH (NDH-1) dehydrogenase back to the PQ

pool or directly back to cytochrome b_6f complex and then to PSI (46). This cyclic electron flow around PSI has also been shown to be essential for photosynthesis as it helps to prevent over-reduction caused by accumulation of NADPH (56).

In contrast, the respiratory electron transport flux in cyanobacteria involves succinate dehydrogenase (SDH) and NADPH-dehydrogenase activities (NDH-1). Two types of NADPH dehydrogenase have been identified in cyanobacteria; NDH-I which prefers NADPH as substrate and NDH-II which prefers NADH. The dehydrogenases, NDH-I and NDH-II control the oxidation-reduction state of NADP and NAD, respectively, thus indirectly regulating electron flow through SDH into the PQ pool or respiratory electron transport flux (57). Cooley et al. (58) showed that the cyanobacteria, *Synechocystis* PCC 6803 mutants lacking SDH displayed significantly slower electron flow rates into the PQ pool compared to wild type and NDH-1 mutants, suggesting that SDH also plays an important role in the flow of respiratory electron into the PQ pool.

Electrons generated from the oxidation of NADPH and succinate to NADP and fumarate respectively flow into the PQ pool. The protons produced by the redox reactions during the transfer of electrons from the PQ pool to the soluble PC is pumped into the lumen to produce a hydrogen ion concentration and charge gradient which consistently generates a proton motive force (PMF) used by ATP synthase to generate ATP in the thylakoid membrane. Photosynthetic electron flux activity is comparatively higher than respiratory electron flow activity under abundant light condition (46). All cyanobacteria can carry out respiration in the dark using oxygen as the terminal electron acceptor.

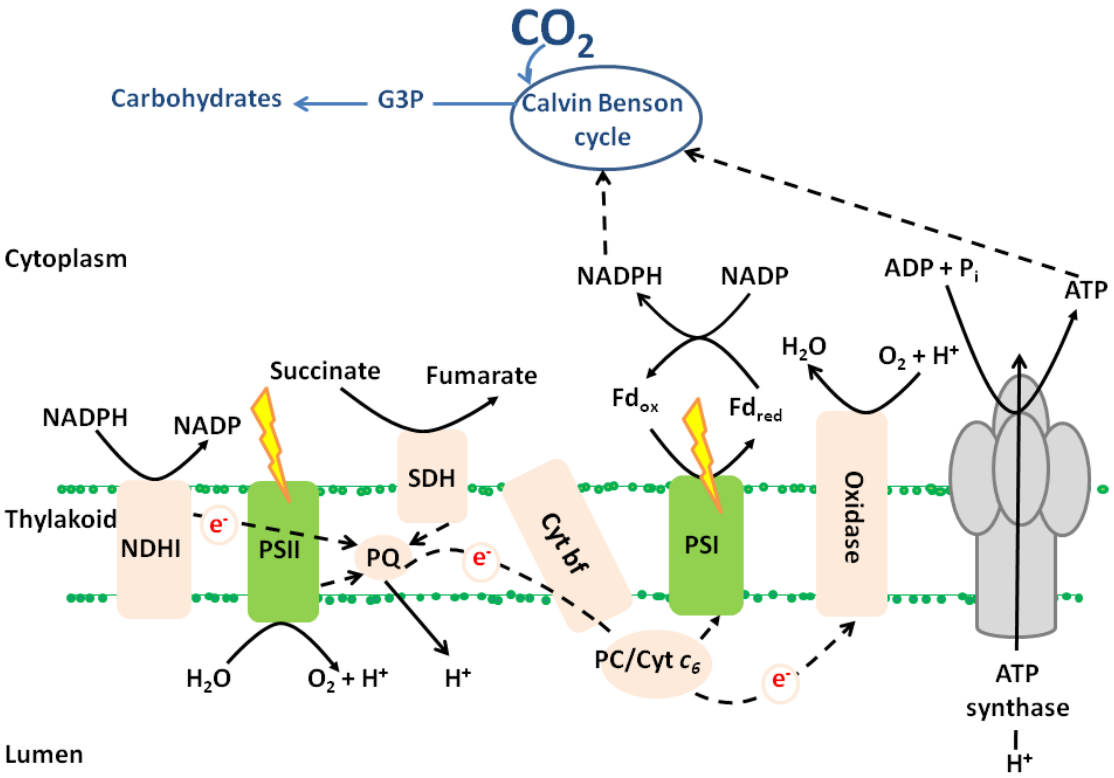

Figure 2. Photosynthetic and respiratory electron flux pathways in thylakoid membranes of cyanobacteria. Arrows indicate the directions of electron flow as well as products formed. The Yellow thunderbolts represent light that triggers the redox reactions in both PSI and PSII. Electron transfer complexes that are specifically involved in photosynthetic electron flux pathway are PS II and PS I, while those specific for respiratory electron transfer include NDH-1, SDH, and the terminal oxidase. The PQ, cyt b_6f and PC/ cyt c_6 are shared by both electron transfer pathways. The presence of either PC or cyt c_6 is determined by copper availability in the environment. Abbreviations: cyt b_6f, the cytochrome b_6f complex; Fd_{ox} and Fd_{red}, Ferredoxin in oxidized and reduced forms, respectively; NADP(H), Nicotinamide – adenine dinucleotide phosphate (reduced form); NDH-1, type 1 NADPH dehydrogenase; Oxidase, terminal oxidase; PC, plastocyanin; cyt c_6, cytochrome; PQ, plastoquinone; SDH, succinate dehydrogenase; G3P, glyceraldehydes-3-phosphate; TCA, tri-carboxylic acid cycle.

Cyanobacteria as Cell Factories for Biofuels Production

The term algal biofuel refer to 'green fuels' generated from microalgae, cyanobacteria and macroalgae (or seaweed). The main themes driving the development of algal biofuels for decades have been the search for a cleaner and cheaper energy, reduction in green-house gas (GHG) or carbon emissions and more importantly, saving the environment from further consequences of global climate change. According to the US Environmental Protection Agency (EPA), fossil fuels are a major source of GHG pollution and carbon-dioxide (CO_2) identified as the primary GHG pollutant; with increasing global levels of atmospheric CO_2 implicated in global climate change (59).

Biofuels development started with the first generation liquid biofuels derived from sugar cane and corn, and such fuels were marred by concerns about food shortages leading to increase in food prices, as well as relevant ethical and ecological questions as to the use of high-value arable land for the cultivation of these crops for energy purposes rather than as food sources (60). These challenges spurred the development of second generation biofuels utilizing lignocellulosic biomass from non-edible crops (e.g. switch grass), with its peculiar challenges of cost-effectiveness, feed stock availability and technology (61). However, the third generation biofuels (also described as algal biofuels), produced from cyanobacteria and microalgae offer further advantages over the other biofuel generations and has attracted the interests of researchers.

Cyanobacteria and microalgae exhibit a higher photosynthetic efficiency than terrestrial plants (62) based on their relatively higher photosynthetic and biomass production rates and this provides a major attraction for utilization of these organisms for

biofuel generation. Cyanobacteria and microalgae are useful model organisms for production of biofuel and other valuable co-products because of the following reasons, 1) high productivity, 2) a non-food based resource, 3) they can be cultivated on non-arable land, 4) they can also grow on brackish and wastewater, and 5) useful for recycling carbon-dioxide and other nutrient waste streams (63). Cyanobacteria and macroalgae accumulate mainly polysaccharides such as glycogen, mannitol or fucoidin as storage reserves (64) while certain eukaryotic algae naturally accumulate high amounts of triacylglycerides (about 30-60% dry weight) (65). These energy-rich compounds and biosynthetic by-products stored in relatively high amounts in cyanobacteria and several algal species can be explored for the production of biodiesel, or as precursor compounds for production of high energy-density biofuels (including isoprene).

In order to provide sustainable energy for the future and reduce dependence on fossil fuels; alternative carbon neutral energy sources must be explored. A good example of such alternative bio-energy solution relies on the ability of plants or algae to use sunlight to fix atmospheric CO_2 into organic matter or cellular biomass, thereby reducing the atmospheric concentration of CO_2. Cyanobacteria have advantages that make them a suitable alternative and a sustainable source of renewable energy. They can tolerate a high CO_2, possess a comparatively efficient CO_2 concentrating mechanism (CCM) which helps to concentrate CO_2 by a 1000-fold around the RuBisCo enzyme (51), and are easier to manipulate genetically because of their fast growth, prokaryotic cell structure, and smaller genome sizes (36) of 1.6 Mb (*Prochlorococcus* sp.) to 9.2 Mb (*Nostoc punctiforme*) (66) compared to eukaryotic algae.

Our lab uses the model cyanobacterium; *Synechococcus sp.* PCC 7002 (Figure 3) which possesses a number of characteristics that enhances its suitability as a model strain for functional genomics and biotechnological applications. These characteristics include 1) a fast doubling time of ~ 4 hours, 2) high light tolerance, 3) relative ease of natural transformability, 4) facultatively photoheterotrophic (i.e. can grow on glycerol (55), and 5) fully sequenced genome of about 3.4 Mbp. The *Synechococcus sp.* PCC 7002 strain carries 6 - 8 copies of its chromosome and six endogenous plasmids; pAQ1, pAQ3, pAQ4, pAQ5, pAQ6 and pAQ7 with sizes of: 4809; 16,103; 31,972; 38,515; 124,303; and 186,459 bp, respectively (67); (See Kyoto Encyclopedia of Genes and Genomes, http://www.genome.jp/keggbin/showorganism?org=syp). Although the copy number of these plasmids may depend on growth conditions, the pAQ6 and pAQ7 plasmids have similar copy numbers as the chromosome while the pAQ1 plasmid shows the highest copy number (about 50 – 100 copies per cell) under exponential growth phase (67).

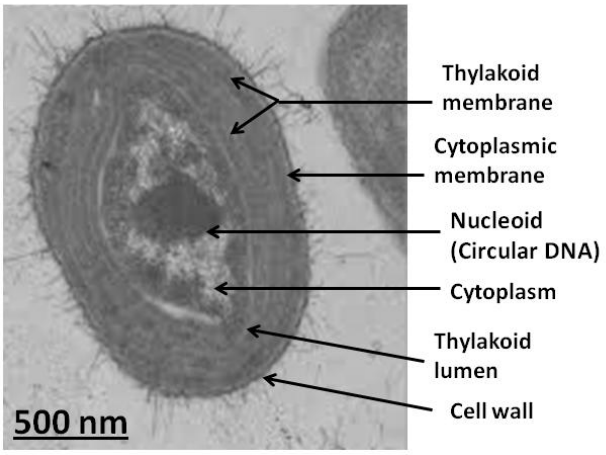

Figure 3: Transmission electron micrograph of *Synechococcus* sp. PCC 7002. Scale bar, 500 nm. (Credit: original image by Prof. Donald Bryant's lab, Penn State University)

Isoprene Synthesis in Cyanobacteria

Isoprene (C_5H_8) (Figure 4), also known as 2-methyl-1, 3-butadiene, is a colorless compound that can be polymerized to yield high-energy liquid biofuels. Isoprene is a volatile hydrophobic compound and passes through cellular membranes allowing it separate from the cyanobacterial biomass and then be captured in the headspace of a bioreactor or sealed container for collection (68). It is an important precursor compound for the production of synthetic rubber and thousands of high-value terpenoid compounds, which makes isoprene a relatively high-value chemical.

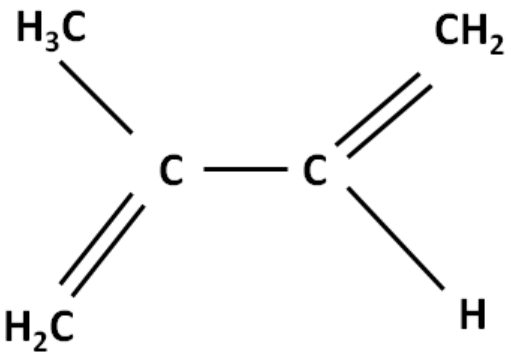

Figure 4. Chemical structure of isoprene

Bio-based isoprene does not have the same adverse environmental impacts as petroleum-based isoprene and is potentially more economical than that produced from petroleum. The development of bio-based isoprene from sustainable renewable energy

sources is expected to drive a competitive process less dependent on increasing crude-oil prices.

Isoprenoids (or terpenoids) are a large family of compounds useful in biological functions such as hormone-based signaling, electron transport, regulation of transcriptional and post-translational processes, protein degradation and glycoprotein biosynthesis (69). Isoprenoids are also an important component of organelles and cell membranes (70) and also offer a natural reserve of useful compounds that can be exploited in biomedicine and biotechnology. Isoprenoids such as sterols are important components of membranes in eubacterial and eukaryotic cells and dolichols are structural components of glycoprotein and bacterial cell wall biosynthesis (70).

Isoprenoid biosynthesis in living organisms is required for the production of compounds such as carotenoids, vitamins, quinones, chlorophyll, and the primary constituents of essential oils in plants (71). In all photosynthetic organisms including cyanobacteria, microalgae and particularly plants, the carotenoids, β-carotene, zeaxanthin and tocopherol (vitamin E) have been suggested as functioning in a photoprotective role either by dissipating excess excitation energy as heat or by scavenging singlet oxygen or other reactive oxygen species (ROS) (72). In plants, isoprene is emitted through leaves and helps plants withstand the effects of reactive oxygen species and heat flecks (3). Heat flecks result from rapid temperature changes in leaves due to high radiant energy fluxes and very low heat capacity of leaves (3).

Terpenoids or isoprenoids are compounds of terpenes modified by chemical oxidation and contain functional groups. Terpenes are composed of isoprene units and vary in structure from linear to ring arrangements. Terpenes can also be grouped according to their sizes depending on the number of isoprene units (Table 1).

Table 1. Examples of Terpenes and Isoprene units

Terpenoids	Number of isoprene units	Examples
Hermiterpenes (C_5H_8)	1	Isoprene, prenol (hemiterprenoid)
Monoterpenes ($C_{10}H_{16}$)	2	Limonene, geraniol
Sesquiterpenes ($C_{15}H_{24}$)	3	Farnesol, humulene
Diterpenes ($C_{20}H_{32}$)	4	Cafestol, taxadiene
Sesterterpenes ($C_{25}H_{40}$)	5	Geranylfarnesol
Triterpenes ($C_{30}H_{48}$)	6	Squalene
Sesquarterpenes ($C_{35}H_{56}$)	7	Ferrugicadiol
Tetraterpenes ($C_{40}H_{64}$)	8	α-, β-, γ-carotenoids
Polyterpenes	> 8	Natural rubber

Two different terpenoid biosynthesis pathways (see Figure 5) are known; 1) the mevalonate acid (MVA) pathway (7) found in archaea, eukaryotes and some bacteria, and 2) the non-mevalonate or 2C-methyl-D-erythritol-4-phosphate (MEP) pathway in cyanobacteria, algae, eubacteria and plant chloroplasts (73). The mevalonic acid (MVA) pathway, which involves seven enzymes, starts with the formation of four molecules of acetoacetyl-CoA after condensation of two acetyl-CoA molecules in a reaction catalyzed by thiolase. A third acetyl-CoA condenses with acetoacyl-CoA to form 3-hydroxy-3-methylglutaryl-CoA (HMG-CoA) by a HMG-CoA synthase which is converted to mevalonic acid by HMG-CoA reductase. The mevalonic acid is phosphorylated

sequentially to mevalonic acid diphosphate by mevalonate kinase and diphosphomevalonate kinase. The mevalonic acid diphosphate is decarboxylated by mevalonate diphosphate decarboxylase to generate Isopentenyl diphosphate (IPP) (69, 70). The last step in generating isoprenoids precursors in the MVA pathway requires IDI isomerase to maintain the DMAPP supply by catalyzing the isomerization of the IPP to DMAPP.

The MEP pathway and associated genes, defined originally from studies in *E. coli*, were used to identify homologous genes from different organisms including cyanobacteria by comparative genomics and bioinformatics (particularly sequence information) (74). The MEP pathway starts with 1-deoxy-D-xylulose-5-phosphate (DXP), formed from the condensation of pyruvate and glyceraldehyde 3-phosphate (G3P) in a reaction catalyzed by 1-deoxy-D-xylulose-5-phosphate synthase (DXS*)* using thiamine pyrophosphate as a cofactor. A reductoisomerase, 2C-methyl-D-erythritol 4-phosphate (IspC) converts DXP to 2C-methyl-D-erythritol-4-phosphate (MEP). Then, MEP reacts with cytidine 5'-triphosphate (CTP) in a CTP dependent reaction to produce 4-diphosphocytidyl-2C-methyl-D-erythritol (CDP-ME) in a reaction catalyzed by IspD (a transferase). 4-diphosphocytidyl-2C-methyl-D-erythritol 2-phosphate (CDP-MEP) is formed by the ATP-dependent phosphorylation of CDP-ME in a reaction catalyzed by IspE (a kinase). The enzymatic reaction catalyzed by IspF produces 2C-methyl-D-erythritol-2, 4-cyclodiphosphate (ME-cPP) from 4-diphosphocytidyl-2C-methyl-D-erythritol 2-phosphate. Also, IspF catalyzes the formation of 2C-methyl-D-erythritol 3, 4-cyclophosphate, although at a slower rate. The ME-cPP is first converted to 1-hydroxy 2-

methyl-2-(E)-butenyldiphosphate in a reaction catalyzed by IspG and then converted to 4-hydroxy-3-methyl-2-butenyl-4-diphosphate (HMBPP) in a reduction reaction. In addition, the IspH enzyme catalyzes further reduction of the 4-hydroxy-3-methyl-2-butenyl-4-diphosphate intermediate to IPP and DMAPP (69, 75, 76).

In vivo studies by Rohdich et al. (77) showed that the ratio of IPP and DMAPP is 5:1 in *E. coli* strains overexpressing the IspH enzyme. Therefore, the addition of IPP to chains of isoprenoid molecules depends on DMAPP availability and thus IDI catalyzes the isomerization of IPP to DMAPP. Two types of IDI have been identified (10); IDI-I which is found in eukaryotes, eubacteria and plants, and IDI-II found in archaea and some bacteria (78). The type I IDI requires only divalent cations as cofactors for activity (79). Type II IDI are flavoenzymes and different from type I IDI (80). Type II IDI requires flavin mononucleotide (FMN), nicotinamide adenine dinucleotide phosphate (NAD[P]H) and divalent cofactors such as Mg^{2+}, Mn^{2+}, and Ca^{2+} (79). The simultaneous production of DMAPP and IPP in the MEP pathway may explain why IDI isomerase is not essential for survival, as shown in *E. coli;* however, it is useful in maintaining the proper IPP/DMAPP ratio in cells (81).

It has been suggested that the MEP pathway in cyanobacteria may involve other substrates besides pyruvate and G3P and that these substrates, from the pentose phosphate pathway enter the MEP pathway at other points in the pathway (71). Ershov et al. (71) suggested that xylulose-5-phosphate (XY5P) could be a precursor for DMAPP synthesis in *Synechocystis sp.* PCC 6803. Under photoautotrophic conditions, XY5P is converted to 2, 4 hydroxymethyl cyclodiphosphate (HME-2, 4-cPP) via a series of

enzymatic reactions. The HME-2, 4-cPP is analogous to 2-C-methyl-D-erythritol 4-phosphate -- the product of the reductase formation of MEP from deoxyxylulose-5-phosphate (DXP) (71).

It is not clear yet how the MEP pathway in cyanobacteria is regulated, but this regulation may involve the accumulation of products in the pathway, effector molecules, transcriptional control, (69) or a combination of these mechanisms. Covalent modifications such as enzyme phosphorylation may also play a role in regulating enzymes and subsequent downstream reactions within the pathway (69). Most studies on the regulation of the MEP gene and pathway have involved plants (82, 83, 84, 85), but the identified regulatory mechanisms can also provide insight into MEP regulation in cyanobacteria. Both share similar MEP pathway genes, athough their distribution and expression patterns vary. Studies involving transgenic plants have shown that overexpression or antisense repression of DXS resulted in corresponding increases or decreases in accumulation of isoprenoid products (86), suggesting that the DXS enzyme catalyzes a rate limiting step for IPP and DMAPP synthesis and isoprenoid final products.

In addition, DXP reductoisomerase (87) and 4-hydroxy-3methylbut-2-enyl diphosphate reductase (88) have been suggested as having rate-limiting roles in IPP and DMAPP synthesis. It has been observed that MEP genes are found in different sites throughout the genome with no evidence of a shared, transcriptional regulator. In contrast, genes for the MVA pathway (especially in gram positive bacteria) are found in an operon, suggesting that the MVA genes are transcriptionally controlled (69). Further understanding of the transcriptional regulation of MEP genes will help researchers

improve favorable transcriptional flux towards enhanced by-products yields such as isoprene.

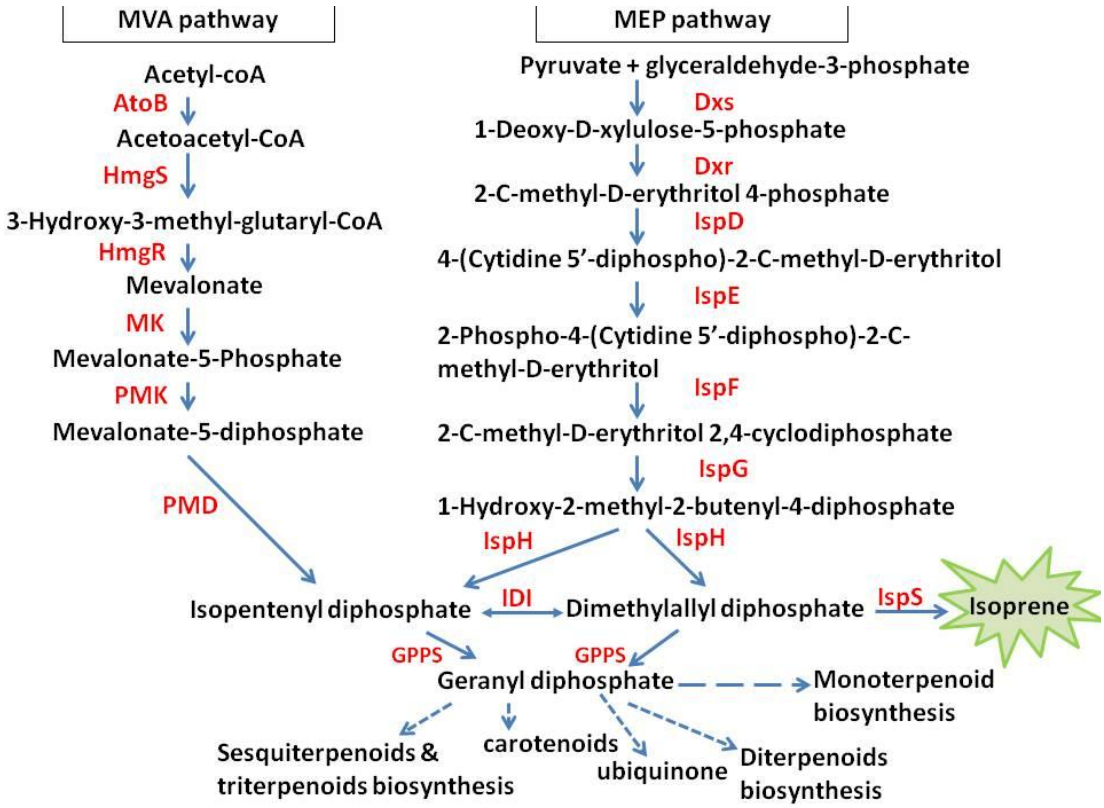

Figure 5. Substrate flux via the MEP and mevalonate (MVA) pathways for isopentenyl diphosphate (IPP) and dimethylallyldiphosphate (DMAPP) synthesis. Arrows indicate direction of products formed. MVA pathway enzymes: AtoB, Acetyl-CoA-acetyltransferase; HmgS, Hydroxymethylglutaryl-CoA synthase; HmgR, Hydroxymethylglutaryl-CoA reductase; MK, Mevalonate kinase; PMK, phosphomevalonate kinase; PMD, phosphomevalonate decarboxylase. MEP pathway enzymes: Dxs, 1-deoxy-D-xylulose-5-phosphate synthase; Dxr, 1-deoxy-D-xylulose-5-phosphate reductoisomerase; IspD, 2-C-methyl-erythritol 4 phosphate cytidyltransferase; IspE, 4-diphosphocytidyl-2-C-methyl-D-erythritol kinase; IspF, 2-C-methyl-D-erythritol 2, 4-cyclodiphosphate synthase; IspG, 4-hydroxy-3-methylbut-2-en-1-yl diphosphate synthase; IspH, 4-hydroxy-3-methylbut-2-enyl diphosphate reductase; IDI, isopentenyl diphosphate isomerase; GPPS, geranyldiphosphate synthase; IspS, isoprene synthase.

Rationale and Objectives of the Study

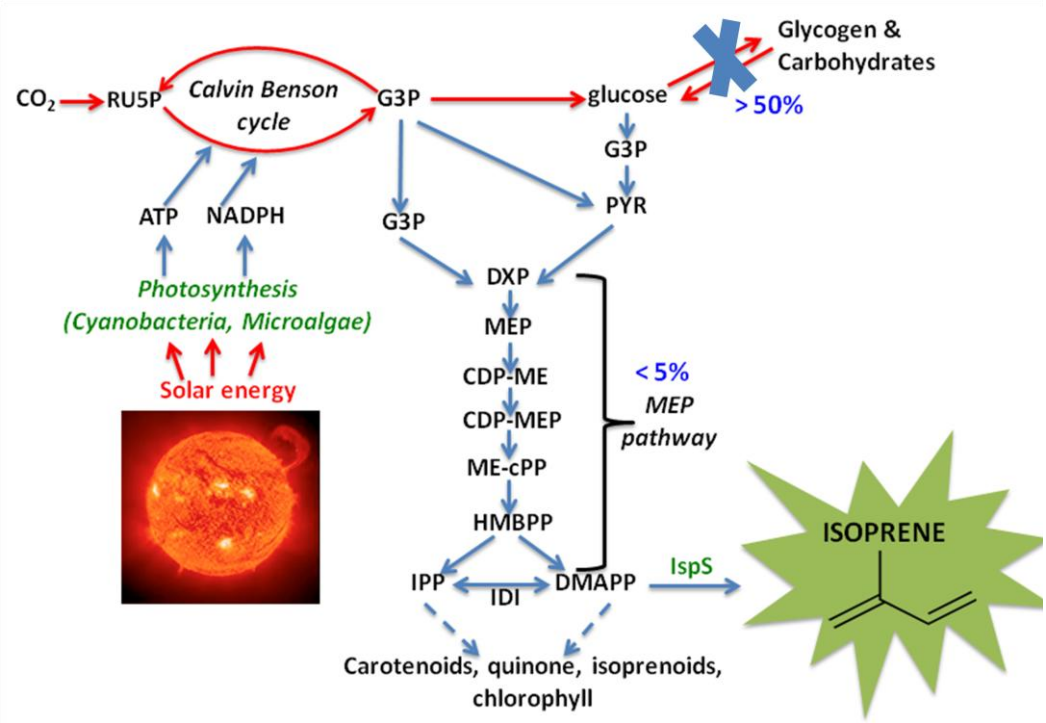

Figure 6. Isoprene production in cyanobacteria via the MEP pathway and competing carbon pathway for glycogen synthesis. A codon-optimized heterologous *IspS* gene from an isoprene producing plant is introduced into a model cyanobacterial species- *Synechococcus sp.* PCC 7002 so that the isoprene precursor, dimethylallyl diphosphate (DMAPP) can be converted into isoprene. Isoprene biosynthesis in cyanobacteria occurs via the Methyl erythritol phosphate (MEP) pathway. Inactivation of the glycogen biosynthesis pathway may increase the pool of MEP substrates; pyruvate and glyceraldehydes-3-phosphate (G3P) for enhanced isoprene production.

Towards improving isoprene yield in the cyanobacterium, *Synechococcus sp.* PCC 7002, the glycogen synthase genes *glgA1 and glgA2* were inactivated. Inactivation of these genes is part of a strategy to channel carbon to the MEP pathway for improved

isoprene yield. Inactivation of the *glgA1* and *glgA*2 genes should prevent the storage of carbon as glycogen, the major storage carbohydrate of cyanobacteria (Figure 6). Therefore, I hypothesized that the inactivation of a competing glycogen biosynthesis pathway will allow carbon previously channeled into this pathway to be re-routed to the MEP pathway for enhanced isoprene production.

In cyanobacteria, glycogen is synthesized by the enzymes: ADP-glucose phosphorylase (GlgC) EC = 2.7.7.27 [SYNPCC7002_A0095], glycogen synthase (GlgA) EC = 2.4.1.21 *glgA1* [SYNPCC7002_A1532]; *glgA2* [SYNPCC7002_A2125] and glycogen branching enzyme (GlgB) EC = 2.4.1.18 [SYNPCC7002_A1865] (45). The end-product of glycogen biosynthesis, the major storage polysaccharide, is a α -D-(1-4) homoglucan polymer formed from glucose residues linked through α-1, 4-glucosidic bonds and α-1, 6-glucosidic linkages (~10% of the carbon-carbon bonds (64)) at branching points and are usually stored as granules in the cytoplasm between the thylakoids of cyanobacterial cells (89). Under optimal photosynthetic and nitrate replete conditions; glycogen can accumulate to over 50% of cyanobacterial dry weight (90).

There are differences in the numbers of genes coding for glycogen biosynthesis enzymes in different cyanobacteria, but *Synechococcus sp*. PCC 7002 carries two isogenes for glycogen synthase; *glgA1* and *glgA2*. In contrast, other cyanobacteria such as *Synechococcus* sp. PCC 7942 carry only one gene coding for a glycogen synthase. Glycogen biosynthesis has been observed to be linked to environmental factors such as nitrogen limitation, as glycogen may serve as a source of energy for surviving nitrogen

starvation (91, 92, 93). Glycogen also plays a physiological role as observed in studies with cyanobacterial mutants with impaired glycogen synthesis (45, 94). In a study with *Synechococcus sp.* PCC 7942, glycogen synthase mutants showed a decrease in photosynthetic activity and an increased sensitivity to high light stress compared to the wild type (45). *Synechocystis* sp. PCC 6803 glycogen synthase mutants also showed impaired viability under dark conditions indicating that glycogen serves as an important respiratory substrate in the absence of light (94).

With respect to the physiological role of the glycogen synthase enzymes; GlgA1 [SYNPCC7002_A2125] and GlgA2 [SYNPCC7002_A1532] in *Synechococcus sp*. PCC 7002, Xu et al. (89) observed that mutants carrying inactivated copies of these isogenes (i.e., 7002 ΔGlgA1A2 null mutants) showed accumulation of glucosylglycerol and glucosylglycerate. The 7002 ΔGlgA1A2 mutants accumulated more sucrose, glucosylglycerol and glucosylglycerate under hypersaline conditions, whereas under optimal growth conditions, the 7002 ΔGlgA1 and 7002 ΔGlgA2 single mutants accumulated more sucrose (89). These observations suggest that glycogen plays a physiological role in cyanobacteria under salt stress conditions.

Energy (ATP) drives the transport of solutes and ions across the membrane as well as synthesis of enzymes and heat shock proteins that help counteract the effect of reactive oxygen species produced during osmotic, salt and oxidative stresses in cyanobacteria (95). Grundel et al. (94), reported significant 'overflow' (i.e. loss) of energetically important metabolites such as pyruvate and 2-oxoglutarate occur under strictly photoautrophic condition in glycogen defective *Synechocystis sp.* PCC 6803

mutants. This observed overflow was a result of the inability of the excess carbon to be channeled into glycogen biosynthesis. Therefore, the absence of an important carbon source such as glycogen may deprive cyanobacterial cells of considerable energy. Notwithstanding, the inactivation of glycogen biosynthesis in the euryhaline *Synechococcus sp.* PCC 7002 is expected to improve isoprene yield if the 7002 ΔGlgA1A2 mutant strains are cultivated under optimal photosynthetic and continuous light conditions. Isoprene production is a metabolic process associated with photosynthetic activity in the presence of light rather than in dark conditions, where glycogen serves as substrate for respiration.

In our lab, previous strategies to introduce optimized genes for the substrate-limiting *IDI* isomerase, and poplar isoprene synthase, *IspS*, genes into *Synechococcus sp*. PCC 7002 involved targeting these genes to the high-copy pAQ1 plasmid. Declining isoprene yield observed in such strains after several days of growth (data not shown) may be a consequence of plasmid loss or the result of metabolic burden by multiple copies of these genes, highly expressed from plasmid pAQ1. Thus, it may be advantageous to express such transgenes in the host chromosome rather than on high-copy plasmids, as plasmid loss is a major cause of reduced heterologous gene expression in plasmid-based systems.

Chromosomal gene targeting may lead more readily to complete replacement of target sites via segregation and thus stable integration of transgenes without the need for selective pressure through the addition of adjacent antibiotic resistance genes. Chromosomal integration of genes of interest may also enhance the expression of such

gene compared to plasmid-based systems. In addition to gene stability, chromosomal integration offers minimal metabolic burden on plasmids (96). Expression of heterologous genes in host organisms causes changes in metabolism described as either metabolic load or burden. Metabolic burden is often described in terms of resources such as energy and essential nutrients. These resources are needed to maintain and express heterologous genes (or replicate antibiotic resistance marker gene(s) carried by the heterologous genes targeted to plasmids) in the host cell (96). Chromosomal integration ameliorates the burden of plasmid maintenance and replication, and as such, cellular resource expenditure may be minimal to maintain the heterologous genes in the host cells. In addition, once the target genes are fully segregated and stably integrated to the chromosome, the host cell requires no further antibiotic selection to maintain the heterologous genes (97).

In the absence of complete segregational loss of the native target plasmid, the maintenance of high-copy plasmids expressing heterologous genes will require selective pressure provided by the growth medium which in turn, increases cost and thus becomes impractical on a commercial scale. Consequently, a strategy was developed for targeting the *IspS* and *IDI* genes to the *petJ2* [SYNPCC7002_A2391] chromosomal location. The *petJ2* gene codes for a c_6-like cytochrome protein whose functional role has not been clearly elucidated. Cytochrome c_6 (Cyt-c_6), is a soluble electron carrier essential for electron transport in cyanobacteria. Cyt-c_6 plays essential roles including electron transfer from the Cyt b_6f complex to the PSI complex during photosynthetic electron transport and during respiratory electron transport, to the cytochrome oxidase complex in the

thylakoid or plasma membranes (98). Genes for isoforms of this protein have been identified in the genome of both unicellular and filamentous cyanobacteria. Two isogenes, *petJ1* and *petJ2* of Cyt- c_6 like cytochromes have been identified in *Synechococcus sp.* PCC 7002 (98). Growth studies involving *petJ1* and *petJ2* mutants of *Synechococcus sp.* PCC 7002 showed that the PetJ1 protein plays an important role in electron transport while *petJ2* inactivation showed no effect (99). The PetJ1 and PetJ2 cytochromes differ significantly in their electrostatic and redox properties, thereby casting doubt on whether PetJ2 functions as an electron acceptor for the Cyt b_6f complex during photosynthesis (100).

A DNA construct carrying the codon-optimized *IspS-IDI* genes under the transcriptional control of a strong *CpcB* promoter (Figure 7), was targeted to the *petJ2* gene in the *Synechococcus* 7002 chromosome. The codon make-up of the *IspS-IDI* genes derived from poplar differs from the codon usage in the *Synechococcus* sp. PCC 7002 cyanobacterial host. Thus, for successful heterologous gene expression, optimized copies of the *IspS* and *IDI* genes with codons similar to those frequently used in *Synechococcus* 7002 were designed by Matthew Nelson, UW Oshkosh. The transgene DNA construct includes a linked streptomycin-spectinomycin antibiotic resistance gene cassette, transcription terminator, and flanking sequences homologous to a target site on plasmid pAQ1, as described by Xu et al. (67).

I proposed that targeting the *IspS-IDI* genes to a chromosomal site would enhance the genetic stability of these genes in *Synechococcus* 7002. The chromosomal integration

of these genes is expected to enhance mRNA transcript stability for the reasons described above and thus allow continuous, stable, isoprene production for a longer period than previously observed. In addition, since *Synechococcus sp.* PCC 7002 carries about 8 copies of its chromosome (67), this strategy, combined with *IspS-IDI* genes integrated in plasmid pAQ1, was likely to increase the total copy number of these genes in *Synechococcus* 7002. This in turn should increase the mRNA transcript level of these genes and thus increase IspS and IDI enzyme activity and isoprene yield.

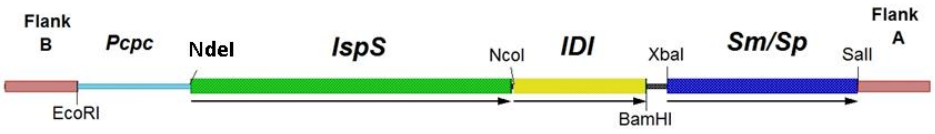

Figure 7. Illustration of the DNA construct carrying codon-optimized isoprene synthase (IspS) and Isopentenyl diphosphate isomerase (IDI) transgenes from poplar plant. This gene construct was introduced into *Synechococcus sp.* PCC 7002 to generate isoprene-producing strains. The heterologous *IspS-IDI* genes are transcriptionally controlled by a *PcpcB* promoter from *Synechococystis sp*. 6803. Original design and construction by Matthew Nelson, UW-Oshkosh.

In this thesis, I describe the successful construction of recombinant plasmids carrying inactivated copies of the *Synechococcus* sp. PCC 7002 *glgA1*and *glgA2* genes. These were introduced into *Synechococcus* to generate a 7002 ΔGlgA1A2 null mutant defective in glycogen synthesis. Optimized poplar *IspS-IDI* genes were introduced into the 7002 ΔGlgA1A2 strain to generate a 7002 ΔGlgA1A2 (*IspS-IDI*) glycogen synthase mutant to assess the impact of glycogen biosynthesis inactivation on isoprene yield. The *petJ2* gene was investigated as a chromosomal site for targeting heterologous genes, and the *IspS-IDI* genes were targeted to this site to assess stability and isoprene production from chromosomally targeted genes. *Synechococcus* carrying *IspS-IDI* genes targeted to *petJ2* produced isoprene at ~1.5 times the rate of strains with *IspS-IDI* genes targeted to the high-copy pAQ1 plasmid. Reverse-transcriptase quantitative PCR (RT-qPCR) showed that *IspS* transcript levels were stable over at least a week and more than 100-times higher in dense cultures than in strains with *IspS-IDI* targeted to plasmid pAQ1. *Synechococcus* with *IspS-IDI* targeted to the chromosomal *petJ2* site produced isoprene stably for a period of at least one month.

MATERIALS AND METHODS

Strains and Culture Conditions

The wild type (WT) *Synechococcus sp.* PCC 7002 (hereafter *Synechococcus* 7002), a euryhaline, gram-negative, rod shaped, unicellular prokaryotic organism, was isolated from the Magueys mud flats of Puerto Rico (101). *Synechococcus* 7002 grows well under photoautotrophic conditions, requires vitamin B_{12} for growth and can also grow photoheterotrophically on glycerol. *Synechococcus* 7002 is capable of growth over a wide range of sodium chloride (NaCl) concentrations and is extremely tolerant of high-light irradiation (27, 102). Under optimal conditions [37 – 39°C, 1 – 3 % (v/v) CO_2 in air, and saturating irradiation of ~250 μmol photons m^{-2} s^{-1}], *Synechococcus* 7002 has a doubling time of ~3.5 hours. *Synechococcus* 7002 is naturally transformable (102) and its genome is completely sequenced and (available on the National Center for Biotechnology Information website, http://www.ncbi.nlm.nih.gov/).

The DH5α *Escherichia coli* strain was used to propagate the recombinant plasmids. Its geneotypic characteristics include the following; F-, *lacZ-β* fragment, *recA-*, *endA-*, *gyrA96* (nalidixic acid resistance). DH5α forms blue colonies on medium containing Isopropyl β-D-1-thiogalactopyranoside (IPTG) and X-gal, when it carries a plasmid that carries the lacZ-α fragment. DH5α was grown on either Luria-Bertani (LB) medium or Minimal Salts/glucose/thiamine medium (103).

The *Synechococcus* transformant strains that were available previously or generated in this study and their characteristic genotypes are shown in Table 2.

Table 2. *Synechococcus* sp. PCC 7002 mutant strains used in this study

Strains	Genotype and Charactersistics	Source
7002 Wild type	*Synechococcus* sp. PCC 7002, control strain	Pasteur Culture Collection
7002 (1108)-IspS-IDI	pAQ1::*IspS-IDI*-Sp^R/Sm^R A transformant strain carrying *IspS* and *IDI* transgenes targeted to plasmid pAQ1. The DNA construct confers streptomycin and spectinomycin resistance.	Matthew Nelson, UWO
7002 ΔGlgA1	*GlgA1*::Km^R Carries a kanamycin resistance gene cassette inserted into the glycogen synthase *glgA1* gene.	Brandon Thomas & Andrea Felton, UWO
7002 ΔGlgA2	*GlgA2*::Em^R Carries an erythromycin resistance gene cassette inserted into the glycogen synthase *glgA2*.	This study
7002 (1305) ΔGlgA1A2-IspS-IDI	*GlgA1*::Km^R, *GlgA2*::Em^R, pAQ1::*IspS-IDI*-Sp^R/Sm^R Transformant strain carrying inactivated *glgA1 and glgA2* genes, and *IspS-IDI* genes targeted to plasmid pAQ1. Carries resistance to Km, Em, and Sm/Sp.	This study
7002 ΔpetJ2	*petJ2::IspS-IDI*-Sp^R/Sm^R Transformant strain carrying *IspS-IDI* genes inserted into the chromosomal *petJ2* gene. Carries resistance to Sm/Sp.	This study
7002 (1401) 'Dual' IspS-IDI	*PetJ2::IspS-IDI*-Sp^R/Sm^R, pAQ1::*IspS-IDI*-Km^R Carries dual sets and multiple copies of the *IspS* and *IDI* genes. Carries *IspS-IDI* genes inserted into the chromosomal *petJ2* gene and the high-copy pAQ1 plasmid. Carries resistance to Sm/Sp and Km.	This study

Growth and Maintenance of Stock Cultures

Stock cultures of both WT and mutant strains of *Synechococcus* 7002 were grown and maintained in liquid A (D7) and A (D7) agar media (see Appendix) containing appropriate antibiotics concentrations. Fresh stock cultures were grown with shaking (100 - 150 rpm) on an orbital shaker positioned in a Percival incubator (Percival scientific, Iowa, USA) with controlled growth conditions (at 39^{o}C and light intensity of ~200 µmol photons m^{-2} s^{-1}). Longer-term stock cultures were maintained at room temperature with slow shaking on an orbital shaker under light intensity of ~ 80 µmol photons m^{-2} s^{-1} supplied by cool-white fluorescent lamps.

Stock cultures of WT and mutant strains were checked for contamination by streaking samples onto Luria-Bertani (LB) agar medium, followed by overnight incubation at 37^{o}C. Depending on the age and appearance of the stock culture, samples streaked onto LB were incubated at 24 – 26^{o}C (or room temperature) for up to a week or more to determine possible contamination. Subsequently, cultures that were free of contamination were used as inocula for growth experiments. To ensure that strains do not show unnecessarily long lag phases during growth experiments, a fresh, sterile A (D7) medium, e.g. 50 mL, containing appropriate antibiotics was inoculated with 300 – 500 µL of stock culture followed by incubation with shaking at 39^{o} C and light intensity of ~ 200 µmol photons m^{-2} s^{-1} in a Percival incubator until the culture reached an optical density [$O.D_{750nm}$] of 1.5 – 2.0. Depending on the growth experiment required, Roux flask bottles or septum-capped culture bottles were used to mimic continuous or closed-vessel growth

conditions (or systems), respectively. Cultures in Roux bottles were supplied with 3% (v/v) CO_2 in air, while cultures grown in capped bottles were saturated with 100% CO_2 to pH between 6.0 and 6.5 (usually pH ~6.5). Culture bottles were then maintained in aquaria at 39^{o}C with constant stirring using a magnetic stir bar and light intensity of ~ 200 or 2000 µmol photons m^{-2} s^{-1} for optimal or high-light conditions, respectively.

Optical Density (O.D) Measurements and Analysis of Growth

An Agilent 8453 UV-visible spectrophotometer was used for optical density (OD) measurements of cultures at 750 nm in 1.0 cm light-path cuvettes. Before cell density measurements are taken, double-distilled water (ddH_2O) was used as a blank. Then, 1.0 mL of culture was drawn from culture flask from which 100 µL is transferred into the cuvette for OD measurement. The OD values recorded are plotted as logarithmic values against time using Kaleidograph software.

Electrotransformation of DH5α Competent *E. coli* Cells

Electrocompetent cells were prepared as described in the Appendix. For transformation of recombinant DNA constructs prepared by 'Gibson Assembly' (described below), 2 µL of Gibson Assembly reaction product containing a desired recombinant plasmid construct (~20 ng of plasmid DNA) was added to 40 µL electrocompetent *E. coli* DH5α cells. The tube containing the mixture was flicked several times, followed by incubation on ice for 2 minutes. The cell suspension was transferred into a cold 0.2 cm gap electroporation cuvette and placed into a pre-chilled electroporation chamber in a BioRad Gene Pulser device set to 25 µF constant

capacitance and 200 Ω resistance, and pulsed once at 2 KV (~ 4.5 ms).Then, 0.5 mL SOC medium (see Appendix) was immediately added to the cuvette and the cell suspension transferred into a sterile 15 mL culture tube. An additional 0.5 mL SOC was used to rinse the cuvette. The cell suspension was incubated at 37°C with shaking (~150 rpm) for 1 hour. Then, 500 µL of the electro-transformant cell suspension was spread onto LB plates containing antibiotic (as determined by the antibiotic resistance gene cassette used for gene interruption) at appropriate concentrations to select for recombinant plasmids. Transformation plates were allowed to dry under sterile conditions and then incubated overnight at 37^{o}C.

DNA Manipulations and Cloning

Standard molecular genetics techniques were used according to Maniatis et al. (104) unless otherwise stated. *Synechococcus* genomic DNA used as the template for amplifying upstream and downstream regions of genes of interest was extracted from 0.6 mL wild type cells (typically OD_{750nm} 0.5 or greater) using a modification of the 'Chelex extraction method' developed by Berthold et al. (105) for DNA extraction from *Chlamydomonas*. Briefly, 0.6 mL of wild-type cells was concentrated by centrifugation at 14,000 x g and suspended in 40 µL cold ethanol (50% v/v), followed by addition of 0.2 mL Chelex-100 [Bio-Rad] suspension (5% w/v). The suspension was vortexed for 1 minute, heated in boiling water for 10 minutes, and then immediately cooled on ice. After cooling, the suspension was vortexed briefly and centrifuged for 7 minutes at 14,000 x g

to pellet cell debris and resin. The supernatant was transferred into a clean, sterile microcentrifuge tube and stored at -20^{o}C.

Quantification of DNA and RNA

An Agilent 8453 UV-visible spectrophotometer was used according to the manufacturer's recommendation. Samples were diluted (e.g by a factor of 20 or 30) into distilled water. DNA concentration were calculated relative to a net absorbance of 1.0 (A_{260nm}-A_{320nm}) = 50 µg/mL double-stranded DNA or 1.0 A_{260nm}-A_{320nm}) = 33 µg/mL single-stranded RNA.

Polymerase Chain Reaction (PCR)

Master mixes were prepared based on 1x PCR reactions. A typical 1x reaction contained: 0.5 µL HF Phusion DNA polymerase (2U/µL) [Thermo Fischer], 200 µM deoxynucleoside triphosphates (dNTPs), 0.2 µM of each primer, 1x Phusion DNA polymerase buffer, template DNA and nuclease-free water in a final volume of 50 µL. One (1.0) ng of plasmid DNA or 100 – 200 ng of genomic DNA was used as template DNA for PCR. Reactions, in an Eppendorf gradient thermalcycler, were typically run with the cycle profile: 98^{o}C for 2 minutes initial denaturation, followed by 30 cycles of 98^{o}C for 30 seconds, 30 seconds at optimal annealing temperature for primer pair (see Table 3), 72^{o}C extension (based on estimated DNA synthesis rate of 40 seconds per 1000 bp), and a final extension of 10 minutes at 72^{o}C.

Gel Electrophoresis

DNA samples were run in gels using Tris-Borate-EDTA buffer (see Appendix). Briefly, 5 µL of PCR or enzyme digestion products were mixed with 3 µL of 1x loading buffer and 2 µL of Syber green (1/1000 dilution) and loaded onto an 0.8% (w/v) agarose gel. 5 µL of 1 kb DNA ladder (NEB) was loaded as a standard. The gel apparatus was supplied with a constant voltage of 100 volts for 40 minutes. After electrophoresis, gels were scanned using either a Bio-Rad FX® scanner or Gel Doc imager®.

Construction of Recombinant Plasmids

To generate recombinant plasmids carrying desired inactivation constructs, component fragments were first amplified from genomic DNA or plasmid DNA templates by polymerase chain reaction (PCR). A DNA inactivation construct design is composed of an upstream gene fragment, an antibiotic resistant gene cassette and a downstream gene fragment, respectively. To facilitate replacement of wild type copies of gene(s) of interest by homologous recombination, flanking DNA fragments of ~ 500 – 800 bp in size with homology to the upstream and downstream regions of gene of interest were used to target the linear inactivation DNA constructs to the desired chromosomal or plasmid sites.

The recombinant plasmids constructed in this study used a pUC57 plasmid backbone fragment, amplified from plasmid pOSH1108 (see Figure 10). The pUC57 DNA fragment carries both an origin of replication and an ampicillin resistance gene cassette, Ap^R. The amplification of DNA fragments by PCR was achieved with primers

shown in Table 3. Lastly, an in-vitro, Gibson Assembly technique, was used to assemble the component DNA fragments into a recombinant circularized plasmid. The assembled DNA (recombinant plasmid) was either used directly for transformation or as a template for PCR.

Recombinant plasmids were generated by an in-vitro assembly technique known as Gibson Assembly developed by Daniel Gibson and colleagues in 2009**.** The Gibson Assembly reaction allows for assembly of multiple overlapping DNA (deoxyribonucleic acid) fragments in-vitro. The Gibson Assembly Master Mix contains 1) An exonuclease that chews back 5' ends to create 3' single-stranded overhangs that anneal to fragments that share complementary overlap regions, 2) A DNA polymerase that fills gaps within each annealed fragment, and 3) A DNA ligase that seals the nicks in the assembled DNA (106, 107).

The concentration of each DNA fragment used in the Gibson assembly reaction was calculated as recommended by NEB. Thus: concentration (pmol) = [weight (ng) x 1000] / [fragment size (bp) x 650 Daltons]. Each DNA component (at 0.1 - 0.2 pmol) was added to 10 µL Gibson assembly mix followed by addition of nuclease-free water for a final volume of 20 µL. The reaction mixture was incubated at 50^{o}C for 1-2 hours followed by inactivation at 98^{o}C for 2 minutes.

Table 3. PCR Primers used in this study.

Primers	Nucleotide sequence (5'-3' direction)	T_m used
GlgA1-a1	GACTGCATGCGCAATATCCAATGTCCGACC	63°C
GlgA1-a4	CTGAGAATTCCAAACCTGTGCTATCTTGCC	63°C
GlgA2-a1	GACTGCATGCGAATAATGCCGTCCTGTTGCG	63°C
GlgA2-a2	CTCTTGCGGGATATCGTCCATCAGACTAAGCT CGCGACTG	63°C
GlgA2_a3	GTGAATCGATAAGCTTGCATGCTATACACCGT GTACCCAGAGG	63°C
GlgA2_a4	GACTGGATCCTGCGTAGGGCAACTTCTCCG	63°C
pRL409-Em^R-F2	GATGGACGATATCCCGCAAGAG	63°C
pRL409-Em^R-R	GCATGCAAGCTTATCGATTCAC	63°C
GlgA2-F-pUC57-R	GACGGCATTATTCGCATGCAGTCTGGCGTAAT CATGGTCATAGC	63°C
GlgA2-R-pUC57-F	GTTGCCCTACGCAGGATCCAGTCGTGCACTCT CAGTACAATCTG	63°C
PetJ2-a1	CGACCAGGTCATTCGCCAG	62°C
1108-IspS-IDI-F_PetJ2-a2	CGAATTCGCCTCCTGAATAAAT-CCCTGGTCGAGATCAGCAC	62°C
1108-IspS-IDI-R_PetJ2-a3	CTAACAATTCGCTCGACGTCGAC-GGCAATATGTCCGCCTACG	62°C
PetJ2-a4	CGATTGGCTACGCAACTATC	62°C
PetJ2-a4-pUC57-R	GATAGTTGCGTAGCCAATCG-TGGCGTAATCATGGTCATAGC	62°C
PetJ2-a1-pUC57-F	CTGGCGAATGACCTGGTC-GTGCACTCTCAGTACAATCTG	62°C
1108-IspS-IDI-F	ATTTATTCAGGAGGCGAATTCG	62°C
1108-IspS-IDI-R	GTCGACGTCGAGCGAATTGTTAG	62°C
pAQ1- F	CTCTCACCAAAGATTCACCTG	68°C
pAQ1-flank AR	GCATGCGGGGTTTTCTCGTGTTTAGGC	68°C
pAQ1-R	CATGAGTGGGGGAAAACGAACC	68°C

The melting temperatures, T_m, represent the temperatures at which the primer pairs anneal to the template binding regions. The T_m indicates annealing temperature for each primer pair as determined by gradient PCR. The nucleotide sequences underlined represent the restriction site(s) introduced into the primer sequences by design. The nucleotide sequences in red represent primer overhangs to allow annealing of overlapping complementary regions of component DNA fragments in Gibson Assembly reactions.

Construction of the *Synechococcus* 7002-IspS-IDI Strain

The 7002-IspS-IDI strain was constructed using the wild type *Synechococcus* 7002 strain as host. This strain was constructed by a genetic engineering strategy that targeted the optimized *IspS* and *IDI* genes to a high-copy plasmid pAQ1 (see Figure 8). A DNA construct, 5014 bp in size flanked by pAQ1 upstream and downstream regions and carrying a spectinomycin-streptomycin linked antibiotic resistant gene cassette was generated by PCR from plasmid pOSH1108 (see Figure 10) using the pAQ1-F/pAQ1-flank R primer pair (see Table 3). The purified DNA construct generated from PCR was used to transform wild type *Synechococcus* 7002 with targeting to the high copy plasmid pAQ1. This strain was generously provided by Matthew Nelson, UW-Oshkosh.

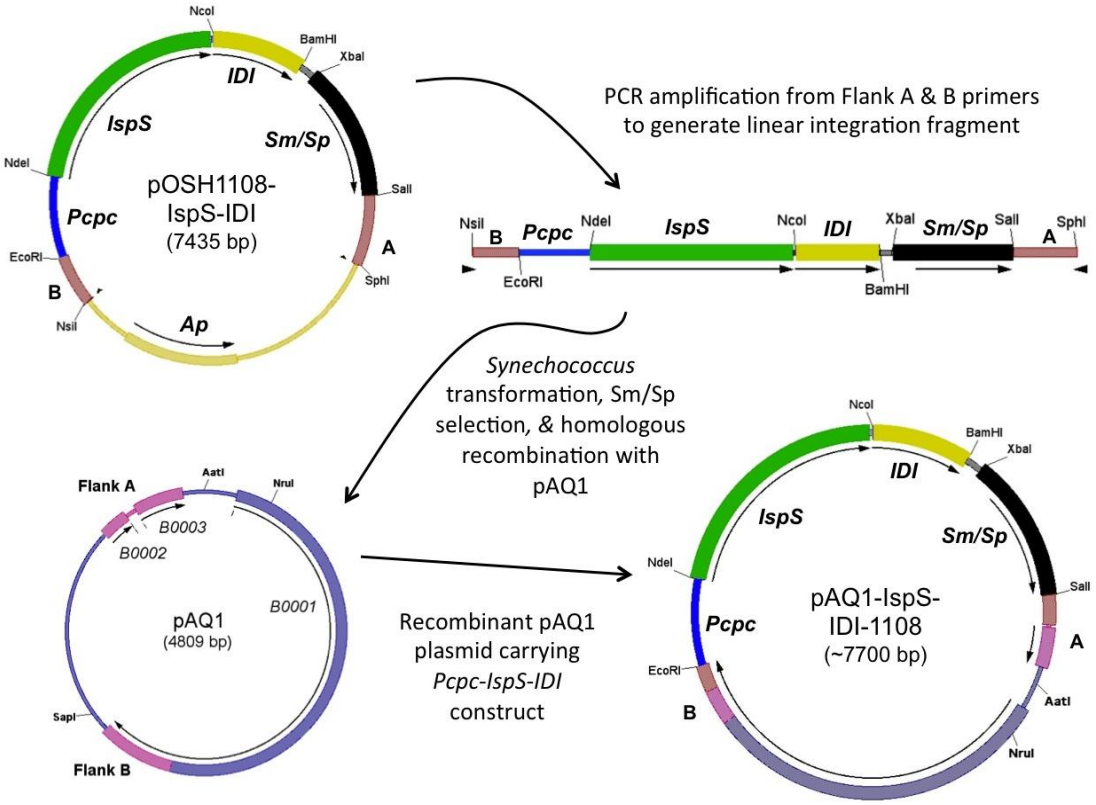

Figure 8. Genetic engineering strategy for targeting codon-optimized *IspS* and *IDI* transgenes to plasmid pAQ1. First, the DNA construct carrying the codon-optimized transgenes is amplified from the pOSH1108 parent plasmid and the generated amplicon is targeted to the high copy pAQ1 plasmid, in *Synechococcus* 7002 and transformant cells. Originally adapted from Xu and Bryant, 2011 (Credit: Matthew Nelson, UW-Oshkosh).

Restriction Enzyme Digestion

To ensure that there was no carry-over of parent plasmid DNA into Gibson assembly reactions, plasmid templates were linearized using restriction enzymes that cut only at unique restriction sites. 400ng of plasmid pRL409 (Figure 9) was linearized using *Nde*I restriction enzyme [NEB], 2 μL of 10x NEB 4 buffer and sterile double–distilled water (ddH_2O) for a 20 μL final reaction volume. Also, 500ng plasmid pOSH1108 (Figure 10) was linearized using *Nco*I enzyme [NEB], 2 μL of 10x NEB 3 buffer and ddH_2O for a final volume of 20 μL. The digestion reactions were incubated at 37^{o}C for 2 hours, followed by heat inactivation at 65^{o}C for 5 minutes. Successful digestion reaction was confirmed by agarose gel electrophoresis.

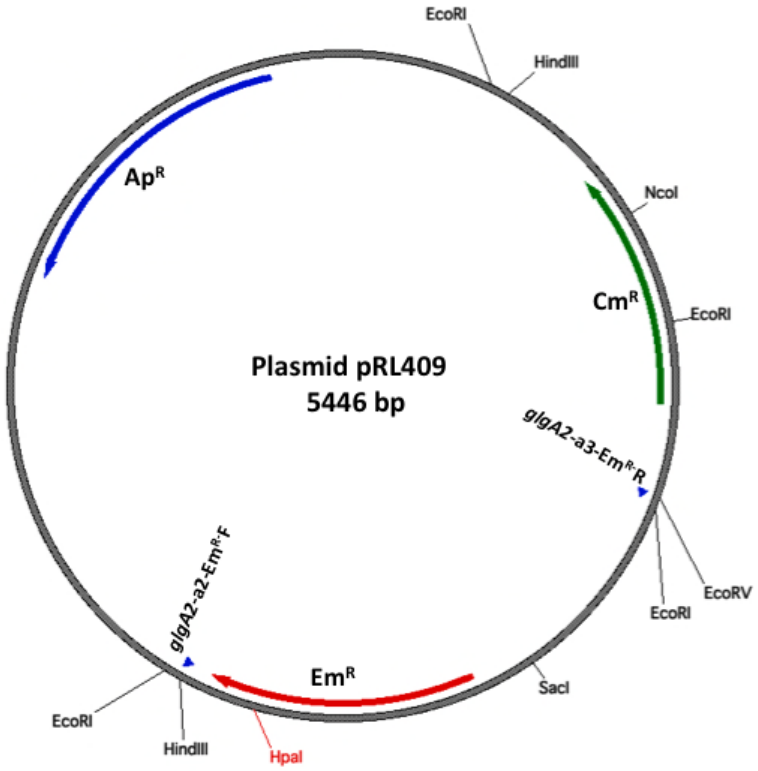

Figure 9: Plasmid pRL409. The red arrow shows the region on the plasmid DNA encoding the erythromycin resistance gene cassette, Em^R. The primer pair pRL409-Em^R-F2 and pRL409-Em^R-R amplifies the DNA fragment carrying the Em^R gene cassette. The Em^R gene cassette was used to generate a recombinant plasmid carrying the *glgA2*-Em^R inactivation construct using in-vitro Gibson Assembly technique.

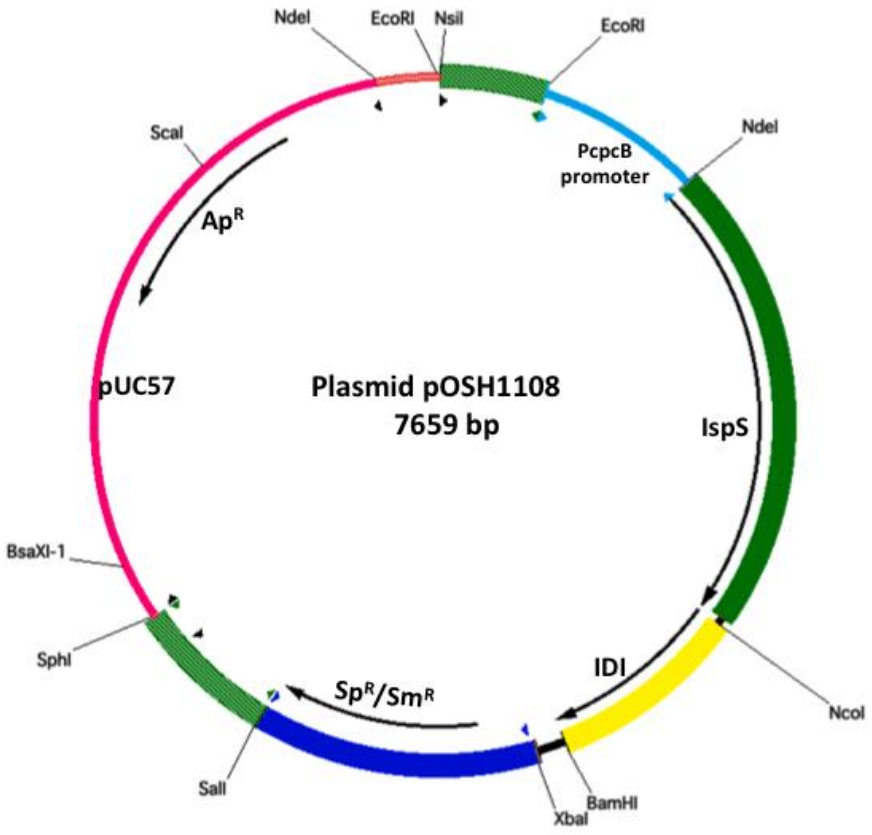

Figure 10: Plasmid pOSH1108. The region shown in red represents the plasmid pUC57 DNA fragment. The pUC57 DNA region which carries the sequence encoding the origin of replication also carries an ampicillin resistance gene cassette, Ap^R. These features made the pUC57 DNA fragment a suitable plasmid backbone for generation of recombinant plasmids in this research. The region between the EcoRI and SaII restriction sites represents the sequence encoding the DNA construct carrying the *PcpcB* promoter (from *Synechocystis sp*. 6803), the *IspS* and *IDI* transgenes from poplar plant and a streptomycin-spectinomycin, Sp^R/Sm^R linked, resistance gene cassette. This DNA construct enables isoprene production in genetically transformed *Synechococcus* 7002 strains. (Constructed by Matthew Nelson, UW Oshkosh.)

Glycogen Assay

Cells were harvested as described by Xu et al. (89), to obtain cells equivalent to OD_{750nm} x culture volume (mL) = 2.5 (i.e., for a culture at 1.0 OD_{750nm}, 2.5 mL cells were harvested). Harvested cell culture was transferred into a sterile tube and centrifuged at 10,000 x g for 10 minutes. The tube was inverted to allow the pellet to dry. The pellet was suspended in 500 uL diluent (10mM Tris-HCl pH 7.5, 10mM NaCl) for the 10x BugBuster™ (Novagen) protein extraction reagent. The resuspended cell pellet in 500 µL of 1x BugBuster™ reagent was mixed by vortexing gently. Before the next step, lysozyme and DNase I, were added to 2.5 mg/mL and 30 µg/mL final concentrations, respectively, and incubated at 37°C for 10 – 30 minutes but 2 hours was used to ensure complete reaction. After incubation, samples were centrifuged at 14,000 x g for 20 minutes at 4°C. The supernatant was transferred to a clean screw-cap microcentrifuge tube and stored at -20° C.

A portion (150 µL) of the saved 'Bugbuster' supernatant from above was transferred to a clean screw-cap microcentrifuge tube for glycogen assay. Prior to transferring from the BugBuster extract, tubes were centrifuged for 6 minutes at 4°C for 14,000 x g. For the glucose assay, a fresh 5 mg/mL amyloglucosidase (70 U/mg from *A. niger*) solution was prepared in 100 mM sodium acetate (pH = 5.1). The 150 µL supernatant sample was added to 300 µL of 100 mM sodium Acetate (pH= 5.1), and 50 µL of 5mg/mL amyloglucosidase stock solution. The reaction mixture was incubated

overnight at 50^{o}C in roller tubes in the Robins Scientific 310 hybridization incubator to allow mixing.

After overnight incubation, the reaction mixture was centrifuged for 6 minutes at 4^{o}C for 14,000 x g. Thereafter, 100 µL of the supernatant was transferred to a new tube for glucose determination. Glucose released from overnight samples (containing extracted glycogen) was determined as described in the Sigma Glucose Assay Kit (Sigma Aldrich) protocol. To determine the amounts of glucose released from glycogen samples extracted from *Synechococcus* 7002 strains, glucose standards were prepared for standard curves as shown in Table 4.

Table 4. Glucose standard preparation and concentrations

Tube	**Volume of diluent (µL water)**	**Volume of glucose standard added (µL stock solution, 1mg/mL)**	**Final Concentration (µg/mL)**
Standard 1 (Blank)	100µL Bugbuster Reagent (1X)	NIL, No glucose standard added	0
Standard 2	98	2	20
Standard 3	96	4	40
Standard 4	94	6	60
Standard 5	92	8	80
Standard 6	90	10	100

In addition to the glucose standards (Table 4), an assay reagent was prepared by adding 0.8 mL o-dianisidine reagent to 39.2 mL of glucose-oxidase/peroxidase reagent and protected from light. The assay reagent (200 µL) was added at time t = 0 to the standard 1 tube and mixed well. An interval of 30 to 60 seconds was allowed between additions to subsequent standards, 2 to 6, (as shown in Table 4 above). Each tube was

incubated at 37^{o}C for exactly 30 minutes and the reaction was stopped by addition of 200 µL 12N sulphuric acid. The overnight samples were also treated with assay reagent and the reactions quenched with sulpuric acid as described above. Reaction products (300 µL) were transferred to a clean micro titer dish and absorbance at 540 nm was read against the reagent blank (see Table 4 above) in a Spectra Max plus 384 (Molecular Devices) microtiter plate spectrophotometer. A standard curve of absorbance (A_{540nm}) as a function of glucose concentration was prepared using the SoftMax pro software. The concentration of glycogen (as units of glucose) in each sample was determined relative to the standard curve.

RNA Isolation and Purity Check

A hot-phenol RNA-isolation procedure was used as described by Mohamed and Jansson (108) with some modifications. First, crude RNA was isolated from cultures grown to a desired $O.D_{750nm}$ by harvesting 2 x 40 mL of cultures and injecting rapidly into two (2) 50 mL Oakridge tubes containing 5 mL cold 10x metabolic stop solution (50% equilibrated phenol, 48% 0.5M sodium ethylenediaminetetraacetic acid (Na_2EDTA) pH 8.0 and 2% β-mercaptoethanol by volume). After vigorous shaking to mix the contents of the tubes, samples were centrifuged at 4^{o}C for 15 minutes at 10,000 rpm, using SR-30 GSA rotor in a Sorvall RC5C centrifuge. After centrifuging, the supernatant was discarded and the tube blotted on clean Kimwipes to remove remaining supernatant. The pellets were resuspended in 1 mL resuspension buffer (300 mM sucrose, 10 mM sodium acetate pH 4.5 in DEPC (diethylpyrocarbonate) treated water) and centrifuged at 10,000 x

g for 1 minute at 4^{o}C. The supernatant was discarded and pellets resuspended in 1 mL suspension buffer and the process repeated. The pellets were drained of residual buffer solution before storage at -80^{o}C.

Afterwards, these pellets were thawed on ice, followed by addition of 38 µL of 0.5 M Na_2EDTA pH 8.0, 320 µL of cell resuspension buffer, 340 µL of 111 mM sodium acetate pH 4.5 and 38 µL of 20% Sodium dodecyl sulfate (SDS), respectively. The suspended cells were vortexed after addition of 20% SDS, and incubated at 65^{o}C for 10 minutes. During incubation, tubes were mixed by inversion at 2 minutes intervals. After incubation, 700 µL of hot acidic phenol (incubated at 65^{o}C) was added and the resultant mixture was incubated for 5 minutes. During incubation at 65^{o}C tubes were mixed twice. Following incubation, the cell mixtures were immediately cooled at -80^{o}C for 45 - 60 seconds. After cooling, the suspension was centrifuged at room temperature for 10 minutes at 14,000 x g. The aqueous phase was carefully transferred to a clean sterile screw-cap microcentrifuge tube, followed by further addition of 100 - 200 µL extraction solution (38 µL 0.5 M Na_2EDTA, 320 µL cell suspension buffer, and 340 µL sodium acetate, pH 4.5) to increase the volume of the aqueous phase for easier recovery. The aqueous phase was treated twice with an equal volume of 25:24:1 phenol/chloroform/isoamyl alchohol, with thorough mixing after each treatment, followed by centrifugation at 14,000 x g for 1 minute.

The aqueous phase was recovered and treated twice with an equal volume of 24:1 chloroform/isoamyl alcohol, with each step followed by thorough mixing and

centrifugation at 14,000 x g for 1 minute at room temperature. The recovered aqueous phase was then transferred into a clean microcentrifuge tube. One-fourth (1/4) volume of 10 M lithium chloride was added to the recovered aqueous phase followed by addition of 2.5 volumes of absolute (100%) ethanol. The resulting mixture was incubated at -20^{o}C for 60 - 75 minutes to allow for RNA precipitation, followed by centrifugation at 14,000 x g for 20 minutes at 4^{o}C. The crude RNA precipitate or pellets (contaminated by DNA) was carefully washed with 70% ethanol to prevent loss of the pellets and this process was repeated twice. After washing, pellets were allowed to dry in the laminar flow hood before resuspension in DEPC-treated 10T/0.1E buffer, pH 8.2 (containing 10 mM Tris-HCl and 0.1 mM disodium EDTA).

The Second step required the removal of DNA contamination from the crude RNA. The isolated RNA was treated with Ambion DNAse supplied in Turbo DNA-free kit according to the manufacturer's recommendation. Ten (10.0) μg of crude RNA was added to 5 μL 10x Turbo DNase buffer, 1 μL Turbo DNase enzyme (2 U/μL) and DEPC treated water for a final volume of 50 μL. This was followed by incubation at 37^{o}C for 45 minutes and addition of 5 μL Turbo DNase inactivation reagent after incubation. Samples were centrifuged at 10,000 rpm for 2 minutes at room temperature and supernatants carefully transferred into sterile microcentrifuge tubes and stored at -80^{o}C. This step was repeated, if treated RNA still contained DNA contamination. This is to ensure complete removal of DNA from the RNA samples. In that case, 1 μL of Turbo DNase enzyme (2U/μL) and a Turbo second DNase digest buffer was added to one-tenth of the volume of sample from the first treatment. The samples were incubated at 37^{o}C for 60 minutes

after which Turbo DNase inactivation buffer was added to 1/10th the sample volume. This was followed by incubation at room temperature for 2 minutes after which samples were centrifuged for 2 minutes at 10,000 rpm. The recovered supernatant from each sample was transferred to a clean tube.

Third, RNA purity was checked by PCR and RT-PCR analysis. PCR and RT-PCR reactions were set up to determine the purity of isolated RNA using Access RT-PCR reagents (Promega). For PCR, 1 µL of RNA sample was added to 10 µL of 5x AMV (Avian Myeloblastosis virus) reverse transcriptase, 5x Tfl (Thermus flavus) DNA polymerase buffer, 5 µL of 10 mM dNTPs, 2.5 uL each of 20 µM forward and reverse primers, 2 µL of 25 mM Magnesium sulphate (MgSO4), 1 µL Tfl polymerase (5U/µL) and nuclease-free water for a final reaction volume of 50 µL. For RT-PCR reactions, the reagents included those used for PCR and 1 µL AMV reverse transcriptase (5U/µL) in addition. A positive control reaction contained 2.5 attomoles RNA supplied by Promega and other components for RT-PCR (as explained above). The thermalcyler (Eppendorf mastercycler gradient^{TM}) profile used was an initial reverse transcription cycle of 45^{o}C for 45 minutes, followed by 94^{o}C for 2 minutes for AMV reverse transcriptase inactivation. The second step of 40 cycles each with initial denaturation of 94^{o}C for 30 seconds, annealing at 60^{o}C for 1 minute and extension at 68^{o}C for 2 minutes. The products of the PCR, RT-PCR and RT-PCR control reactions were analyzed using agarose gel electrophoresis. The primer-pair TL-F, 5'ACGATCACCGTTTCCTTC 3' and TK-2, 5'AGCCATCGCCACCGGACGAC 3,' amplified a 800 bp fragment of the

PetBD operon of *Synechococcus* 7002, and was used for positive control for RNA quality by RT-PCR and detection of DNA contamination by PCR.

Complementary DNA (cDNA) Synthesis for Reverse Transcriptase Quantitative PCR (RT-qPCR)

After carrying out RT-PCR and PCR purity check described above, the status of DNA-free RNA was confirmed and cDNA synthesis proceeded. Following pure RNA quantification, 500 ng of DNA-free RNA was added to 25mM magnesium chloride, 5x AMV reverse transcriptase buffer, 10 mM dNTP, 1 μL of RNAsin plus (40U/μL), AMV reverse transcriptase (5U/μL), 1 μL random hexamers (0.3 μg/μL) and nuclease free water as described in the Access RT-PCR protocol (Promega). The mixture was placed in an Eppendorf mastercycler thermalcycler and incubated at 42^{o}C for 60 minutes, followed by AMV RT inactivation and RNA-cDNA primer denaturation at 94^{o}C for 2 minutes. After the completion of the reaction, the cDNA products were maintained on ice while the concentration of the cDNA was determined using the Agilent spectrophotometer.

Primers and Probes for RT-qPCR

Primers and 'Taqman' probes originally designed by Matthew Nelson and Toivo Kallas were provided for use. The design was based on the following parameters; For primers: annealing temperature, T_m = 57 - 61^{o}C with difference in primer pair T_m not exceeding 2^{o}C, a GC content of 45-60% with presence of G or C nucleotide at the 3' position of the primers and length of primer about 15 - 22 bp. For probes; T_m = 67 - 70^{o}C, a maximum T_m difference of 5-6^{o}C between primer and probe, GC content of 45 - 60%,

and length of probe should be 23 - 27 bp. For probes, guanine should be avoided at the 5' end. The primers and probe (shown in Table 5) were designed for *Synechococcus* 7002 codon-optimized, poplar *IspS* transgene nucleotide sequence. The probe was designed to carry a fluorescent 5-carboxyfluorescein dye (5-FAM) at the 5' end and a Black-hole quencher (BHQ-1) dye at the 3' end.

Table 5. Probe and primers designed for RT-qPCR

Gene	Type	Sequence
IspS (codon-optimized)	Syn 7002-IspS-CO Taq Probe	TTCGCCGTGCATTAGATCGGT TTGTG
	Syn 7002-IspS-CO-F primer	GTTTGGGTTACCGGTTTGAG
	Syn 7002-IspS-CO-R primer	TCTTGGTCACCGCATCAAAG

Primer-Probe Validation and Efficiency Determination

Normalization of results obtained from the described primer-probe set requires the validation of such primers and probes for qPCR or RT-qPCR experiments. Reaction volumes were scaled down to 20 µL and plasmid template DNA or crude RNA was serially diluted 10 fold over 5 $\log_{10}$ values (e.g., from 10 ng/µL to 0.1 pg/µL). Thus, for the primer-probe set, five reaction tubes and a no-template negative control were set up. The reaction master mix was set up thus: 10 µL of 2x Bull's Eye Taqman PCR master mix, 1 µL of both forward and reverse primer (final concentration 1 µM), 0.25µL of corresponding probe (final concentration=200 nM), and nuclease free or DEPC-treated water for a final volume of 20µL. Reactions were run in an Applied Biosystems (ABI Step One^{TM}) real-time PCR machine using a cycle profile of 95^{o}C for 10 minutes for

DNA polymerase activation, followed by denaturation of double-stranded DNA at 95^{o}C for 15 seconds, and primer annealing and extension at 60^{o}C for 1 minute, repeated for 40 cycles. The validation reactions were set up using the 'Quantitation standard curve' program with threshold cycle values automatically set to 0.05 by the software. The cycle to threshold (C_T) values obtained for each dilution points for the primer-probe set were plotted as a function of the $\log_{10}$ concentration of the starting template. The efficiency of the primer-probe set was determined from the slope of the line on this graph. Percent Efficiency = (E – 1) x 100 % where Amplification Efficiency, E =$10^{-1/slope}$. A PCR efficiency of 92% or greater was considered acceptable for direct comparisons.

RT-qPCR Gene Expression Studies

The reaction components and cycling profile for these experiments were similar to those described above for primer-probe efficiency tests. However, the method of analysis used was comparative C_T (or ΔC_T). The means of cycle to threshold (C_T) values of three technical replicates for each sample (or biological replicate) was used as the cycle to threshold value for each biological replicate. RNA templates were extracted from strains grown to either low optical densities (OD_{750nm}) of 0.5 – 1.0 or high OD_{750nm} of 4.0 - 8.0. The threshold values were manually adjusted to 0.05 for all samples. Complementary DNA (cDNA) pools generated from DNA-free RNAs extracted from 'Dual IspS-IDI', 7002-IspS-IDI and ΔPetJ2 strains were used as templates for the RT-qPCR gene expression studies. As an internal control, each of the technical triplicates was separately spiked with 67.2 pg/μL of a plasmid pOSH1108 DNA (which carries the

codon-optimized *IspS* gene sequence) corresponding to ~ 8 x 10^6 million copies of the plasmid. The plasmid copy number was calculated as recommended by ABI: weight in Daltons (g/mole) = (size of plasmid) (660 Da/bp). Then, copy number (g/molecule) = Weight of plasmid ÷ Avogadro's number.

The gene expression levels were determined by normalizing to the *IspS* transcript level in the strain that showed the highest cycle to threshold, C_T, values. These C_T values were obtained from the mean C_T values of three biological replicates in the three transformant strains grown to low- and high- cell densities. By this approach the ΔC_T (gene-expression) values obtained can be expressed as relative transcript levels ($\log_2$ scale) as a function of cell density (optical density) in the harvested cultures.

Isoprene Toxicity Test

Sealed, 250 mL septum-capped Boston round bottles were set up to mimic a closed photobioreactor system. Cultures grown in sealed bottles were saturated with 100% CO_2 to a pH of 6.0 to 6.5 (usually pH of 6.5) prior to incubation. Culture bottles were inoculated with wild type *Synechococcus* 7002 to 0.1 OD_{750nm} and maintained in an aquarium at 39^{o}C with constant stirring from a magnetic stirrer and light intensity of ~200 µmol photons $m^{-2}s^{-1}$. Dilutions of liquid isoprene (MW 68.12 g/mol, Sigma Aldrich), prepared in 100% ethanol, were added to the cultures in the sealed bottles. Each dilution series was prepared by adding liquid isoprene and ethanol for a final volume of 200 µL. A control culture had no liquid isoprene added. A clean syringe was used to draw

1.0 mL culture samples at intervals, from each culture bottle for optical density measurements at 750 nm and growth rate determinations.

Isoprene Production Assays

For isoprene production assays, *Synechococcus* cells were inoculated to a starting OD_{750nm} of 0.5 and grown overnight in 200 mL volumes of A (D7) medium in a 250 mL sealed Boston round bottle at 37^{o}C with constant stirring at 200 μmol photons $m^{-2}s^{-1}$ light intensity. The culture was saturated with 100% (v/v) CO_2 to a pH of 6.5 prior to incubation. To eliminate carry-over of isoprene traces from previous assays, bottles were thoroughly rinsed with ethanol (95% v/v), and then dried. Isoprene accumulated in the culture head-space was analyzed by a Gas Chromatography - Mass Spectrometry (GC-MS). Head-space gas was drawn through the septum-cap of the sealed culture bottle with a 100 μL Hamilton gas tight syringe and immediately injected into the GC. To determine the relative quantity of isoprene in sample gases, a calibration curve showing isoprene peak height from chromatogram as a function of isoprene amount (ppm) injected in the GC was constructed. To plot the calibration curve, a serial dilution of vaporized pure liquid isoprene standard (Sigma Aldrich, USA) of known concentration (ng/μL) was prepared. For the high end dilution, 2.5 μL of liquid isoprene standard was added to a tightly sealed septum-capped bottle and allowed to completely evaporate into gaseous phase by placing in an oven at 37^{o}C for ~ 20 minutes. Following the preparation of several dilutions, 100 μL samples drawn from each dilution was injected and analyzed by the GC.

Isoprene analysis was performed using a Focus GC linked to a DSQ-II Mass Spectrometer (Thermo Scientific) with a Restek PLOT (Porous Layer Open Tubular) Rt-U-BOND column (Restek Inc., Bellefonte, PA) with Xcalibur software. The GC oven temperature was maintained at 150^{o}C and held for 5.5 minutes. The ion source temperature was 200°C and samples injected into GC with split ratio of 1:10. Single Ion Monitoring (SIM) method was used to identify isoprene from samples using a low mass exclusion of 41 and qualifier ions set to 53, 67, and 68 *m/z*. The peak retention time for isoprene was 5.5 minutes. Isoprene was identified by comparing the retention times of sampled gas with that of a standard sample and its full scan mass spectrum.

Fast Isoprene Sensor (FIS) for Real-Time Isoprene Measurements

The Fast Isoprene sensor (FIS) [Hills Scientific Boulder, Colorado USA], is a sensitive detecting system and can measure isoprene from less than 1 ppb to ppm isoprene. The FIS works on the basis that isoprene reacts with ozone to produce violet light of 435 nm. The violet light produced is detected and counted by a photon detector for quantitative, real-time detection of isoprene using the LabView software provided by manufacturer. According to manufacturer's recommendation, oxygen and the ozonizer were switched on for at least 1 hour (and preferably overnight) before calibrations to allow FIS warm up and signal to fully stabilize. Sample gas was run until a continuous steady state was achieved to eliminate the possibility of sampling pre-existing isoprene in the culture head space. Before each calibration, the standard gas supply was purged for 10 seconds to remove degraded isoprene held in the tubing and connections (109). For

sample analysis, the FIS pump actively draws headspace gas into the reaction cell at a user-defined and electronically controlled flow rate. Oxygen was supplied at a pressure and flow rate recommended by manufacturer to ensure that there was sufficient ozone to react with the sample isoprene.

The culture volume in sealed photobioreactors was kept at two-thirds or less of the vessel volume to allow sufficient headspace for gas sampling while concurrently preventing bubbling-induced water droplets from entering the sampling outlet and reaching the reaction cell of the FIS. The correspondence between isoprene concentration and FIS signal output (photon counts) is linear over several thousand fold, and a 4 or 5 point calibration provides an excellent reference. The calibration response thus yields both the zero count of background noise for y-intercept and calibration conversion factor represented by the slope of the graph. Isoprene concentrations in the calibration standard and samples were determined as follows:

Isoprene (ppb, gas phase) = (photon counts - base line count) ÷ calibration factor where base-line count = signal count at zero isoprene.

Isoprene (in FIS reaction cell) = (Isoprene standard gas)(isoprene standard gas flow) ÷ gas flow (in reaction cell) where reaction cell flow is a mixture of ozone flow, and flow of either sample-isoprene from a culture head-space or isoprene standard gas. Isoprene in the standard gas was 19.6 ppm isoprene in N_2 gas. Figure 11 illustrates the FIS configuration.

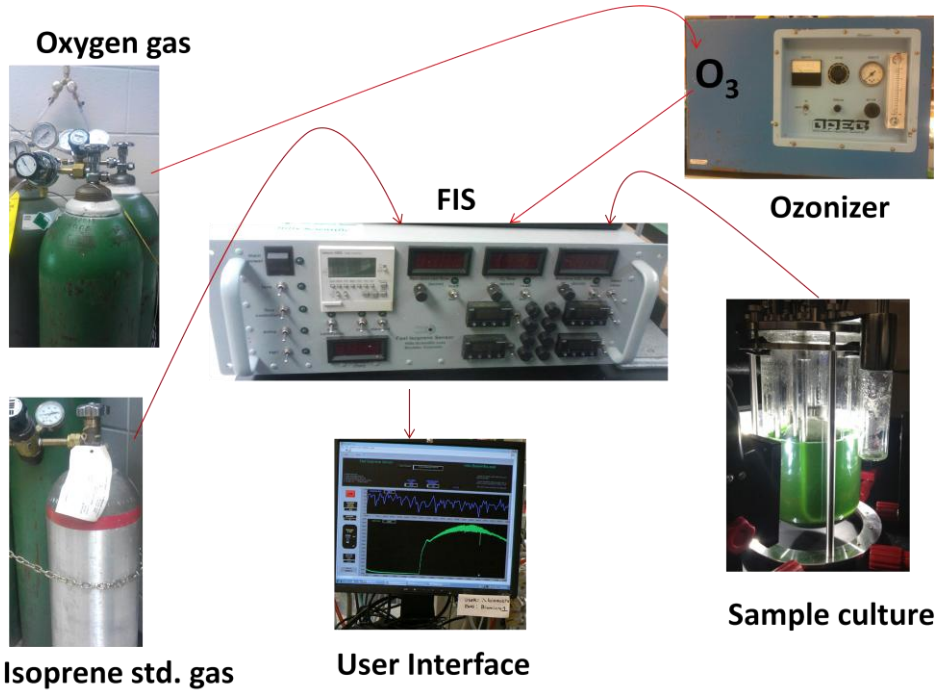

Figure 11. Schematic of the Fast Isoprene Sensor (FIS) for measurement of isoprene from culture head-spaces. Silicone tubing and connectors were used to connect all of the components: oxygen gas, ozone gas from the ozonizer, isoprene standard gas, and head-space gas from the culture vessel to the FIS. Arrows show the directions of the gas flows. Oxygen gas is first converted to ozone (O_3) by an ozonizer and then channeled into the FIS. Ambient air, sample gas, and ozone are mixed via a connector before being channeled into the FIS. The photon signals generated in the reaction cell, amplified by a photomultiplier, and displayed in LabView software.

RESULTS

Inactivation of a Competing Glycogen Pathway

Construction of the pUC57-glgA2-Em^R Recombinant Plasmid.

Following the Gibson Assembly reaction method, primers were designed to produce a recombinant plasmid carrying a DNA inactivation construct containing an erythromycin resistance gene cassette flanked by upstream and downstream regions of the *glgA2* gene. As illustrated in Figure 12, the GlgA2-a1/GlgA2-a2 primer pair amplifies 686 bp upstream while GlgA2-a3/GlgA2-a4 primer pair amplifies 715 bp downstream of the wild-type *glgA2* gene.

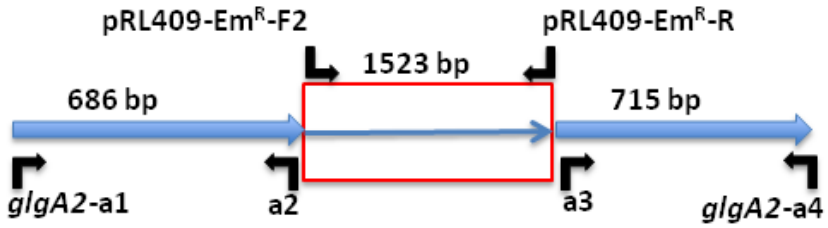

Figure 12. GlgA2-Em^R DNA construct for glycogen synthase *glgA2* gene inactivation. Arrows show the primer pairs for generating the upstream and downstream *glgA2* fragments and the Em^R resistance gene cassette. The primers GlgA2-a1 and GlgA2-a2 amplify the *glgA2* upstream fragment; the GlgA2-a4 and GlgA2-a3 generate the downstream fragment while the pRL409-Em^R-F2 and pRL409-Em^R-R amplify the erythromycin-resistance gene cassette, Em^R.

A 1523 bp erythromycin resistance gene cassette (Em^R) was amplified from the plasmid pRL409 (5.4 kb) using pRL409-Em^R-F2/pRL409-Em^R-R primers. The pUC57 plasmid backbone fragment (2436 bp) carrying an ampicillin gene cassette (Ap^R) was

amplified from the plasmid pOSH1108 (7.6 kb) with the GlgA2-F-pUC57-R and GlgA2-R-pUC57-F primer pair.

Following the Gibson assembly reaction, a 5.3 kb recombinant plasmid product carrying the *glgA2*-Em^R inactivation DNA construct was expected. Two (2) μL of the Gibson assembly product was used to transform DH5α *E. coli* cells by electrotransformation. The transformation mixture was spread on LB plates containing ampicillin (150 μg/mL final concentration). After overnight incubation, colonies were randomly selected and transferred into Luria Bertani (LB) liquid medium containing ampicillin followed by incubation at 37^{o}C for ~ 16 hours.

Following overnight incubation, plasmids were extracted from transformant cell cultures using the Wizard® Plus purification system (Promega) according to manufacturer's recommendation. Isolated plasmid DNA was quantified using the Agilent 8453 UV-visible spectrophotometer, followed by PCR analysis to determine whether the isolated recombinant plasmid carried the expected *glgA2*-Em^R inactivation construct.

Wild type *Synechococcus* 7002 cells grown to 0.4 OD_{750nm} were transformed using ~2 μg of the *glgA2*-Em^R inactivation construct amplified from the product of the Gibson assembly reaction. The transformation suspension was spread onto A (D7) agar medium containing erythromycin (20 μg/mL) and incubated at 37^{o}C under moderate illumination of ~200 μmol photons $m^{-2}s^{-1}$. After a week, a few putative ΔGlgA2 mutant colonies observed on the plates were transferred into liquid A (D7) medium containing erythromycin (20 μg/mL) and incubated with moderate shaking. Genomic DNA extracted

from the 7002 ΔGlgA2 mutants was analyzed by PCR to determine if the isolated mutants carried inactivated copies of the *glgA2* gene.

The gel image shown in Figure 13 indicates that the primers designed to amplify the upstream and downstream fragments of the wild type *glgA2* produced the expected sizes of 686 bp and 715 bp amplicons, respectively.

Figure 13. Gibson Assembly reaction DNA fragments for pUC57-*glgA2*-Em^R recombinant plasmid construction. Lanes 1 and 2 show PCR amplifications of upstream and downstream flanking regions of *glgA2* respectively. Lane 3, NEB 1 kb ladder; Lane 4, pUC57 fragment and Lane 5, Em^R fragment.

The second step involved the linearization of the plasmid pRL409 and subsequent amplification of the Em^R gene cassette from plasmid pRL409. As expected, a 1.5 kb Em^R fragment was amplified from the linearized plasmid pRL409. Also shown in Figure 13, is the pUC57 fragment (2.4 kb), carrying an Ap^R gene cassette amplified from the plasmid pOSH1108. The pUC57 fragment carrying an origin of replication served as the plasmid

backbone for the construction of the recombinant plasmid, pUC57-*glgA2*-Em^R carrying the *glgA2*-Em^R construct.

The expected Gibson reaction product shown in Figure 14 (a pUC57-*glgA2*-Em^R recombinant plasmid carrying the *glgA2*-Em^R DNA inactivation construct) was used to transform DH5α *E. coli* cells. Plasmid DNA extracted from the isolated *E. coli* DH5α transformant clones were characterized by PCR to determine whether the recombinant plasmid carried the expected *glgA2*-Em^R inactivation construct.

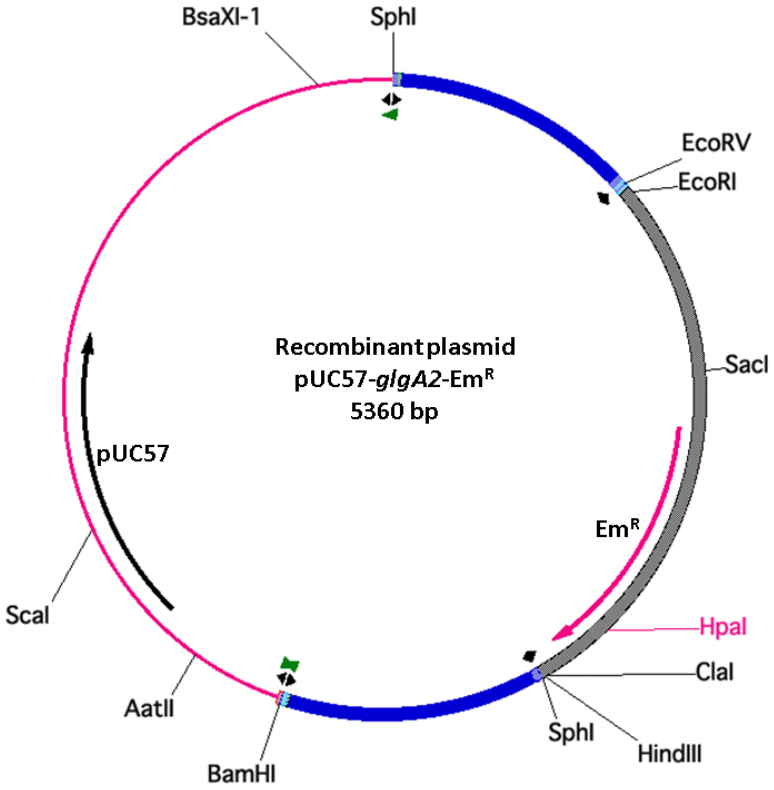

Figure 14. Recombinant plasmid pUC57-*glgA2*-Em^R carrying the *glgA2*-Em^R inactivation DNA construct. The region between the BamHI and SphI restriction sites contains the DNA fragment that carries the *glgA2*-Em^R inactivation construct. A unique HpaI restriction site (shown in red-colored font) is located in the region of the open reading frame (ORF) coding for the erythromycin gene cassette, Em^R.

To characterize the recombinant plasmid pUC57-*glgA2*-Em^R, the Em^R and pUC57 DNA fragments were amplified. As expected, the amplified products produced band sizes of 1.5 and 2.4 kb on an agarose gel. In addition, the size of the *glgA2*-Em^R inactivation DNA construct generated from the recombinant plasmid with the GlgA2-a1/GlgA2-a4 primer pair (which also amplifies the native *glgA2* gene) corresponded with the expected fragment size of 2.9 kb. These results, as shown in Figure 15, indicate that the recombinant plasmid, pUC57-*glgA2*-Em^R carried the inactivation construct, *glgA2*-Em^R (2.9 kb), and that the Gibson Assembly reaction was successful.

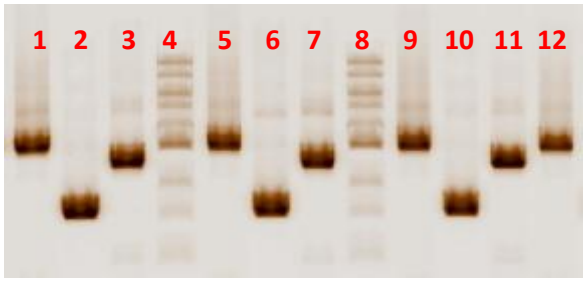

Figure 15. PCR tests to characterize the recombinant pUC57-*glgA2*-Em^R plasmid. Lanes 1, 5, 9 and 12 show the inactivation constructs amplified from GlgA2-a1 and GlgA2-a4 primers; lanes 2, 6 and 10 show Em^R gene fragments amplified from pRL409-Em^R-F2 and pRL409-Em^R-R primers; lanes 3, 7 and 11 show pUC57 fragments amplified from GlgA2-R-pUC57-F and GlgA2-F-pUC57-R primers. Lanes 4 and 8 show size standards (1 kb NEB ladder).

To determine whether putative *Synechococcus* 7002 ΔGlgA2 mutants carried inactivated copies of the *glgA2* gene, genomic DNAs were extracted from these mutants and characterized by PCR. As shown in Figure 16, the GlgA2-a1/GlgA2-a4 primer pair generated a 2.9 kb amplicon from the mutants, while a 2.6 kb fragment was produced from wild type *Synechococcus* 7002 DNA. However, since the PCR products generated

from genomic DNA templates of wild type and 7002 ΔGlgA2 mutants differed by only ~300 bp, it was difficult to discern the difference in sizes of the native *glgA2* and introduced *glgA2*-Em^R copies on agarose gel.

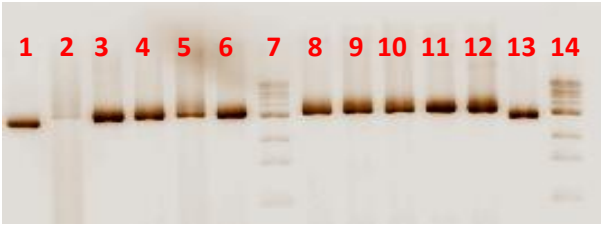

Figure 16. PCR analysis to determine replacement of the native *glgA2* with the inactivated *glgA2*-Em^R gene construct in *Synechococcus* 7002 ΔGlgA2 mutants.
Lanes 2-6 and 8-12 from 7002 ΔGlgA2 mutants; lanes 1 and 13 from wildtype controls. Lanes 7 and 14 show 1 kb NEB ladders.

To further distinguish between the native *glgA2* and introduced *glgA2*-Em^R copy, both PCR products were digested with *Hpa*I restriction endonuclease [NEB]. Since the Em^R gene inserted into the inactivated *glgA2* copy in the 7002 ΔGlgA2 mutants carries a unique *Hpa*I site (see Figure 14), which is not present in the wild type *glgA2* sequence, restriction digestion with *Hpa*I endonuclease should confirm whether the PCR amplicons generated from the 7002 ΔGlgA2 mutants were inactivated alleles of wild type *glgA2* gene**.** The result of the restriction digest analysis, as shown in (Figure 17), indicated that the ΔGlgA2 PCR products digested with *Hpa*I resulted into two bands (1995 bp and 932 bp) as expected, because of the presence of a *Hpa*I restriction site. However, the wild type *glgA2* DNA was not cleaved by this enzyme because it did not carry a *Hpa*I

sequence. These results confirmed that the ΔGlgA2 DNA carried the erythromycin-resistance gene containing the *Hpa*I sequence and thus 7002 ΔGlgA2 mutants carried the inactivated copy of the *glgA2* gene. These results confirmed the replacement of the wild type *glgA2* gene with the interrupted *glgA2*-Em^R allele in the ΔGlgA2 mutants.

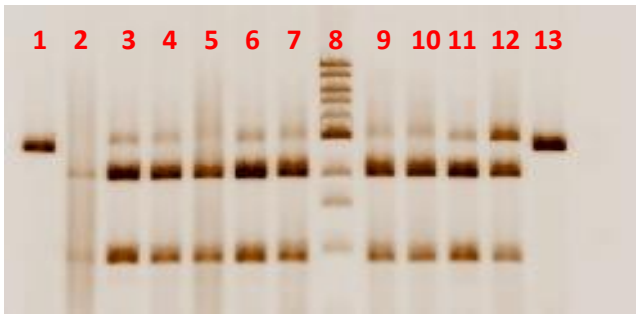

Figure 17. Restriction analysis of *Synechococcus* 7002 ΔGlgA2 mutants. Lanes 1-7 and 9-12 show *Hpa*I digests of PCR product from ΔGlgA2 mutant clones. Lanes 1 and 13 show *glgA2* DNA fragments digested using *Hpa*I enzyme from wild-type controls. Lane 8 shows size standards (1kb NEB ladder). The PCR products were amplified from the a1 and a4 primers that flank the *glgA2* gene.

Construction of the Double Glycogen Synthase Null Mutant (7002 ΔGlgA1A2).

After the successful construction of a recombinant pUC57-*glgA2*-Em^R plasmid carrying the *glgA2*-Em^R inactivation construct, PCR was used to amplify the *glgA2*-Em^R inactivation DNA construct using the GlgA2-a1/GlgA2-a4 primer pair. The product of the PCR was purified using Wizard® PCR clean-up reagents (Promega) according to manufacturer's instructions. The 7002 ΔGlgA1 mutant (constructed by Brandon Thomas and Andrea Felton, UW-Oshkosh) was transformed using ~2 μg of purified *glgA2*-Em^R.

The *Synechococcus* 7002 ΔGlgA1 mutant carries inactivated copies of the glycogen synthase, *glgA1* isogene. The *glgA1* gene sequence was interrupted with a kanamycin resistant gene cassette. After transformation of the *Synechococcus* 7002 ΔGlgA1 mutant, the cells were spread onto A (D7) plates containing both erythromycin and kanamycin at 20 μg/mL and 50 μg/mL final concentrations, respectively.

After two weeks of incubation at 37^{o}C under moderate illumination of ~ 200 μmol photons $m^{-2}s^{-1}$, mutant colonies observed were randomly selected and transferred into fresh liquid medium in 15 mL sterile snap cap tubes. Erythromycin and kanamycin antibiotic solutions were added to ensure selection and growth of only mutants carrying inactivated copies of both *glgA1* and *glgA2* isogenes. Genomic DNA extracted from cells in tubes that showed growth, was used as template for PCR analysis to determine whether the native copies of *glgA1* and *glgA2* had been replaced by the inactivation constructs. The PCR analysis was carried out using two separate pairs of primers GlgA1-a1/GlgA1-a4 and GlgA2-a1/GlgA2-a4 which amplify *glgA1*-Km^R and *glgA2*-Em^R DNA inactivation fragments, respectively.

As expected, the GlgA2-a1/GlgA2-a4 primers generated a 2.9 kb amplicon from mutant DNA whereas a 2.6 kb fragment was produced from wild-type DNA (as control), indicating that the native *glgA2* gene had been replaced by the inactivated *glgA2*-Em^R allele. Further, the GlgA1-a1/GlgA1-a4 primer pair generated a 2.3 kb product from mutant DNA templates relative to a 1.8 kb amplicon from wild type genomic DNA. The results of these PCR analyses (Figure 18) showed that the mutant clones still maintained inactivated copies of *glgA1*. Moreover, these data confirm integration of the inactivated

glgA2-Em^R gene and demonstrate the successful replacement, by homologous recombination, of both the wild type *glgA1* and *glgA2* alleles with the inactivated copies.

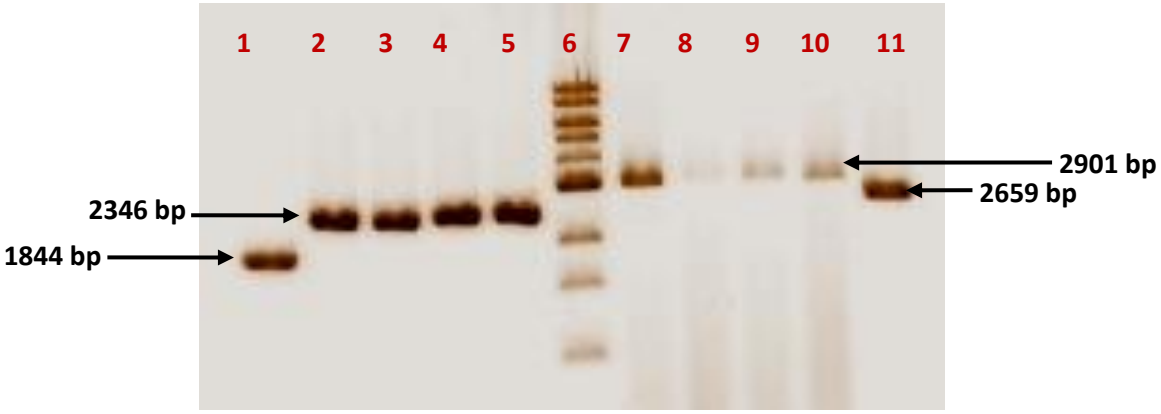

Figure 18. PCR analysis to characterize *Synechococcus* 7002 ΔGlgA1A2 (glycogen synthase null) mutants. Lane 1: Wild type, control *Synechococcus* 7002 genomic DNA amplified from GlgA1-a1/GlgA1-a4 primers. Lanes 2-5: Genomic DNA from ΔGlgA1A2 transformants amplified from GlgA1-a1/GlgA1-a4 primers. Lane 6: NEB 1 Kb ladder, Lanes 7-10: Genomic DNA from the same ΔGlgA1A2 transformant clones (as in lanes 2-5) amplified from GlgA2-a1/GlgA2-a4 primers. Lane 11: Wild type, control *Synechococcus* 7002 genomic DNA amplified from GlgA2-a1/GlgA2-a4 primers.

Impact of glgA1 and glgA2 'Knockouts' on Glycogen Synthesis.

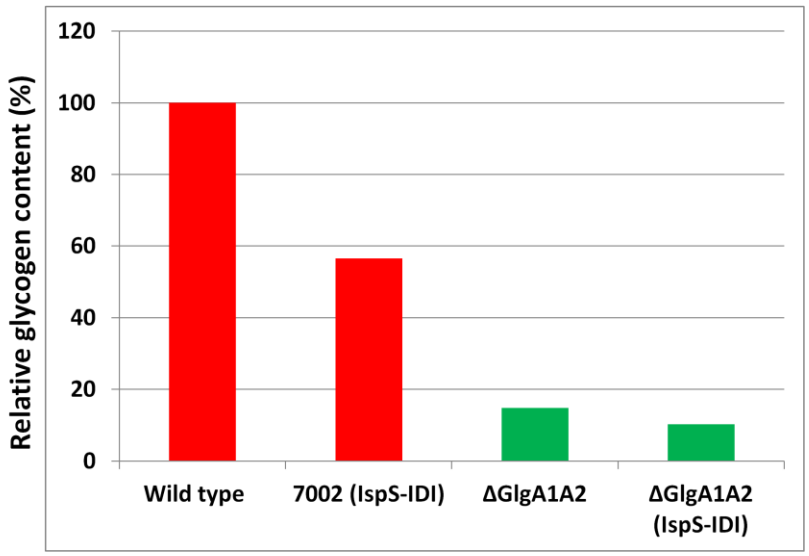

Figure 19. Glycogen content of *Synechococcus* wild type and mutants. The glycogen contents in strains defective in glycogen biosynthesis was compared to wild type *Synechococcus* 7002 and an isoprene-producing strain with functional glycogen synthesis. The relative amounts of glycogen detected were normalized to the glycogen content determined for wild type *Synechococcus* 7002.

A hypothesis for this study was that modifications of carbon partitioning that will enhance carbon flux into the MEP pathway will improve isoprene yield. Therefore, inactivation of the *glgA1* and *glgA2* genes coding for glycogen synthase enzymes was expected to cause an increase in isoprene production in genetically engineered isoprene-producing strains. To evaluate the impact of inactivation of glycogen biosynthesis on isoprene yield, a glycogen assay was used to determine the impact of the *glgA1* and *glgA2* inactivations in 7002 ΔGlgA1A2 mutants. The glycogen contents in three different

strains; 7002 ΔGlgA1A2-IspS-IDI, 7002 ΔGlgA1A2, and 7002-IspS-IDI were compared to glycogen extracted from a wild type *Synechococcus* sp. PCC 7002 control. The results of the glycogen assay (Figure 19) indicated that the ΔGlgA1A2-IspS-IDI and ΔGlgA1A2 mutants produced ~10% and ~15%, respectively, of the glycogen in the wild type. The ΔGlgA1A2-IspS-IDI and ΔGlgA1A2 strains carry inactivated copies of both the *glgA1* and *glgA2* genes. These data show that the inactivation of both *glgA1* and *glgA2* in *Synechococcus* sp. PCC 7002 resulted in greatly reduced glycogen biosynthesis.

Interestingly, the glycogen determined in 7002-IspS-IDI was less than 60% of that detected in the wild type, while the glycogen content in 7002 ΔGlgA1A2-IspS-IDI was also lower than in 7002 ΔGlgA1A2. This observed reduction in glycogen in strains carrying the *IspS* and *IDI* transgenes compared to non-isoprene producing strains (wild type and 7002 ΔGlgA1A2) may indicate increased carbon partitioning into the MEP pathway in strains that actively produce isoprene. This suggests that expression or over-expression of the IspS and IDI enzymes causes carbon previously directed into glycogen biosynthesis to be channeled into the MEP pathway for isoprene production. Thus, it appears that isoprene production also serves as a carbon-sink to ameliorate excess reductant and carbon accumulation in genetically engineered isoprene-producing *Synechococcus* 7002 strains.

Impact of glgA 'Knockouts' on Growth under Continuous Culture Condition.

To determine the impact of glycogen synthase *glgA1* and *glgA2* 'knockouts' on photoautotrophic growth, mutant strains were cultivated under low- and high-light conditions. The mutants tested were 7002 ΔGlgA1, 7002 ΔGlgA2, and 7002 ΔGlgA1A2 carrying inactivated copies of *glgA1*, *glgA2* and both *glgA1* and *glgA2*, respectively. Since high light intensity is a known stress factor, the mutants were first exposed to optimal light (~ 200 μmol photons $m^{-2}s^{-1}$) before shifting to high light intensity (~ 2000 μmol photons $m^{-2}s^{-1}$ or full sunlight intensity). The results of the growth experiment as represented in Figure 20 show estimated doubling time, t_D, of 4 hours for both wild type and 7002 ΔGlgA1 mutant, under both optimal- and high-light intensities (~ 200 and ~ 2000 μmol photons $m^{-2}s^{-1}$ respectively). However, the7002 ΔGlgA2 and 7002 ΔGlgA1A2 showed an estimated t_D of ~ 5 hours under optimal light. In addition, as shown in Figure 20, the exposure of 7002 ΔGlgA2 and 7002 ΔGlgA1A2 mutants to high light intensities, increased their doubling times. The t_D calculated for 7002 ΔGlgA2 under high light intensity was ~ 5 hours, while the t_D estimated for 7002 ΔGlgA1A2 mutant after shifting to high light, increased to ~8 hours.

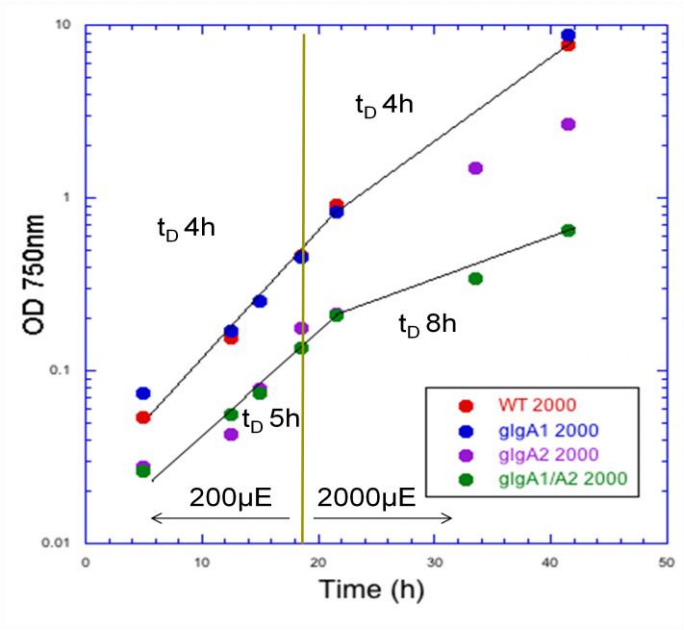

Figure 20. Growth rates of *Synechococcus* glycogen synthase mutants. Cells were grown at 37°C with continuous 3% CO_2 in air (v/v). Cell densities were measured as optical density (OD) at 750nm. The growth rate of 7002 ΔGlgA1, 7002 ΔGlgA2, and 7002 ΔGlgA1A2 mutants were compared to wild type at both moderate and high light intensity of ~200 µmol m^{-2} s^{-1} and ~ 2000 µmol m^{-2} s^{-1}, respectively.

The growth data represented in Figure 20 showed that the inactivation of glycogen synthase genes in all three mutants; 7002 ΔGlgA1, 7002 ΔGlgA2 and 7002 ΔGlgA1A2 had no adverse effect on photoautotrophic growth under optimal photosynthetic condition. However, the growth of the 7002 ΔGlgA1A2 mutant was slower compared to the wild type, 7002 ΔGlgA1 and 7002 ΔGlgA2-strains under high light stress condition. These observations indicate that glycogen synthesis and glycogen are not essential for photoautotrophic growth of *Synechococcus* sp. PCC 7002 under

optimal photosynthetic conditions, but may provide an advantage for cells growing at high light intensity.

Impact of glgA 'Knockouts' on Growth under Closed Culture Condition.

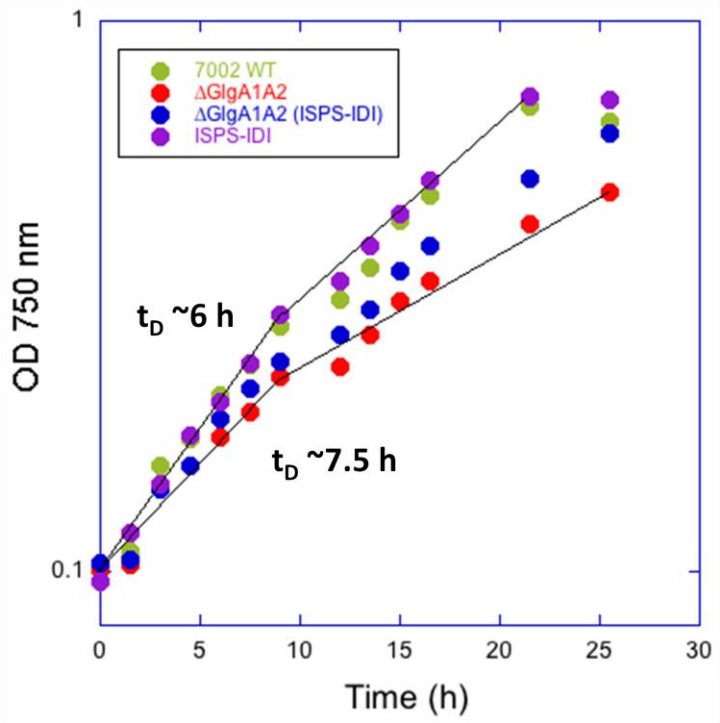

Figure 21. Impact of glycogen synthase mutations on growth of isoprene-producing glycogen mutant strains in sealed bottles. Cells were saturated with 100% CO_2 to pH = 6.5 prior to incubation at ~ 200 µmol photons $m^{-2} s^{-1}$ at 38ºC.

Since a closed photobioreactor system will be necessary for capturing the volatile isoprene produced in genetically engineered mutants expressing *IspS* and *IDI*, it was important to evaluate growth of such strains under closed culture conditions. To determine the impact of inactivating the glycogen biosynthesis pathway on growth, the

7002 ΔGlgA1A2, 7002 ΔGlgA1A2-IspS-IDI, and 7002-IspS-IDI strains were grown in sealed bottles. The growth of 7002 ΔGlgA1A2, 7002 ΔGlgA1A2-IspS-IDI, and 7002-IspS-IDI strains was compared to wild-type *Synechococcus* 7002 (as control) under optimal photosynthetic conditions (38^{o}C, ~ 200 μmol photons m^{-2} s^{-1} light intensity). The calculated doubling time, t_D, for both control and 7002-IspS-IDI was ~ 6 hours compared to ~7.5 hours calculated for both 7002 ΔGlgA1A2-IspS-IDI and 7002 ΔGlgA1A2 mutant strains carrying inactivated copies of both *glgA1* and *glgA2*. The result of the growth experiments (as shown in Figure 21) suggested that inactivations of the glycogen synthase, *glgA1* and *glgA2* genes did not affect the growth of strains carrying such defective glycogen background under optimal photoautotrophic conditions in closed culture vessels .

Impact of Glycogen Inactivation on Isoprene Yield

Construction of 7002 ΔGlgA1A2-IspS-IDI Transformant.

The 7002 ΔGlgA1A2 mutant strain carrying inactivated copies of the glycogen synthase *glgA1* and *glgA2* genes was constructed by transformation with a purified DNA construct carrying isoprene synthase, *IspS* and *IDI* isomerase transgenes and a linked streptomycin-spectinomycin antibiotic resistance gene cassette. The DNA construct (4817 bp, Figure 7) is flanked by upstream and downstream pAQ1 fragments homologous to target regions on the high-copy plasmid pAQ1 in *Synechococcus* 7002, and was amplified from a plasmid pOSH1108 template using the pAQ1-F/pAQ1-R

primer pair. The DNA construct generated by PCR was purified and then used to transform the 7002 ΔGlgA1A2 mutant host. The transformation mixture was spread onto A (D7) agar containing spectinomycin and streptomycin (each at 50 μg/mL final concentration). Colonies observed on plates were randomly selected and transferred into 15 mL sterile snap cap tubes containing liquid A (D7) medium with spectinomycin and streptomycin. Genomic DNA extracted from transformant cells in tubes that showed culture growth was used as templates for PCR.

Isolated transformant clones were characterized by PCR to determine integration of *IspS* and *IDI* into target plasmid pAQ1. The results of the PCR analysis (Figure 22, panel A) showed that *IspS* and *IDI* genes were successfully targeted to copies of the high-copy plasmid pAQ1 in the 7002 ΔGlgA1A2 mutant strain. The result of the PCR analysis presented in panel A suggested that not all copies of this plasmid were successfully targeted since plasmid pAQ1 is a high copy number plasmid. Gel images shown in panel B and panel C, confirmed the 7002 ΔGlgA1A2 mutant strain still maintained inactivated copies of *glgA2* and *glgA1*.

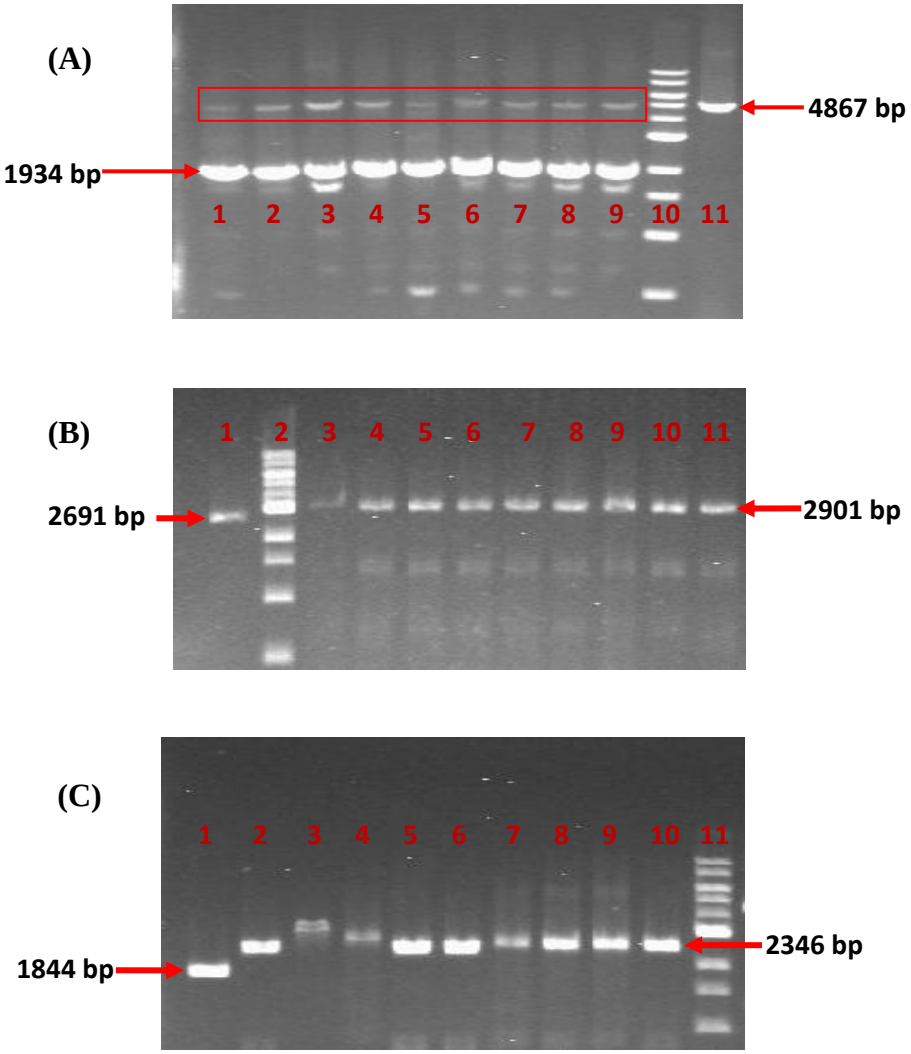

Figure 22: PCR analysis to characterize 7002 ΔGlgA1A2-IspS-IDI transformants.
PCR analysis to confirm integration of *IspS* and *IDI* into plasmid pAQ1 and the replacement of native glycogen synthases, *glgA* genes with inactivated copies. **Panel A.** Lane 1-9: Genomic DNA from transformant clones amplified with pAQ1-F/pAQ1-R primers. Lane 10: NEB 1 kb ladder Lane. 11: plasmid pOSH1108 DNA (as control) amplified with pAQ1-F/pAQ1-R primers. The bands marked by the red box represent the integration of the DNA construct to a targeted neutral site on the high copy pAQ1 plasmid, while the intense bands represent the target region on the native plasmid pAQ1. **Panel B.** Lane 1: Wild type *Synechococcus* 7002 genomic DNA (as control) amplified with GlgA2-a1/GlgA2-a4 primers. Lane 2: NEB 1 kb ladder. Lane 3-11: Genomic DNA from transformant clones amplified with GlgA2-a1/GlgA2-a4 primers. **Panel C.** Lane 1: Wild type *Synechococcus* 7002 genomic DNA (as control) amplified with GlgA1-a1/GlgA1-a4 primers. Lane 2- 10: Genomic DNA from transformant clones amplified with GlgA1-a1/GlgA1-a4 primers. Lane 11: NEB 1 kb ladder.

Isoprene Production in 7002 ΔGlgA1A2-IspS-IDI Transformant.

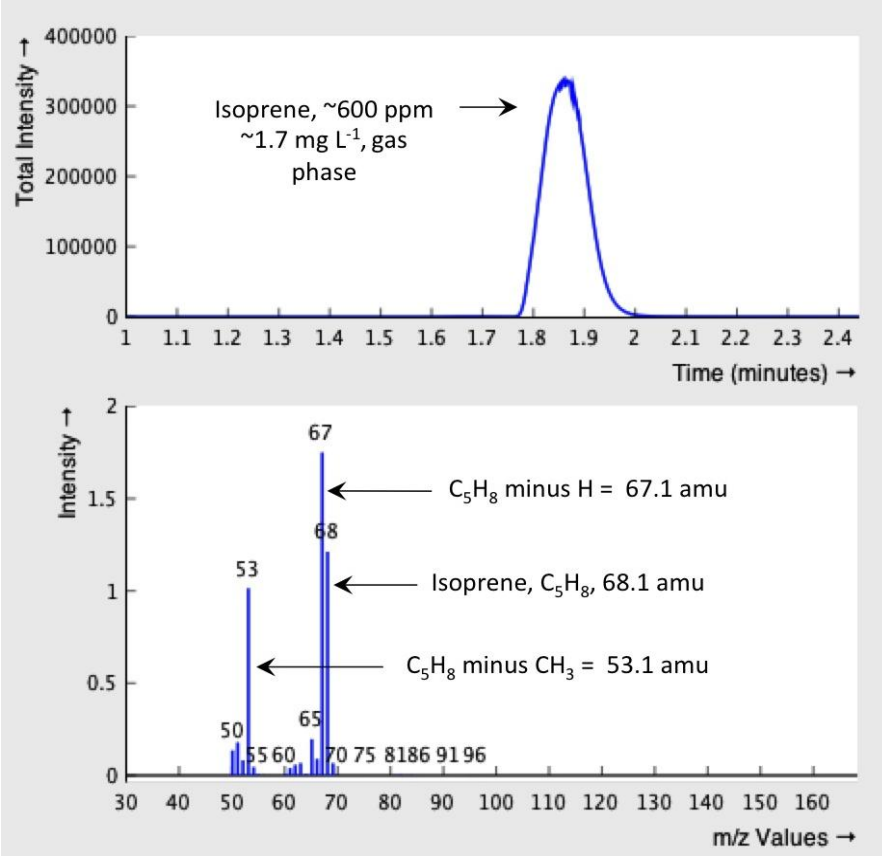

Figure 23. Representative Gas Chromatography-Mass Spectrometry (GC-MS) chromatogram of isoprene production in an isoprene-producing *Synechococcus* PCC 7002 strain (1108, pAQ1::*Isps-IDI*). A) GC-MS chromatogram showing isoprene accumulated in the culture head-space. Isoprene concentration in the culture head-space was ~1.7 mg L^{-1} indicating a production rate of ~330 µg isoprene gDW^{-1} h^{-1}. **B)** Fragment ion spectra from GC peaks a and b shows that both contained isoprene (58.1 atomic mass units [amu]) and characteristic degradation products. (Credit: Mathew Nelson, UW-Oshkosh)

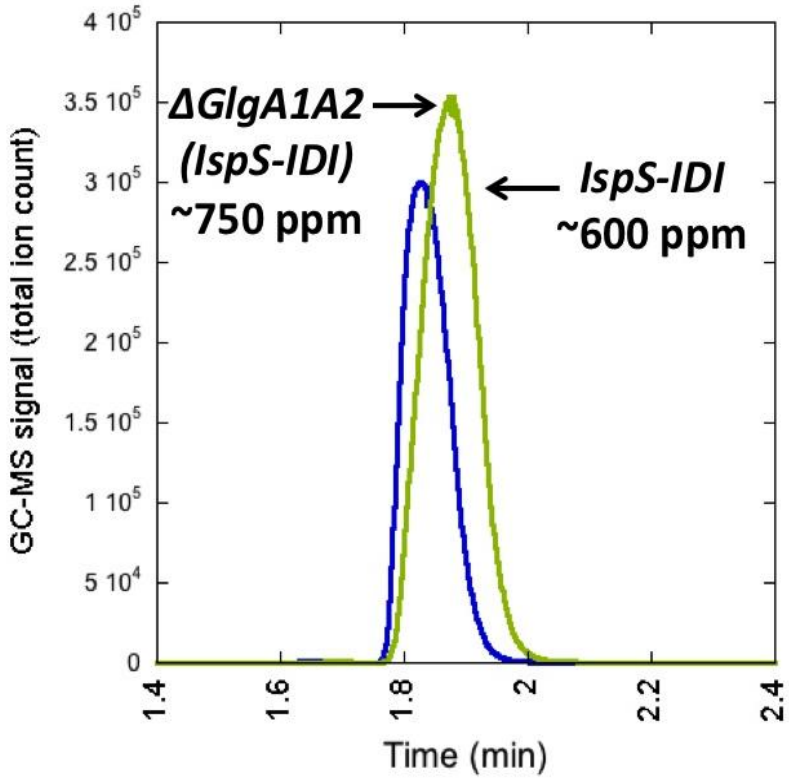

Figure 24. (GC-MS) chromatogram of isoprene produced by a *Synechococcus* 7002 ΔGlgA1A2 'knockout' strain. The green peak represents the isoprene total ion count as measured from 7002-IspS-IDI strain while the blue peak represents isoprene ion count from 7002 ΔGlgA1A2-IspS-IDI strain. The 7002-IspS-IDI strain has the codon-optimized *IspS* and *IDI* transgenes targeted only to the pAQ1 plasmid while 7002 ΔGlgA1A2-IspS-IDI has the *IspS* and *IDI* transgenes targeted to pAQ1, in addition to carrying inactivated copies of the *glgA1* and *glgA2* glycogen synthases gene.

As previously mentioned, I hypothesized that the inactivation of the competing glycogen biosynthesis pathway will result in the channeling of carbon previously used for glycogen into the MEP pathway for increased isoprene production. To determine the impact of inactivation of glycogen synthase *glgA1* and *glgA2* genes on isoprene production, the 7002 ΔGlgA1A2-IspS-IDI and 7002-IspS-IDI strains were cultured under closed culture conditions. The closed culture system is needed for accumulating and harvesting a specific quantity of isoprene per unit time in the head-space of photobioreactor. The result of the GC-MS analysis to determine isoprene accumulated in the head-space of sealed culture-bottles is shown in Figure 24. The results show a total ion count of 3.5×10^5 corresponding to ~ 750 ppm (parts per million) isoprene produced by the 7002 ΔGlgA1A2-IspS-IDI strain compared to the 3×10^5 ion counts corresponding to ~ 600 ppm isoprene produced by the 7002-IspS-IDI strain. Both strains carry the *IspS* and *IDI* transgenes targeted to a high-copy plasmid pAQ1 only. These results indicate that the 7002 ΔGlgA1A2-IspS-IDI strain produced ~ 20% more isoprene compared to the 7002-IspS-IDI strain. This result showed that the inactivation of the glycogen synthase genes, *glgA1* and *glgA2* in *Synechococcus sp*. PCC 7002 resulted in an increase in isoprene production, although the ~ 20% increase observed was significantly lower than anticipated. Therefore, the result suggests that carbon used previously for glycogen biosynthesis was rather channeled into a carbon biosynthesis pathway other than the MEP pathway.

Isoprene Toxicity Test.

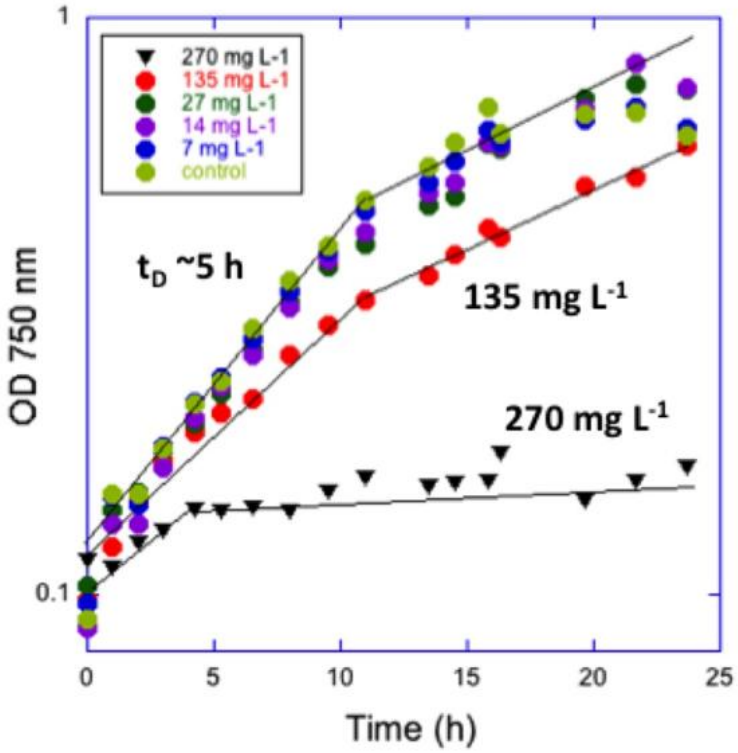

Figure 25. Impact of isoprene on growth of *Synechococcus* sp. PCC 7002. Wild-type *Synechococcus* cells were grown in sealed bottles and saturated with 100% CO_2, to pH = 6.5, prior to incubation at 38°C and ~ 200 µmol photons $m^{-2}s^{-1}$. Liquid isoprene was added to the cultures in the sealed bottles prior to incubation. Optical Density measurements at 750 nm were taken at different intervals within 24 hours. The condition for this growth experiment mimics a closed culture system where isoprene is expected to accumulate in the culture head-space.

The inactivation of the *glgA* genes in 7002 ΔGlgA1A2-IspS-IDI strain resulted in only ~ 20% increase in isoprene production compared to a 7002-IspS-IDI control strain capable of glycogen synthesis. A possible explanation for the lack of a larger impact from the *glgA* genes knockout in 7002 ΔGlgA1A2-IspS-IDI is that further increases in

isoprene production may result in toxicity to the cells. To determine the impact of isoprene on photoautotrophic growth, wild type *Synechococcus sp.* PCC 7002 cells were grown in sealed culture bottles. Cultures of *Synechococcus* were spiked with different dilutions (concentrations) of liquid isoprene. The results of the growth experiments (Figure 25) showed a calculated doubling time, t_D, of 5 hours for cells spiked with isoprene concentrations corresponding to 7 mg/L, 14 mg/L, and 27 mg/L, similar to that of the control culture (i.e. without liquid isoprene addition). Although the doubling time of cells spiked with 135 mg/L isoprene, was higher than t_D of ~5 hours calculated for the control culture, no substantial growth inhibition was observed. However, cells spiked with 270 mg/L isoprene showed an almost complete inhibition of growth after ~ 6 hours of incubation. These data show that isoprene; is not toxic to *Synechococus* 7002 cyanobacteria, but can inhibit photoautotrophic growth at high concentrations that are far in excess of current production levels. Also from these preliminary data we do not know whether the cells continue to produce isoprene when growth has been limited by isoprene accumulation. In summary, these growth data confirmed that isoprene is not toxic at current production levels in the strains expressing the *IspS* and *IDI*, poplar transgenes.

Chromosomal Integration of *IspS* and *IDI* for Improved Genetic Stability

Construction of pUC57-petJ2-IspS-IDI-Sp^R/Sm^R Recombinant Plasmid.

To construct the recombinant plasmid pUC57-*petJ2*-IspS-IDI-Sp^R/Sm^R, component DNA fragments as shown in Figure 26 were first generated by PCR.

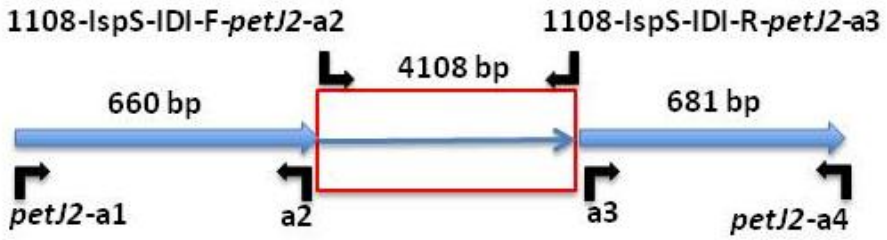

Figure 26. *PetJ2-IspS-IDI*-Sp^R/Sm^R DNA construct for inserting *IspS-IDI* genes into the chromosomal *petJ2* gene -- The primer pairs used for generating the component fragments of the Gibson Assembly reaction were as follows: petJ2-a1/petJ2-a2 generates the *petJ2* upstream fragment, petJ2-a4 / petJ2-a3 generates the *petJ2* downstream region, and 1108-IspS-IDI-F_PetJ2-a2/1108-IspS-IDI-R_PetJ2-a3 generates the *PcpcB-IspS-IDI*-Sp^R/Sm^R fragment.

The upstream and downstream *petJ2* DNA fragments were amplified by PCR from genomic DNA extracted from wild type *Synechococcus*. The petJ2-a1/1108-IspS-IDI-F_PetJ2-a2 primer pair amplified a 660 bp *petJ2* upstream fragment, while 1108-IspS-IDI-R_PetJ2-a3/petJ2-a4 primer pair amplified a 681 bp *petJ2* downstream fragment from the wild type DNA template. The primers 1108-IspS-IDI-F /1108-IspS-IDI-R generated a 4108 bp fragment carrying a linked spectinomycin-streptomycin antibiotic resistance gene marker, isoprene synthase (*IspS*), and *IDI* isomerase transgenes

transcriptionally fused to a *CpcB* promoter. The 4108 bp *PcpcB-IspS-IDI*-Sp^R/Sm^R DNA construct was generated from the pOSH1108 parent plasmid (provided by Matthew Nelson, UW-Oshkosh). In addition, the pUC57 plasmid backbone fragment (2436 bp) was amplified from the plasmid pOSH1108 with the PetJ2-a1-pUC57-F/PetJ2-a4-pUC57-R primer pair. These DNA fragments were then added to a Gibson Assembly reaction mix. Following Gibson Assembly, 2 µL of the assembly product was used to transform DH5α *E. coli* cells by electrotransformation. The transformation mixture was spread onto LB plates containing ampicillin (150 µg/mL final concentration), spectinomycin (25 µg/mL final concentration) and streptomycin (25 µg/mL final concentration).

After overnight incubation, colonies were selected and transferred into liquid LB medium containing ampicillin, spectinomycin and streptomycin followed by incubation at 37^{o}C for ~16 hours. After incubation, plasmids were extracted from overnight cultures by Wizard® Plus purification reagents (Promega) according to the manufacturer's instructions. One (1.0) ng of the extracted DNA was used as the template for PCR analysis to determine whether the isolated plasmid DNA carried the expected *petJ2-PcpcB-IspS-IDI*-Sp^R/Sm^R inactivation construct. Figure 27 shows the recombinant plasmid pUC57-*petJ2-IspS-IDI*-Sp^R/Sm^R expected from the Gibson Assembly reaction.

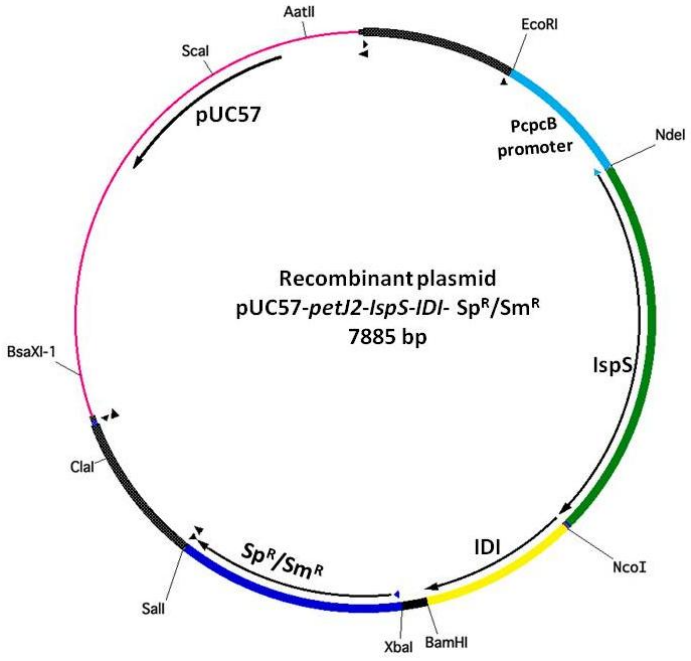

Figure 27. Recombinant plamid pUC57-*petJ2-IspS-IDI*-Sp^R/Sm^R carrying the *petJ2-IspS-IDI*-Sp^R/Sm^R construct. The regions shaded in black represent the *petJ2* upstream and downstream DNA sections. The red region represents the pUC57 plasmid backbone, carrying the origin of replication and an ampicillin resistance gene cassette, Ap^R. The region between the SaII and EcoRI restriction sites represents the *PcpcB-IspS-IDI*-Sp^R/Sm^R fragment carrying the codon-optimized isoprene synthase and IDI isomerase transgenes for isoprene production, and an antibiotic resistance gene marker that confers both spectinomycin and streptomycin resistance. The IspS-IDI-Sp^R/Sm^R fragment was generated from the pOSH1108 parent plasmid.

Plasmid DNAs extracted from the DH5α *E. coli* cells transformed with the Gibson reaction products were tested by PCR to determine whether the assembled recombinant plasmid carried the inactivation DNA construct of interest. Since the recombinant

plasmid was designed to carry *petJ2*-IspS-IDI-Sp^R/Sm^R inactivation construct for targeting to *Synechococcus* PCC 7002, I expected that amplification of this DNA fragment from the recombinant plasmid DNA template would generate a 5471 bp product. As expected, the petJ2-a1/petJ2-a4 primer pair produced a 5471 bp product (Figure 28) which confirmed that the recombinant plasmid carried the *petJ2-IspS-IDI*-Sp^R/Sm^R inactivation DNA construct, and that the Gibson Assembly reaction was successful.

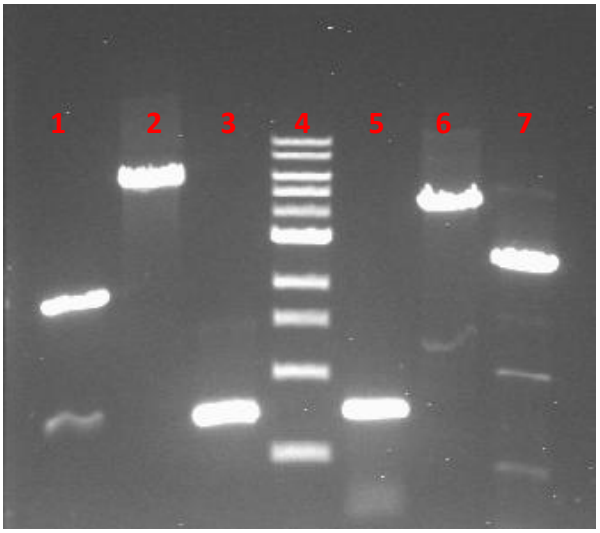

Figure 28. PCR analysis to characterize recombinant plasmid pUC57-*petJ2-IspS-IDI*-Sp^R/Sm^R. Lane 1**:** Wild type control, *Synechococcus* 7002 genomic DNA amplified from petJ2-a1/petJ2-a4 primers. Lane 2: Inactivation construct, *petJ2-IspS-IDI*-Sp^R/Sm^R amplified from petJ2-a1/petJ2-a4 primers. Lane 3: petJ2 uptream DNA fragment amplified from petJ2-a1/petJ2-a2 primers. Lane 4: NEB 1kb ladder. Lane 5: petJ2 downstream DNA fragment amplified from petJ2-a3/petJ2-a4 primers. Lane 6: The *PcpcB-IspS-IDI*-Sp^R/Sm^R fragment carrying the codon-optimized isoprene synthase, *IspS* and *IDI* isomerase transgenes for isoprene production amplified from 1108-IspS-IDI-F-PetJ2-a2/1108-IspS-IDI-R-PetJ2-a3 primers. Lane 7: pUC57 fragment amplified from petJ2-a1-pUC57-F/ petJ2-a4-pUC57-R primers.

Construction of a ΔpetJ2 Mutant.

Wild type *Synechococcus* cells grown to an OD_{750nm} of ~0.3 were transformed with ~3 μg of the *petJ2-PcpcB-IspS-IDI*-Sp^R/Sm^R inactivation fragment amplified from the product of the Gibson assembly reaction described above. The transformation suspension was spread onto A (D7) agar medium containing spectinomycin (50 μg/mL final concentration) and streptomycin (50 μg/mL final concentration) followed by incubation at 37^{o}C under moderate illumination. After two weeks, transformant colonies observed on the plates were transferred into 15 mL sterile snap cap tubes containing liquid A (D7) medium with addition of spectinomycin and streptomycin, followed by incubation with moderate shaking at 37^{o}C under optimal light intensity. Genomic DNA extracted from cells that showed growth was analyzed by PCR to determine whether the isolated mutants carried inactivated copies of the *petJ2* gene.

As expected, the petJ2-a1/petJ2-a4 primers generated a 5471 bp fragment from template DNA extracted from mutants while a 1490 bp fragment was amplified from wild type genomic DNA (as control). The result of this PCR analysis as shown in Figure 29, indicate successful integration of the *petJ2-IspS-IDI*-Sp^R/Sm^R inactivation DNA fragment and segregational loss of the wild type *petJ2* allele. Thus, the PCR analysis confirmed the replacement via homologous recombination of the wild.type *petJ2* gene copy with an interrupted *petJ2* allele (*petJ2-IspS-IDI*-Sp^R/Sm^R).

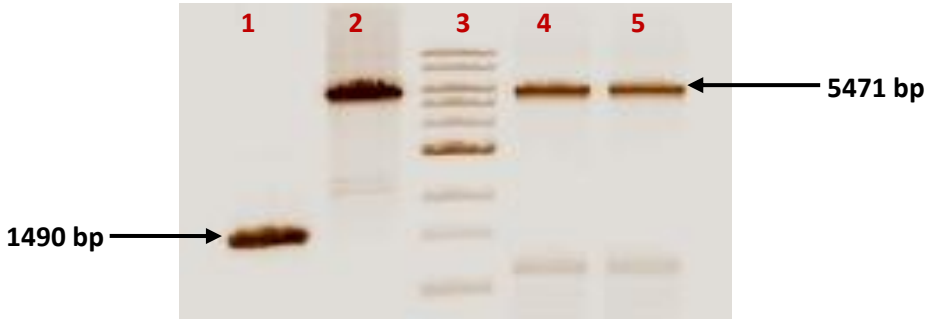

Figure 29. PCR analysis to characterize 7002 ΔpetJ2 mutants. All samples were amplified from petJ2-a1/petJ2-a4 primers. Lane 1**:** Wild type *Synechococcus* 7002 genomic DNA (as control). Lane 2: pUC57-petJ2-IspS-IDI-Sp^R/Sm^R Recombinant plasmid DNA (as control). Lane 3: NEB 1kb ladder. Lanes 4 and 5: Genomic DNAs from two putative *Synechcococcus* ΔpetJ2 mutant clones.

***Chromosomal Integration of IspS-IDI Transgenes Increases Gene Stability*.**

The *Synechococcus* 7002-IspS-IDI strain with *IspS-IDI* transgenes targeted to the high-copy pAQ1 plasmid (i.e. pAQ1::*IspS-IDI*) consistently showed declining isoprene production after continuous cultivation, usually within a week. The observed declining yield may have resulted from loss of pAQ1 plasmids carrying the *IspS-IDI* transgenes. To enhance the genetic stability of isoprene-producing strains and achieve stable, continuous isoprene production, the optimized *IspS* and *IDI* genes were targeted to the *petJ2* chromosomal site, as described above.

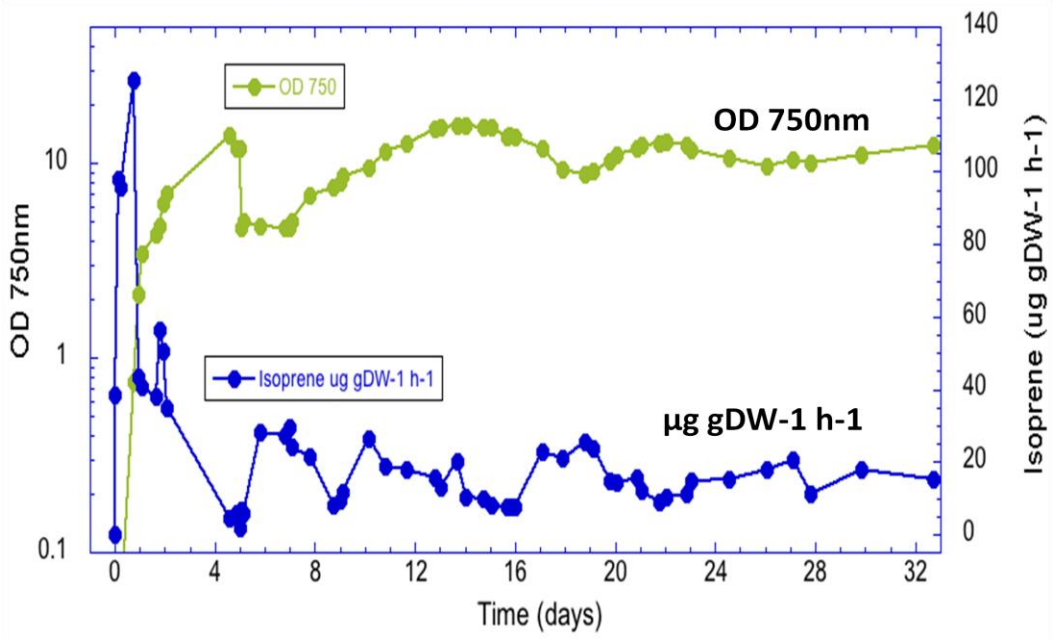

Figure 30. Stable and continuous isoprene production in a 7002 ΔpetJ2 strain. Isoprene concentration in the culture head space gas was measured in real-time with a Fast Isoprene Sensor (FIS). The y-axes show cell density (OD_{750nm}) and isoprene production expressed as µg isoprene per gDW per hour.

Isoprene production remained stable for at least 4 weeks in such strains (Figure 30) indicating that chromosomal integration of the *IspS-IDI* genes increased their stability and prevented the declining yield associated with transgene targeting to the pAQ1 plasmid. As in other experiments, Figure 30 shows that peak isoprene production occurred under dilute culture condition indicating that light penetration remains an important limiting factor for phototrophic isoprene production.

Increased Copies of Optimized *IspS* and *IDI* for Improved Isoprene Yield

Construction of 'Dual IspS-IDI' Strain.

This transformant strain was constructed using as host a *Synecococcus* 7002 ΔPetJ2 mutant carrying the *petJ2::PcpcB-IspS-IDI*-Sp^R/Sm^R inactivation cassette (Figure 11) as a replacement for its native *petJ2* gene. A similar DNA construct (5244 bp in size) flanked by upstream and downstream regions of plasmid pAQ1 and carrying a kanamycin selective marker instead of a spectinomycin-streptomycin resistance gene cassette was generated from plasmid pOSH1309 (Figure 31) using the pAQ1-F/pAQ1-R primer pair. Plasmid pOSH1309 was generously provided by Matthew Nelson, UW-Oshkosh.

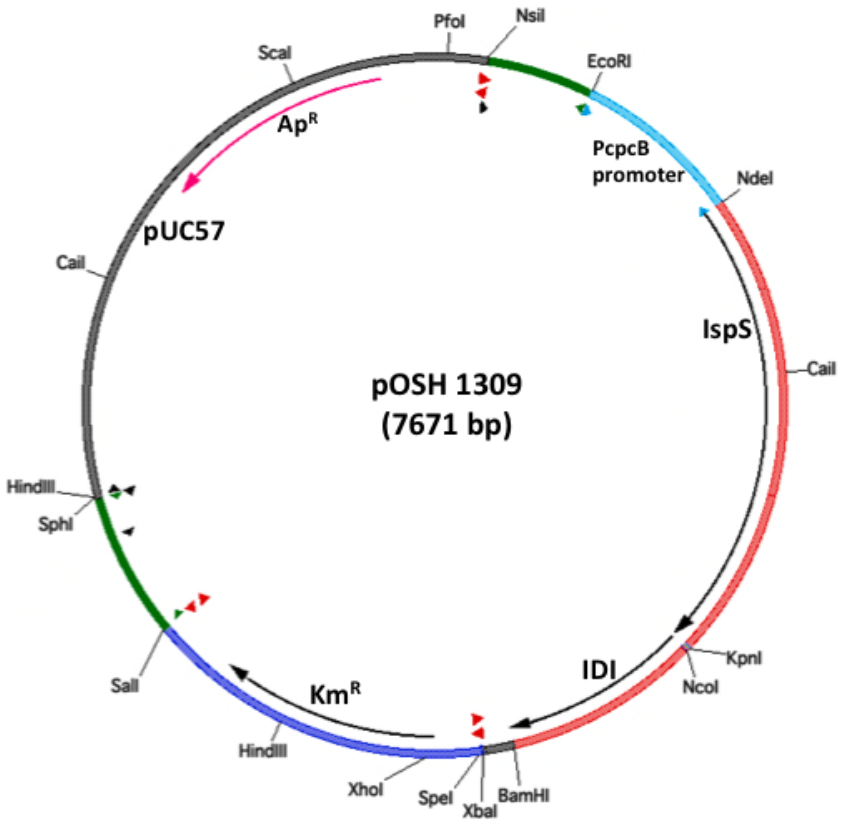

Figure 31. Plasmid pOSH1309 for targeting *Isps-IDI-Km*^{R} genes to the plasmid pAQ1 plasmid of *Synechococcus.* The green segments represent pAQ1 flanking DNA regions. The black region represents the pUC57 plasmid backbone from the pOSH1108 plasmid and carries an ampicillin resistance gene cassette, Ap^R. The region between the EcoRI and SaII restriction sites represents the DNA construct expressing the codon-optimized isoprene synthase, *IspS*, and IDI-isomerase transgenes and a kanamycin resistance gene cassette. (Constructed by Matthew Nelson, UW Oshkosh)

The *PcpcB-IspS-IDI-Km*^{R} DNA construct generated by PCR was purified with Wizard® Plus purification reagents (Promega) according to the manufacturer's protocol. Three (3.0) µg of the purified, linear DNA was used to transform the *Synechococcus* 7002 ΔPetJ2 mutant host. The DNA constructs for targeting the *IspS-IDI* genes to both the chromosomal *petJ2* and plasmid pAQ1 sites were similar but carried different antibiotic resistance gene markers as illustrated in Figure 32.

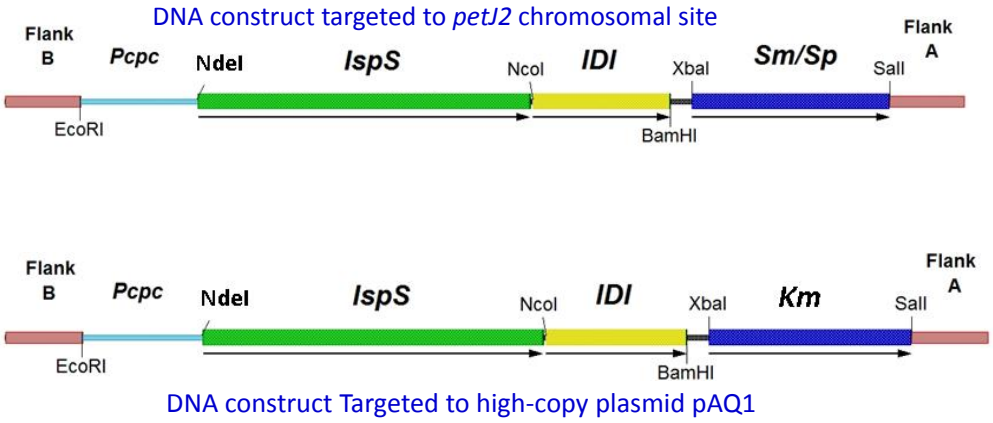

Figure 32. Illustration of *IspS-IDI* gene constructs targeted to the chromosomal *petJ2* and plasmid pAQ1 sites. A. The DNA construct that carries linked spectinomycin and streptomycin resistance marker genes for targeting to the *petJ2* chromosomal site. **B**. The DNA construct that carries a kanamycin resistance gene cassette and flanking regions for targeting to plasmid pAQ1.

The cyanobacterial transformation suspensions were spread onto A (D7) agar containing spectinomycin, streptomycin and kanamycin (each at 50 μg/μL final concentration). Colonies observed on plates were randomly selected and transferred into 15 mL sterile snap cap tubes containing liquid A (D7) medium with spectinomycin, streptomycin and kanamycin as antibiotic additions. To characterize the transformants, genomic DNA was extracted from cells that showed growth in liquid culture and used as template for PCR analysis.

PCR products generated from *Synechococcus* transformants with the pAQ1-F/pAQ1-R primer pair are shown in Figure 33. The gel image shows a faint, high molecular weight band about the size expected for successful integration of the DNA construct to the plasmid pAQ1 target site. The intense low molecular weight band observed in addition to the expected band size in Figure 33 may suggest a partial segregation of the targeted construct or the inability of the inactivation DNA constructs to target all available copies of the plasmid pAQ1.

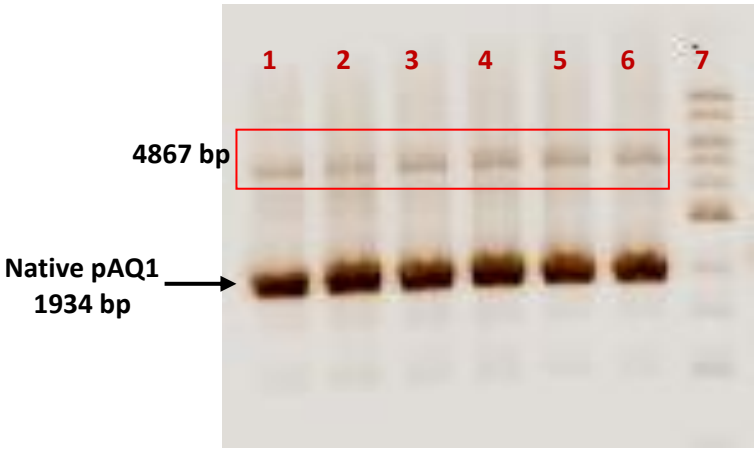

Figure 33. PCR analysis of *IspS-IDI* genes targeted to plasmid pAQ1 in the 'Dual IspS-IDI' strain. Lanes 1-6: Genomic DNAs from *Synechococcus* transformant clones amplified from primers pAQ1-F/pAQ1-R. The higher molecular weight amplicons (faint bands marked by the red box) are from the target regions of pAQ1 plasmids carrying the *IspS-IDI*-Km^R construct while the intense lower molecular weight bands represent the target region on the native, high copy, pAQ1 plasmid. Lane 7: NEB 1 kb ladder.

Impact of Increased Copies of Optimized IspS and IDI on Isoprene production.

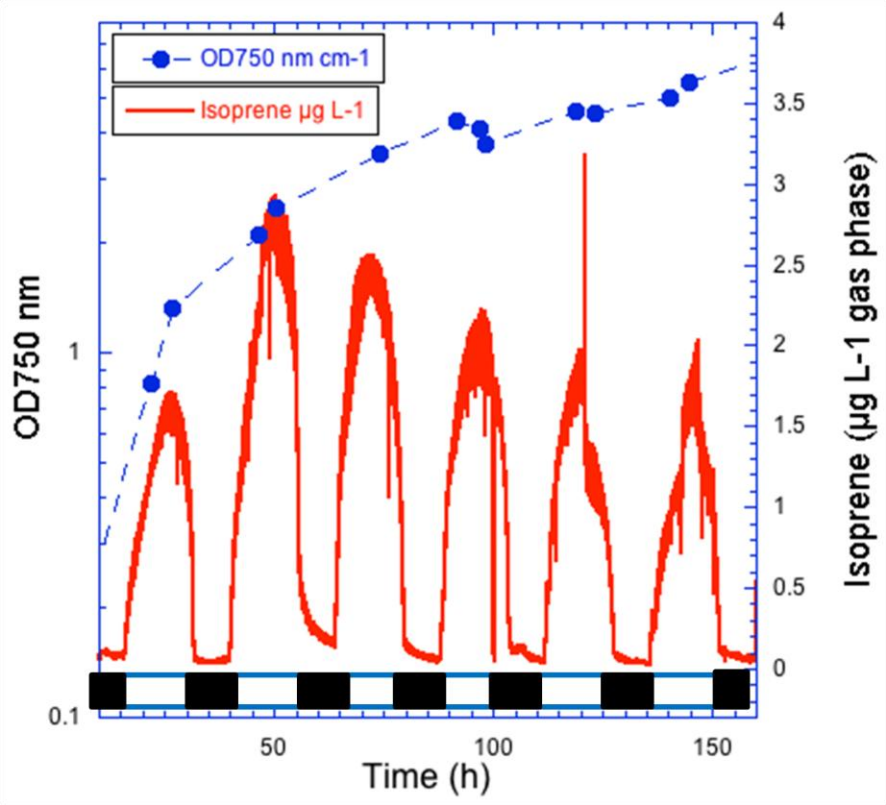

Figure 34. Real-time Fast Isoprene Sensor (FIS) measurements of isoprene production in a 'Dual-IspS-IDI' *Synechococcus* 7002 strain. Isoprene concentration in the head-space (gas phase) of the culture was quantified as µg/L based on a calibration factor calculated from isoprene standards at different flow rates. Culture conditions were 3% CO_2 and 39°C with alternating 16h/8h light-dark periods, and a sinusoidal illumination pattern with a peak light intensity of ~ 2000 µmol photons $m^{-2}s^{-1}$. The red trace shows the isoprene concentration in the culture head-space as measured by the FIS. The blue trace shows optical density (OD_{750nm}) measurements. (Data from Matthew Nelson and Toivo Kallas, UW-Oshkosh)

To determine the impact of the additional copies of the optimized *IspS* and *IDI* transgenes in the 'Dual-IspS-IDI' strain, isoprene production was measured in real time using a Fast Isoprene Sensor (FIS, Hill Scientific). Figure 34, shows isoprene production at a maximal concentration of ~1.5 μg/L in the 'Dual-IspS-IDI' strain at a cell density of ~1.0 OD_{750nm} compared to ~1.0 μg/L in the 7002-IspS-IDI strain that carries optimized *IspS* and *IDI* transgenes on plasmid pAQ1 only (data not shown). The results show that the 'Dual-IspS-IDI' strain produced ~ 1.5 times more isoprene than the 7002-IspS-IDI strain. In addition, isoprene production measured in terms of cell dry weight was estimated at 2.8 mg/g dry weight (gDW) per 12h day in 'Dual-IspS-IDI' strain compared to 1.8 mg/gDW per 12h day in the 7002-IspS-IDI strain. These studies with the 'Dual-IspS-IDI' strain further confirmed that the *petJ2* gene is a suitable chromosomal location for targeting heterologous genes or synthetic operons.

As illustrated in Figure 34, the 'Dual-IspS-IDI' culture was exposed to an alternating dark-light cycle with peak light intensity corresponding to full sunlight intensity (~2000 μmol photons m^{-2} s^{-1}). Isoprene production was detected primarily during periods of illumination indicating that the production of isoprene is a highly light-dependent process, limited by the amount of available light energy for optimal photosynthesis and carbon fixation. The peak isoprene production observed was recorded in dilute culture of optical densities (OD_{750nm}) less than 3. As shown in Figure 34, isoprene production decreased as the cell density increased. This observation indicates that culture density is an important factor in isoprene production under photoautotrophic growth condition. Photosynthetic efficiency per cell is reduced in very dense cultures

because there is self-shadowing among cells and light cannot penetrate deep into the culture. This reduction in photosynthetic activity limits the amount of fixed photosynthate available for isoprene biosynthesis. In conclusion, the FIS data showed that increased copies of the *IspS-IDI* transgenes achieved by targeting to both chromosomal and plasmid sites in the 'Dual-IspS-IDI' strain resulted in increased isoprene production.

RT-qPCR Gene Expression Analysis

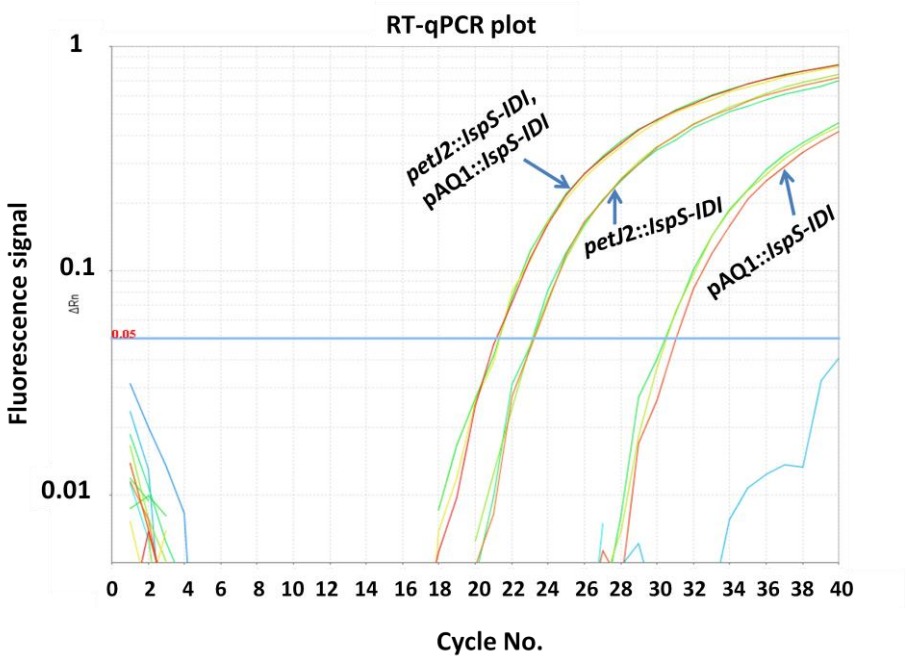

Figure 35. Reverse Transcriptase Quantitative PCR (RT-qPCR) amplification plot of *IspS* transcript abundance in *Synechococcus* strains with chromosomal and plasmid targeted *IspS-IDI* genes. RNAs were isolated from 'Dual IspS-IDI', 7002 ΔpetJ2 and 7002-IspS-IDI strains with the genotype *petJ2*::*IspS-IDI*, pAQ1::*IspS-IDI*; *petJ2*::*IspS-IDI*; and pAQ1::*IspS-IDI* respectively. mRNA transcript abundance was analyzed by 'TaqMan' RT-qPCR as described in Materials and Methods. The plot shows fluorescence signal intensity as a function of PCR amplification cycle. Relative mRNA quantities are determined by the number of cycles taken to reach a signal threshold set at 0.05.

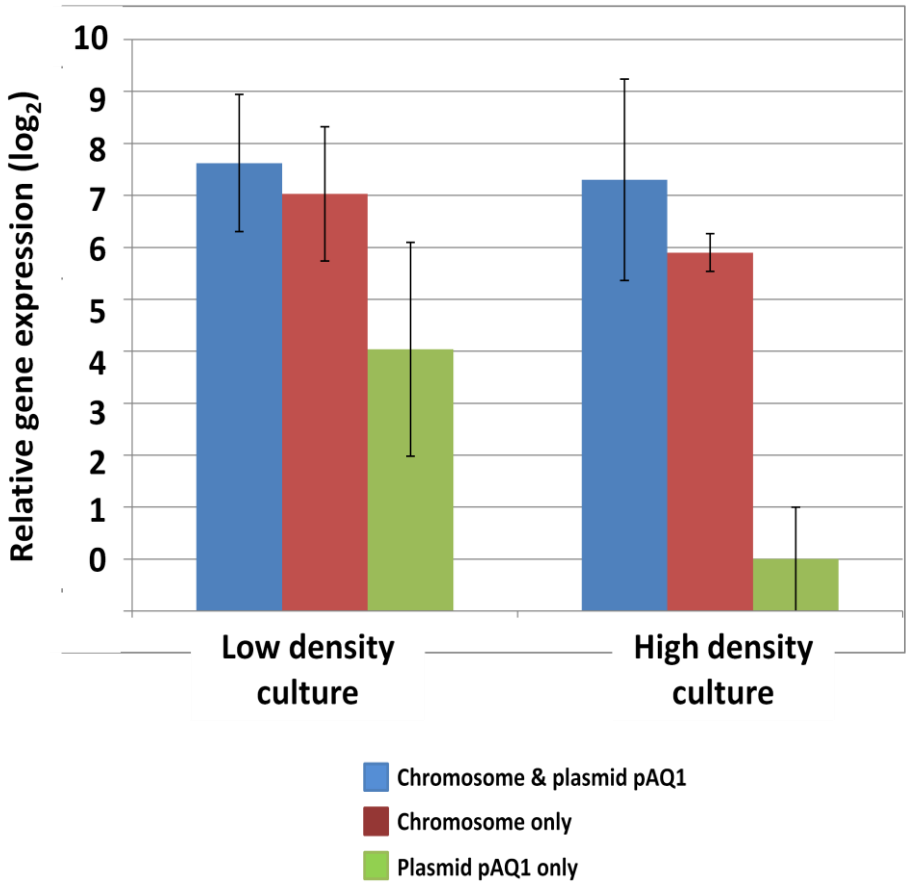

Figure 36. Relative *IspS* transcript abundance in *Synechococcus* strains with chromosomal and plasmid targeted *IspS-IDI* genes. RNAs were harvested from cells at both high- and low – optical densities and analyzed by 'TaqMan' RT-qPCR from data such as those shown in Figure 35. Error bars represent the standard errors from the mean cycle to threshold (C_T) values from three independent biological replicates. Cells were harvested at OD_{750nm} of 0.5 – 1.0 from low density cultures and OD_{750nm} of 4.0 - 8.0 from high density cultures. The error bars show standard errors.

Reverse transcriptase quantitative PCR (RT-qPCR) experiments were conducted to determine whether the increased isoprene production observed in the 7002 'Dual IspS-IDI' strain arose from increased copies of the isoprene synthase genes leading to increased mRNA transcript levels. As shown in Figure 36, the results of the qPCR analysis indicate that the 'Dual-IspS-IDI' strain maintained similar levels of *IspS* transcripts at both low and high culture densities. The 'Dual-IspS-IDI' carries *IspS* transgenes targeted to both a *petJ2* chromosomal location and the high-copy plasmid, pAQ1. The transcript level of *IspS* in the 7002 ΔpetJ2 strain grown at low density was ~ 2 times higher than at high cell density, but still within standard deviations. However, the *IspS* transcript in 7002-IspS-IDI (with *IspS-IDI* genes in plasmid pAQ1 only) in low-density cultures was ~ 16 fold higher than in this strain grown to a high density. The *IspS* transcript levels in 7002-IspS-IDI cells harvested from week-old, dense cultures were several hundred fold lower than in both the 7002 ΔpetJ2 and 'Dual-IspS-IDI' cells harvested from similar conditions. This observed decline in *IspS* transcripts in 7002-IspS-IDI under high density culture condition may be attributed to loss of the recombinant plasmid pAQ1:: *IspS-IDI* carrying the *IspS* transgenes. Interestingly, strains carrying the *IspS* genes targeted to the chromosomal *petJ2* site and grown to high or low culture densities showed similar *IspS* transcript levels. These data suggest that increased copies of the *IspS* transgene led to increased *IspS* transcript levels, resulting in the ~1.5 fold increase in isoprene production in the 'Dual-IspS-IDI' strain relative to 7002-IspS-IDI, which has a set of *IspS-IDI* genes in plasmid pAQ1 only.

DISCUSSION

In recent years, photosynthetic organisms such as cyanobacteria and algae have been identified as potentially viable biofactories for biofuels production. The ability of cyanobacteria to harness abundant solar energy and atmospheric carbon dioxide through photosynthesis makes them particularly attractive as model organisms for generation of 'green fuels' (or environmentally-friendly fuels). Cyanobacteria have higher photosynthetic efficiencies than terrestrial plants (62), are amenable to genetic engineering, can grow to high densities in photobioreactors (culture chambers), and have a much faster growth rate than plants. All of these features make them ideal as host organisms for synthesis of terpenoids and industrially-relevant biochemicals. Despite these advantages and recent developments in algal biofuels research, the challenge of achieving significant biofuels production for commercial exploitation is still a major concern for researchers and as such, different strategies for circumventing these challenges have been proposed.

Towards improving terpenoid (or bioproduct) yields in cyanobacteria, a suite of genetic engineering strategies will be required toward enhancing photosynthetic efficiency, optimizing carbon utilization, and partitioning to increase carbon flow to desired biosynthetic pathways. These strategies may include inactivating competing carbon pathways to allow carbon to be redirected to a desired pathway, expressing specific or complete suites of heterologous genes for alternative pathways, and targeting of such heterologous genes to chromosomal sites for improved genetic stability. Isoprene

is a volatile, hydrophobic compound with a global market demand of 770,000 metric tons per year estimated at 3 billion dollars annually, and an important precursor for industrial and biofuels applications. Matthew Nelson in our lab has successfully engineered isoprene production in *Synechococcus* sp. PCC 7002 cyanobacteria, but isoprene yields need to be significantly improved to realize the dream of commercial production.

In this research work, I hypothesized that the inactivation of a competing carbon pathway for glycogen biosynthesis would significantly improve isoprene production in *Synechococcus* 7002. This hypothesis was premised on the assumption that if *Synechococcus* cannot store excess carbon as glycogen, then this carbon will be channeled into other pathways including the MEP pathway for isoprene production. Contrary to this expectation, as shown in Figure 24, isoprene production in the glycogen synthase knockout strain, 7002 ΔGlgA1A2-IspS-IDI, was only ~ 20% greater than in the 7002-IspS-IDI strain, which retains glycogen synthesis, indicating that most of the carbon pool was rather channeled into a pathway different than the MEP pathway. The glycogen content in the 7002-IspS-IDI strain was already ~ 50% lower than in wild type *Synechococcus* 7002. This suggests that a fraction of the carbon normally used for glycogen synthesis is already partitioned into the MEP pathway for isoprene production in strains that carry active *IspS-IDI* genes. In other words, isoprene biosynthesis via the MEP pathway in the strains carrying the *IspS* and *IDI* genes may already provide an efficient ‘carbon-sink’ for ameliorating excess carbon and reductant.

A similar observation was reported by Bentley et al. (7), who found that rates of isoprene production in the *Synechocystis* sp. PCC 6803 cyanobacteria that are defective in glycogen biosynthesis but express a heterelogous isoprene synthase gene (*IspS*) are comparable to those in strains with normal glycogen biosynthesis that express the same heterelogous isoprene synthase gene (*IspS*). That result showed that inactivation of glycogen biosynthesis in a cyanobacterial strain did not result in re-routing of carbon into the MEP pathway and thus, may help explain why the inactivation of the glycogen biosynthesis in *Synechoccocus* 7002 that express heterologous *IspS-IDI* genes did not result in a significant increase in isoprene production in the current study.

Although it is not clear yet how carbon partitioning is regulated in cyanobacteria and microalgae, Xu et al. (89) recently showed that inactivation of glycogen biosynthesis in *Synechococcus* 7002 caused carbon previously used for glycogen synthesis to be re-routed into production of soluble sugars. A plausible explanation for this observation may be that since both the glycogen and soluble sugar biosynthetic pathways in cyanobacteria share some of the same metabolic precursors, this may result in competition by enzymes in these pathways for available precursor compounds (89). In addition, Xu et al. (89) reported that *Synechococcus sp.* PCC 7002 mutants carrying inactivated copies of both the glycogen synthase isogenes (i.e., *glgA1* and *glgA2*) showed accumulation of the soluble sugars- glucosylglycerol and glucosylglycerate under hypersaline conditions. These, and similar solutes in other species, play a physiological role in helping cyanobacteria survive salt and low-water activity stress conditions (110, 111, 112). In addition, the production of sugars in cyanobacteria allows for consumption of excess

reducing equivalents and triose phosphate intermediates which alleviates the impacts of photo-inhibition caused by energy imbalances between light absorption and metabolic sink capacities (113). Studies like this show a link between soluble sugar production and the ability of glycogen-defective cyanobacteria to survive salt stress. For this reason it may be argued that an alternative sugar biosynthesis pathway is favored in glycogen synthase null mutants to allow such strains to survive and grow in saline environments such as in the marine medium A (114), that we use to grow *Synechococcus* 7002 in the lab.

Therefore, it will be interesting to determine if the inactivation of the sucrose, glucosylglycerol and glycerate biosynthesis pathways in genetically engineered strains grown under hyposaline conditions can cause the excess carbon pool to be re-directed into the MEP pathway for improved isoprene yield. In addition, understanding of the carbon flux mechanisms and regulation in cyanobacteria will allow for effective optimization of carbon flux to either inductively or constitutively redirect carbon into the MEP pathway for enhanced isoprene yield.

In continuous isoprene production from genetically engineered cyanobacteria strains, declining or total loss of production is a major concern. This may be due to genetic instability arising from carbon partitioning strategies that involve inactivation of a competing pathway thus creating a selective pressure favoring spontaneous mutants that restore a functional pathway. Genetic instability may also be caused by the loss of plasmids that carry transgenes for isoprene production leading to low productivity. The

latter requires antibiotic selection to maintain such plasmids -- a strategy which is not feasible for continuous isoprene production on a commercial scale. To improve genetic stability, a chromosomal *petJ2* location was targeted for integration of the exogenous *IspS-IDI* transgenes by homologous recombination. The successful demonstration of continuous stable isoprene production over an extended period of time in a photobioreactor suggests that genes targeted to a chromosome are more likely to be stable in such genetically engineered strains. The continuous stable isoprene production achieved in this research is a significant improvement from the unstable and sometimes declining isoprene production observed in strains that have the *IspS* and *IDI* transgenes targeted to plasmid pAQ1 alone. The genetic stability of the 'Dual-IspS-IDI' strain suggests that the *petJ2* site is a suitable chromosomal site for transgene integration.

As stated, genetic instability may have been a factor in the declining isoprene yield observed in genetically engineered strains expressing the optimized *IspS* and *IDI* from plasmid pAQ1. This instability could have resulted from mutations that accumulated in the introduced transgene(s) over several generations. Alternatively, loss of productivity could have arisen from the loss of plasmids carrying the targeted exogenous transgenes. Metabolic burden arising from continuous unregulated metabolite or biochemical production could also have caused selective pressure against the genetically engineered cyanobacterial cells. Such selective pressure may also select for mutations that lower productivity in any number or ways in the transgenic cyanobacteria. For these reasons, the cyanobacterial isoprene-terpene project will benefit from identification of native regulatable promoters that can help reduce the metabolic burden

on genetically engineered strains, allowing isoprene production only when desired. It is important to identify regulatable promoters that will be useful in the regulation of isoprene biosynthesis so as to reduce the metabolic burden on cells that have been engineered to constitutively synthesize isoprene. Such regulatable promoters may be identified in global gene expression studies via microarray or RNA sequencing ('RNA-Seq') analyses (115) to identify genes and promoter regions that respond, for example, to isoprene production or cell density under different environmental or stress conditions.

The identification of regulatable promoters will allow for controlled isoprene production in *Synechococcus* 7002 cultures and thus, relieve cells of the extra metabolic burden of continuous isoprene production. More so, such regulatable promoters may have potential uses for production of other high-impact biochemical products in the future and provide a means of control for isoprene production over a broad range of environmental conditions. To further improve isoprene yield, it is important to also consider strategies involving either rational or directed evolutionary approaches for protein engineering (15, 116) that will help in identification of isoprene synthase and isomerase IDI proteins with significantly improved enzyme activities. Likewise, the search for even stronger native promoters must be given impetus as evidenced in the study by Zhou et al. (117). The novel Pcpc_{560} promoter (that controls expression of the *cpcB* gene), native to *Synechocystis* sp. PCC 6803, carries 2 predicted promoter regions and 14 predicted transcriptor factor binding sites (TFBS). The chromosomal integration of heterologous genes controlled by the Pcpc_{560} promoter resulted in significantly higher levels of the encoded heterologous proteins (up to ~ 15% of total soluble proteins) in cyanobacteria.

Therefore, it will be important to consider such factor as the TFBS in the choice and design of native cyanobacterial promoters for efficient and improved gene expression.

To increase isoprene yield, the *IspS* and *IDI* gene copy number was increased by targeting the optimized transgenes to both a *petJ2* chromosomal site as well as a neutral site on the high copy pAQ1 plasmid in the 7002 'Dual-IspS-IDI' strain. Isoprene production in the 'Dual-IspS-IDI' strain was compared to that in the 7002-IspS-IDI strain (carrying *IspS* and *IDI* transgenes targeted to plasmid pAQ1 only). The 'Dual-IspS-IDI' strain produced ~ 1.5 times more isoprene than the 7002-IspS-IDI strain. Interestingly, isoprene production peaked at a cell density of ~3.0 OD_{750nm} and declined with increasing culture density, indicating that photosynthetic carbon fixation may have been limited by light penetration into the cyanobacterial culture as it increased in density. This decline in isoprene production in dense cultures may be due to the effect of self-shading by cells preventing the penetration of light into the culture. To ameliorate this, two strategies have been identified: 1) to genetically engineer *Synechococcus* 7002 strains with reduced amounts of light harvesting proteins, and 2) to design photobioreactors or culture vessels that have narrow diameters to enhance light availability to cells over a larger cross-sectional area.

Experiments were conducted to determine whether the difference observed in isoprene yield between the 'Dual-IspS-IDI' strain and 7002-IspS-IDI resulted from differences in the abundance of their isoprene synthase, *IspS*, transcripts. As anticipated, gene expression data (Figure 36) showed that *IspS* mRNA levels were higher in the

'Dual-IspS-IDI' strain relative to a 7002 ΔpetJ2 strain (Δ*petJ2::IspS-IDI*) carrying *IspS-IDI* targeted only to this chromosomal site for cells grown to both low and high optical densities (OD_{750nm}). More significantly, *IspS* transcript levels in both the 'Dual-IspS-IDI' strain and the Δ*petJ2::IspS-IDI* strain were higher than in the 7002-IspS-IDI strain that carries *IspS-IDI* genes targeted to plasmid pAQ1 only. *IspS* gene expression was ~200-fold higher in the Dual-IspS-IDI strain compared to 7002-IspS-IDI cells harvested from dense, week-old cultures. This variability in *IspS* transcript levels may be explained in part by the partial segregation or incomplete replacement of the native pAQ1 plasmid with the pAQ1 construct carrying the *IspS* and *IDI* transgenes.

The inability to achieve full segregation (replacement) of endogenous pAQ1 plasmids with the transgenic pAQ1::*IspS-IDI* plasmids means that the remaining pool of native pAQ1 plasmids may facilitate the replacement of the introduced *IspS-IDI* genes with the native pAQ1 target sequence via homologous recombination. It is not clear yet if the variability in *IspS* transcript levels earlier described is a product of a yet unknown transcriptional, post-transcriptional, translational, post-translational or protein-protein regulation of the IspS protein or a decline in *IspS* gene copy numbers from plasmid loss after periods of continuous cultivation. To help explain this observation, further experiments will be required that involve determining *IspS* gene copy numbers and relative transcript levels of *IspS* genes in the 'Dual- IspS-IDI', *ΔPetJ2::IspS-IDI,* and 7002-IspS-IDI (pAQ1::*IspS-IDI*) strains used in this research. Such experiments will provide insight into reasons for the declining isoprene yield observed in strains with *IspS* and *IDI* transgenes targeted only to plasmid pAQ1 under continuous culture conditions.

Our lab-scale photobioreactor studies showed that incident light (even at ~ 2000 to 4000 μmol photons m^{-2} s^{-1}, equivalent to intensities up to twice full sunlight) is not evenly distributed throughout these cultures. Cells at the surface of bioreactors absorb essential all of the light and prevent light penetration deep into these cultures. Since optimal light penetration is necessary for maximum photosynthetic efficiency and bioproduct production, there has been much interest in engineering algae that carry attenuated light-harvesting antenna proteins (25, 31). Such antenna-depleted mutants should prevent shading of cells in dense cultures and improve photosynthetic efficiency resulting in improved synthesis of bioproducts including isoprene. Indeed, several studies have shown that antenna-depleted mutant of both green algae and cyanobacteria can be grown to higher cell densities than the wild type strains (31, 118, 119). Thus, I expect that inactivation of *cpcB*, the first gene of the c-phycocyanin operon, encoding proteins of the phycobilisome light-harvesting complex of *Synechococcus* 7002 will limit the amount of the light-harvesting proteins and thus help alleviate the problem of self-shading under dense culture condition. This proposal, if successful, is expected to boost isoprene production per liter culture by allowing each cell to receive more light for optimal photosynthetic efficiency.

In typical cyanobacteria ~ 50 - 80% of fixed CO_2 is directed to synthesis of protein, cell wall, storage polysaccharides, and soluble sugars with ~10% for lipids and the remaining ~5% for terpenoids (6). The challenge for metabolic engineering is to redirect carbon flow to desired bioproducts. Nutrient limitation (e.g. nitrogen depletion) and high light stress conditions have been widely used in microalgae to channel carbon

away from protein synthesis or direct it to secondary metabolites that are induced in response to such stresses (120). This strategy has successfully resulted in the increased accumulation of terpenoids such as β-carotene (121, 122) and astaxanthin (123, 124) in *Dunaliella bardawil* and *Haematococcus pluvialis*, respectively. Such strategies are attractive because they do not require genetic engineering. Their success, however, depends on whether carbon can be successfully re-routed into desired pathways such as the MEP pathway rather than to increased production of soluble sugars (89) or other metabolites (125). Such nutrient deprivation or stress strategies have not been fully tested on photosynthetic efficiency and bioproduct production in *Synechococcus* sp. PCC 7002. Because the *Synechococcus* 7002 strains developed in our lab and in this study carry optimized *IspS-IDI* genes and produce isoprene at rates 40 to 80 times those reported previously for cyanobacteria (6, 7), nitrogen-deprivation together with an active MEP pathway for funneling carbon to isoprene may lead to further improved isoprene yields.

CONCLUSION

This research has successfully demonstrated several important proofs-of-concept toward the development of isoprene-producing *Synechococcus* 7002 cyanobacteria for commercial applications. First, targeting optimized *IspS* and *IDI* transgenes to a neutral, *petJ2* chromosomal site, rather than to the high-copy pAQ1 plasmid, significantly enhanced the stability of *IspS* mRNA transcripts as shown by reverse transcriptase quantitative PCR (RT-qPCR) experiments. This further demonstrated that the *petJ2* locus can serve as a target site for chromosomal integration of synthetic operons or gene constructs in future experiments. Second, increasing the copy number of the *IspS-IDI* transgenes increased isoprene production. This was shown in the 'Dual IspS-IDI' strain that carries one set of *IspS-IDI* genes in plasmid pAQ1 and another set in the *petJ2* chromosomal site. Finally, as further evidence of *IspS-IDI* transgene stability when targeted to the chromosome, the 'Dual IspS-IDI' strain produced isoprene continuously for a month in a photobioreactor culture. Overall this research has further demonstrated the amenability of *Synechoccocus* sp. PCC 7002 as a model organism for genetic engineering and an excellent platform for algal bioproducts and biofuels development. This work has contributed toward improved photosynthetic isoprene production in *Synechococcus* cyanobacteria but further genetic engineering approaches will be needed to create a 'super-strain' strain for an economically sustainable algal biotechnology industry.

APPENDIX A

Microbial media

Liquid A (D7) Medium

Add appropriate quantities (in grams) of the salts shown below to 900 mL of MilliQ-H_2O in a 2000 mL conical flask.

Salts	**Powder (g/L)**	**Final concentration (1x)**
NaCl	18	0.3 M
KCl	0.6	0.008 M
$NaNO_3$	1.0	0.012 M
$MgSO_4$	2.41	0.02 M
$CaCl_2$	0.2775	0.0025 M

To the 1x A Base from above, add the Fe-EDTA and D7 micronutrients solutions.

1x A base from above	**Volume (mL) added per liter A Base**	**Final concentration 1x**
15mM Fe-EDTA	1.0	15 μM
1000x D7 micronutrients (Tbl. C)	1.0	1x

After autoclaving the above AFM Base, allow to cool to about 50^{o}C before adding the sterile ingredients shown below.

Ingredients	**Volume (mL) added per liter AFM Base**	**Final concentration (1x)**
0.83M Tris-HCl pH=8.2	10.0 mL	8.3 mM
1.0M KH_2PO_4	0.37 mL	0.37 mM
6 μM (= 8 mg/L) Vitamin B_{12}	1.0 Ml	6 nM

Solid A (D7) Medium

In order to prepare solid A media for agar plates, AFM Base and agar must be prepared and autoclaved separately to avoid formation of toxic or inhibitory productsupon autoclaving. The protocol involves autoclaving separately, 500 mL of 2x AFM base (with addition of 2g $Na_2S_2O_3$; sodium thiosulfate) and 500 mL of 2x 1.2% agar. After autoclaving, allow solutions to cool to about 50^{o}C, and then add the 2x AFM Base to the agar and then mix by stirring on a magnetic stir plate. Then, add sterile solutions of Tris-HCl pH=8.2, KH_2PO_4 and vitamin B_{12} as described above. If necessary, add appropriate concentrations of sterile antibiotic solutions as desired. Mix agar solution by stirring before pouring plates. Store the plates at 4^{o}C.

D7 Micronutrients

This original Arnon D7 formulation (126) shown below may be slightly different from the D7 micronutrients formulation referenced in Buzby et al. (127).

Salts	**g/L (final concentration 1000x)**
H_3BO_3	2.86
$MnCl_2.4H_2O$	1.81
$ZnSO_4.7H_2O$	0.222
$Na_2MoO_4.2H_2O$	1.26
$CuSO_4.5H_2O$	0.079
$NaVO_3$	0.239
$CoCl_2.6H_2O$	0.0403

S.O.C Medium

For a 100 mL , add 2g tryptone, 0.55g yeast extract, 1 mL of 1.0 M NaCl, 1 mL 1.0 M Kcl and Milli-Q H_2O to a final 100 mL volume. Autoclave and allow to cool to room temperature, then add 1 mL of sterile 1.0 M $MgCl_2$ (20.3g $MgCl_2.6H_2O$ to 70 mL Milli-Q H_2O), 1 mL of sterile 1.0M $MgSO_4$ (12g $MgSO_4$ to 70 mL Milli-Q H_2O) followed by 1 mL filter sterile 2.0 M glucose (3.6g glucose in 7 mL Milli-Q H_2O).

Luria-Bertani (LB) Broth [pH=7.0]

Add 15.5 g of LB homogenous powder (US Biological, Massachusetts) to 1 liter of Milli-Q H_2O. Each gram of powder contains 10 g tryptone, 5 g yeast extract and 0.5 g sodium chloride. Ensure powder is completely dissolved in Milli-Q H_2O before autoclaving for 15 minutes at 121^oC. Transfer 200 ml into sterile bottles for use as culture broth for growing *E. coli*. Store at room temperature or at 4^oC for longer shelf-life.

LB Agar

For LB Agar, Add 15.5 g of LB homogenous powder (US Biological, Massachusetts) to 1 liter of Milli-Q H_2O. Then add 12 g of agar powder to the suspension and ensure powder mixture is completely in suspension before autoclaving. Allow to cool to 50^oC before adding appropriate concentrations of antibiotics solutions. Pour plates and store at 4^oC.

APPENDIX B

Buffers and Reagents

TBE Buffer (5x)

Add 54g Tris Base (Tris hydroxymethyl aminomethane) and 27.5g boric acid to 300 mL Milli-Q H_2O. Then, add 20 mL of 0.5 M EDTA (pH=8.0) [93.05g Na_2EDTA in 500 mL Milli-Q H_2O] and bring to a final volume of 1 liter.

Diethylpyrocarbonate (DEPC) Treated Sterile Milli-Q H_2O

First, oven bake glass wares and magnetic stir bars for ~12 hours. Then, to 1.0 L MilliQ-H_2O, add DEPC to 0.1% final concentration and stir overnight. Autoclave solution and preferably transfer solutions into oven-baked 1.0 L Wheaton capped bottles for storage.

DEPC Treated 10T/0.1E (pH=8.0)

Ensure Stock solutions are DEPC treated. Add 500 µL of 1.0 M Tris-HCl (pH=8.2), 10 µL of 0.5 M sodium EDTA (pH=8.0) and DEPC treated Milli-Q H_2O to a final volume of 50 mL. Transfer buffer solution into 1.5 mL sterile screw cap tubes. Aliquots can be stored at 4^oCwhile stock solution can be kept at room temperature.

600 mM Sucrose

Add 20.54 grams of sucrose to an oven baked 250 mL with a stir bar. Add sterile Milli-Q H_2O water to a final volume of 100 mL. Add DEPC to a final concentration of 0.1% and then stir overnight in the laminar flow hood. Following overnight incubation, autoclave the sucrose solution and transfer into sterile 50 mL screw cap tubes.

Sodium Acetate (pH=4.5)

Add 8.2 gram of sodium acetate to 50 mL of sterile Milli-Q H_2O in an oven baked beaker with a magnetic stir bar. Stir to dissolve and then adjust the pH to 4.5 using Glacial acetic acid. Add DEPC to 0.1% final concentration and adjust the final volume to 100 mL. Transfer solution to a 250 mL oven baked flask and stir vigorously overnight. After overnight stirring, autoclave and store in sterile screw cap tubes at room temperature.

0.5 M Sodium EDTA (Disodium Ethylenediaminetetraacetate) [pH=8.0]

Add 148.9 grams of sodium EDTA salt to 600 mL sterile Milli-Q H_2O in an oven baked Wheaton bottle with a magnetic stir bar. Adjust pH and final volume to 8.0 and 800 mL respectively. Add DEPC to 0.1% final concentration and stir overnight with cap loosely fit. After overnight stirring, autoclave and store at room temperature.

0.5 M Tris (Tris Hydroxymethylaminomethane)

Add 15.15 grams Tris Base to an oven-baked flask containing 250 mL sterile Milli-Q H_2O. Autoclave and store at room temperature.

100 mM Tris-HCl (pH=8.2)

Add 1.21 grams of Tris to 100 mL sterile MilliQ-H_2O in an oven baked flask. Autoclave and allow to cool at room temperature. Bubble the flask with argon gas for ~ 3 minutes, and then seal flask before storing at room temperature. To prepare DEPC-treated

Tris-HCl, add DEPC to 0.1% final concentration and stir overnight in the laminar flow hood.

Equilibrated Phenol

Before preparation, autoclave a 500 gram brown bottle, with a magnetic stir bar in the oven at 180^{o}C for ~12 hours. Weight 200 grams of phenol crystals and transfer into the bottle. Add 200 mg of 8-hydroxyquinoline and stir to dissolve. Then, add 250 mL of 0.5M Tris solution with vigorous stirring for 30 minutes. Then, incubate overnight at 4^{o}C to allow the aqueous and organic phases to separate. After separation of phases, aspirate as much of the aqueous phase as possible and then test the pH of the phenol-containing organic phase. With these starting volumes of phenol and Tris solution, the pH should be around 8.0. Add 100 mL of 100 mM Tris-HCl solution and stir mixture vigorously for 30 minutes to allow phase separation before storage at 4^{o}C. The organic phase contains the equilibrated phenol.

10x Metabolic Stop Solution

Add 25 mL equilibrated phenol solution, 24 mL sodium EDTA (0.5 M), and 1 mL β-mecarptoethanol to a clean 50 mL screw cap tube. Ensure the metabolic stop solution is prepared fresh and stored at 4^{o}C or on ice before use. The final volume can be scaled up accordingly depending on harvested culture volume.

Equilibrated phenol/Chloroform/Isoamylalchohol (25:24:1)

Add 25.0 mL equilibrated phenol, 24.0 mL chloroform and 1.0 mL isoamylalchohol to a clean 50 mL screw cap tube. Protect from light (by covering tube with aluminium foil) and store at -20^{o}C for up to 6 months. During use, store at 4^{o}C or on ice.

Chloroform/Isoamylalchohol (24:1)

Add 48 mL chloroform to 2 mL isoamylalchohol in a clean 50 mL screw cap tube. Protect from light (by covering with aluminium foil) and store at -20^{o}C for up to 6 months. During use, store at 4^{o}C or on ice.

Vitamin B_{12} (Cobalamin)

Stock solution was prepared as 800 mg/mL in sterile Milli-Q H_2O, while working stocks were stored as 80 mg/mL aliquots, filter sterilized and transferred into screw cap microcentrifuge tubes. Store aliquots at -20^{o}C protected from light.

Antibiotics

Stock solutions of different antibiotics were prepared as 1000x (w/v) of desired working concentrations. Preparation of Kanamycin (50 mg/mL), Ampicillin (150 mg/ml), Streptomycin (50 mg/mL), and Spectinomycin (50 mg/mL) is by determining the equivalent salt weight and dissolving in 10 mL sterile Milli-Q H_2O. The antibiotic suspensions are sterilized using a clean syringe plugged to a 0.2 micron pore size filter.

However, Erythromycin (20 mg/ml) is prepared by dissolving erythromycin salt in ethanol (95% v/v) and need no filter sterilization.

APPENDIX C

Protocols

DNA Extraction Protocol

This 'quick extraction' protocol was modified from personal communication with Matthew Nelson, UW-Oshkosh. Add a loopful of cyanobacterial cells to 100 µL of 35% ethanol in a screw cap tube. Alternatively, centrifuge 1 mL of a dense liquid culture at 14,000 x g for 6 minutes at room temperature. Discard supernatant and resuspend pellet in 100 µL of 35% ethanol. Ensure complete resuspension of cyanobacterial cells in ethanol, for both methods of cell preparation. Heat cell suspension in boiling water for 5 minutes and immediately cool at -20^{o}C for 5 minutes. Then, vortex and centrifuge at 14,000 x g for 5 minutes at 4^{o}C. Then, carefully transfer supernatant to a sterile microcentrifuge tube and store at -20^{o}C.

Transformation of *Synechococcus sp*. PCC 7002

Synechococcus sp. PCC 7002 strains are grown exponentially in liquid AD7 medium containing appropriate antibiotic concentration at 37^{o}C supplied with ambient CO_2. Cells are harvested at OD_{750nm} of ~ 0.5 and resuspended in fresh A (D7) to OD_{750nm} of ~ 3.0. Then, 2-3 µg of linear DNA construct is added to about 0.8 mL of resuspended cells in 15 mL clean snap cap tubes with overnight incubation at 37^{o}C, 200 µmol photons $m^{-2}s^{-1}$ with ambient CO_2. The transformation mixture is spread on A (D7) agar plate containing appropriate antibiotic concentration and incubated in the Percival incubator (Perry, Iowa, USA) for 3 days at 37^{o}C with moderate illumination (< 150 µmol photons $m^{-2}s^{-1}$). After third day, the plates are exposed to ~ 200 µmol photons $m^{-2}s^{-1}$ illumination

until colonies appear. Colonies are randomly selected and then transferred into a fresh A (D7) medium containing desired antibiotics in a clean 15 mL snap cap tube.

Alternatively, 50mL fresh sterile A (D7) medium containing appropriate antibiotic concentration is inoculated with *Synechococcus* cells to about OD_{750nm} of ~ 0.2. Incubate cells overnight in a 37^{o}C water bath at 200 μmol photons $m^{-2}s^{-1}$, and 3% (v/v) CO_2 in air. Following day, harvest 7.0 mL of the overnight culture and centrifuge using the table-top Bechkamp centrifuge at 3750 rpm for 3 minutes. Discard 95% of supernatant and resuspend cell pellets in remaining supernatant. The cell suspension is further diluted to a final volume of 1.0 mL at OD_{750nm} of ~ 3.0 in a clean sterile screw cap tube using fresh A (D7) medium. Add 3- 5 μg of inactivation linear DNA construct to the cell suspension and mix well. Transfer cell suspension to a clean 15 mL snap cap tube and then add 500 μL of A (D7) medium for a final volume of 1.5 mL. This compensates for possible evaporation of water from medium during overnight incubation. Incubate transformation mixture at 37^{o}C with 200 μmol photons $m^{-2}s^{-1}$light intensity and, 3% (v/v) CO_2 in air bubbled into transformation mixture. After overnight incubation, 500 μL of transformation is spread on A (D7) agar plate containing appropriate antibiotics for positive selection. Incubate A (D7) plates for 3 days at moderate light intensity (< 150 μmol photons $m^{-2}s^{-1}$), e.g., by covering with black wire mesh in a Percival incubator before exposure to optimal light intensity of 200 μmol photons $m^{-2}s^{-1}$.

Preparation of DH5α Electrocompetent *E. coli* cells

Inoculate 4 mL of LB/Nalidixic acid (final concentration = 30μg/mL) with a loopful of DH5α cells and incubate overnight at 37^{o}C with moderate shaking. Following overnight incubation, inoculate 400 mL of LB with 4 mL of overnight culture. Then, incubate at 37^{o}C, with shaking at 100 rpm for ~ 4 hours to early mid-log phase. Centrifuge in sterile cold Oakridge tubes at 5000 x g for 10 minutes at 4^{o}C. Discard supernatant carefully not to displace pellets and gently resuspend pellet in 200 mL ice-cold 10% sterile glycerol. During washing and resuspension, ensure that the pellet is kept on ice. Repeat this process two more times, each time resuspending pellet in 200 mL ice-cold 10% sterile glycerol. Then, centrifuge and resuspend pellets in 100 mL of cold 10% glycerol. Discard supernatant and resuspend in a final volume of 1.2 mL cold 10% glycerol. Transfer 40 μL aliquots to pre-labeled sterile microcentrifuge tubes and freeze immediately in liquid nitrogen and store tubes at -80^{o}C.

REFERENCES

1. Harvey, B. G., Wright, M. E., and Quintana, R. L. (2009). High-density renewable fuels based on the selective dimerization of pinenes. *Energy & Fuels, 24*(1), 267-273.

2. Meylemans, H. A., Quintana, R. L., and Harvey, B. G. (2012). Efficient conversion of pure and mixed terpene feedstocks to high density fuels. *Fuel, 97*, 560-568.

3. Sharkey, T. D., Wiberley, A. E., and Donohue, A. R. (2008). Isoprene emission from plants: Why and how. *Annals of Botany, 101*(1), 5-18.

4. Sharkey, T., Loreto, F., and Delwiche, C. (1991). High carbon dioxide and sun/shade effects on isoprene emission from oak and aspen tree leaves. *Plant, Cell & Environment, 14*(3), 333-338.

5. Shaw, S. L., Gantt, B., and Meskhidze, N. (2010). Production and emissions of marine isoprene and monoterpenes: A review. *Advances in Meteorology, 2010.*

6. Lindberg, P., Park, S., and Melis, A. (2010). Engineering a platform for photosynthetic isoprene production in cyanobacteria, using *Synechocystis* as the model organism. *Metabolic Engineering, 12*(1), 70-79.

7. Bentley, F. K., Zurbriggen, A., and Melis, A. (2014). Heterologous expression of the mevalonic acid pathway in cyanobacteria enhances endogenous carbon partitioning to isoprene. *Molecular Plant, 7*(1), 71-86.

8. Lee, S., and Poulter, C. D. (2006). *Escherichia coli* type I isopentenyl diphosphate isomerase: structural and catalytic roles for divalent metals. *Journal of the American Chemical Society, 128*(35), 11545-11550.

9. Ershov, Y., Gantt, R. R., Cunningham, F. X., and Gantt, E. (2000). Isopentenyl diphosphate isomerase deficiency in *Synechocystis* sp. strain PCC6803. *FEBS Letters, 473*(3), 337-340.

10. Barkley, S. J., Desai, S. B., and Poulter, C. D. (2004). Type II isopentenyl diphosphate isomerase from *Synechocystis* sp. strain PCC 6803. *Journal of Bacteriology, 186*(23), 8156-8158.

11. Yamashita, S., Hemmi, H., Ikeda, Y., Nakayama, T., and Nishino, T. (2004). Type 2 isopentenyl diphosphate isomerase from a thermoacidophilic archaeon *Sulfolobus shibatae*. *European Journal of Biochemistry, 271*(6), 1087-1093.

12. Eisenreich, W., Bacher, A., Arigoni, D., and Rohdich, F. (2004). Biosynthesis of isoprenoids via the non-mevalonate pathway. *Cellular and Molecular Life Sciences CMLS, 61*(12), 1401-1426.

13. Ajikumar, P. K., Xiao, W. H., Tyo, K. E., Wang, Y., Simeon, F., Leonard, E., Mucha, O., Phon, T. H., Pfeifer, B., and Stephanopoulos, G. (2010). Isoprenoid pathway optimization for taxol precursor overproduction in *Escherichia coli*. *Science (New York, N.Y.), 330*(6000), 70-74.

14. Matthews, P., and Wurtzel, d. E. T. (2000). Metabolic engineering of carotenoid accumulation in *Escherichia coli* by modulation of the isoprenoid precursor pool with expression of deoxyxylulose phosphate synthase. *Applied Microbiology and Biotechnology, 53*(4), 396-400.

15. Leonard, E., Ajikumar, P. K., Thayer, K., Xiao, W. H., Mo, J. D., Tidor, B., Stephanopoulos, G., and Prather, K. L. (2010). Combining metabolic and protein engineering of a terpenoid biosynthetic pathway for overproduction and selectivity control. *Proceedings of the National Academy of Sciences of the United States of America, 107*(31), 13654-13659.

16. Xue, J., and Ahring, B. K. (2011). Enhancing isoprene production by genetic modification of the 1-deoxy-d-xylulose-5-phosphate pathway in *Bacillus subtilis*. *Applied and Environmental Microbiology, 77*(7), 2399-2405.

17. Martin, V. J., Pitera, D. J., Withers, S. T., Newman, J. D., and Keasling, J. D. (2003). Engineering a mevalonate pathway in *Escherichia coli* for production of terpenoids. *Nature Biotechnology, 21*(7), 796-802.

18. Kim, S., and Keasling, J. (2001). Metabolic engineering of the nonmevalonate isopentenyl diphosphate synthesis pathway in *Escherichia coli* enhances lycopene production. *Biotechnology and Bioengineering, 72*(4), 408-415.

19. Zurbriggen, A., Kirst, H., and Melis, A. (2012). Isoprene production via the mevalonic acid pathway in *Escherichia coli* (bacteria). *BioEnergy Research, 5*(4), 814-828.

20. Kudoh, K., Kawano, Y., Hotta, S., Sekine, M., Watanabe, T., and Ihara, M. (2014). Prerequisite for highly efficient isoprenoid production by cyanobacteria discovered through the over-expression of 1-deoxy-d-xylulose 5-phosphate synthase and carbon allocation analysis. *Journal of Bioscience and Bioengineering, 118*(1), 20-28.

21. Stephenson, P. G., Moore, C. M., Terry, M. J., Zubkov, M. V., and Bibby, T. S. (2011). Improving photosynthesis for algal biofuels: Toward a green revolution. *Trends in Biotechnology, 29*(12), 615-623.

22. Zhu, X., Long, S. P., and Ort, D. R. (2008). What is the maximum efficiency with which photosynthesis can convert solar energy into biomass? *Current Opinion in Biotechnology, 19*(2), 153-159.

23. Muller, P., Li, X. P., and Niyogi, K. K. (2001). Non-photochemical quenching. A response to excess light energy. *Plant Physiology, 125*(4), 1558-1566.

24. Barber, J., and Tran, P. D. (2013). From natural to artificial photosynthesis. *Journal of the Royal Society, Interface 10*(81), 20120984.

25. Melis, A. (2009). Solar energy conversion efficiencies in photosynthesis: Minimizing the chlorophyll antennae to maximize efficiency. *Plant Science, 177*(4), 272-280.

26. Mitra, M., and Melis, A. (2008). Optical properties of microalgae for enhanced biofuels production. *Optics Express, 16*(26), 21807-21820.

27. Nomura, C. T., Sakamoto, T., and Bryant, D. A. (2006). Roles for heme–copper oxidases in extreme high-light and oxidative stress response in the cyanobacterium *Synechococcus* sp. PCC 7002. *Archives of Microbiology*, *185*(6), 471-479.

28. Work, V. H., D'Adamo, S., Radakovits, R., Jinkerson, R. E., and Posewitz, M. C. (2012). Improving photosynthesis and metabolic networks for the competitive production of phototroph-derived biofuels. *Current Opinion in Biotechnology*, *23*(3), 290-297.

29. Simionato, D., Basso, S., Giacometti, G. M., and Morosinotto, T. (2013). Optimization of light use efficiency for biofuel production in algae. *Biophysical Chemistry*, *182*, 71-78.

30. Polle, J. E., Kanakagiri, S., and Melis, A. (2003). tla1, a DNA insertional transformant of the green alga *Chlamydomonas reinhardtii* with a truncated light-harvesting chlorophyll antenna size. *Planta*, *217*(1), 49-59.

31. Kirst, H., Formighieri, C., and Melis, A. (2014). Maximizing photosynthetic efficiency and culture productivity in cyanobacteria upon minimizing the phycobilisome light-harvesting antenna size. *Biochimica Et Biophysica Acta (BBA)-Bioenergetics*, *1837*(10), 1653-1664.

32. Iwaki, T., Haranoh, K., Inoue, N., Kojima, K., Satoh, R., Nishino, T., Wada, S., Ihara, H., Tsuyama, S., Kobayashi, H., and Wadano, A. (2006). Expression of foreign type I ribulose-1, 5-bisphosphate carboxylase/oxygenase (EC 4.1. 1.39) stimulates

photosynthesis in cyanobacterium *Synechococcus* PCC 7942 cells. *Photosynthesis Research*, *88*(3), 287-297.

33. Tamoi, M., Nagaoka, M., Miyagawa, Y., and Shigeoka, S. (2006). Contribution of fructose-1, 6-bisphosphatase and sedoheptulose-1, 7-bisphosphatase to the photosynthetic rate and carbon flow in the calvin cycle in transgenic plants. *Plant & Cell Physiology*, *47*(3), 380-390.

34. Angermayr, S. A., Rovira, A. G., and Hellingwerf, K. J. (2015). Metabolic engineering of cyanobacteria for the synthesis of commodity products. *Trends in biotechnology*, *33*(6), 352-361.

35. Melis, A. (2013). Carbon partitioning in photosynthesis. *Current Opinion in Chemical Biology, 17*(3), 453-456.

36. Rosgaard, L., de Porcellinis, A. J., Jacobsen, J. H., Frigaard, N., and Sakuragi, Y. (2012). Bioengineering of carbon fixation, biofuels, and biochemicals in cyanobacteria and plants. *Journal of Biotechnology*, *162*(1), 134-147.

37. Tomitani, A., Knoll, A. H., Cavanaugh, C. M., and Ohno, T. (2006). The evolutionary diversification of cyanobacteria: Molecular-phylogenetic and paleontological perspectives. *Proceedings of the National Academy of Sciences of the United States of America*, *103*(14), 5442-5447.

38. Willey, J. (2008). *Prescott, harley, and klein's microbiology-7th international ed./Joanne M. willey, linda M. sherwood, christopher J. woolverton*. New York: McGraw-Hill Higher Education.

39. Schirrmeister, B. E., Antonelli, A., and Bagheri, H. C. (2011). The origin of multicellularity in cyanobacteria. *BMC Evolutionary Biology, 11*, 45-2148-11-45.

40. Speziale, B. J., and Dyck, L. A. (1992). *Lyngbya* infestations: comparative taxonomy of *lyngbya wollei* comb. Nov. (cyanobacteria) 1. *Journal of Phycology, 28*(5), 693-706.

41. Robertson, D. E., Jacobson, S. A., Morgan, F., Berry, D., Church, G. M., and Afeyan, N. B. (2011). A new dawn for industrial photosynthesis. *Photosynthesis Research, 107*(3), 269-277.

42. Pils, D., and Schmetterer, G. (2001). Characterization of three bioenergetically active respiratory terminal oxidases in the cyanobacterium *Synechocystis* sp. strain PCC 6803. *FEMS Microbiology Letters, 203*(2), 217-222.

43. Hoiczyk, E., and Hansel, A. (2000). Cyanobacterial cell walls: News from an unusual prokaryotic envelope. *Journal of Bacteriology, 182*(5), 1191-1199.

44. Liberton, M., Page, L. E., O'Dell, W. B., O'Neill, H., Mamontov, E., Urban, V. S., and Pakrasi, H. B. (2013). Organization and flexibility of cyanobacterial thylakoid membranes examined by neutron scattering. *The Journal of Biological Chemistry, 288*(5), 3632-3640.

45. Suzuki, E., Ohkawa, H., Moriya, K., Matsubara, T., Nagaike, Y., Iwasaki, I., Fujiwara, S., Tsuzuki, M., and Nakamura, Y. (2010). Carbohydrate metabolism in mutants of the cyanobacterium *Synechococcus elongatus* PCC 7942 defective in glycogen synthesis. *Applied and Environmental Microbiology, 76*(10), 3153-3159.

46. Vermaas W. F. J. (2001). Photosynthesis and respiration in cyanobacteria. *Encyclopedia of life sciences.* Nature.

47. Mullineaux, C. W. (2014). Electron transport and light-harvesting switches in cyanobacteria. *Frontiers in Plant Science, 5*.

48. MacColl, R. (1998). Cyanobacterial phycobilisomes. *Journal of Structural Biology, 124*(2), 311-334.

49. Grossman, A. R., Schaefer, M. R., Chiang, G. G., and Collier, J. L. (1993). The phycobilisome, a light-harvesting complex responsive to environmental conditions. *Microbiological Reviews, 57*(3), 725-749.

50. Rae, B. D., Long, B. M., Whitehead, L. F., Forster, B., Badger, M. R., and Price, G. D. (2013). Cyanobacterial carboxysomes: Microcompartments that facilitate CO_2 fixation. *Journal of Molecular Microbiology and Biotechnology, 23*(4-5), 300-307.

51. Badger, M. R., and Price, G. D. (2003). CO_2 concentrating mechanisms in cyanobacteria: Molecular components, their diversity and evolution. *Journal of Experimental Botany, 54*(383), 609-622.

52. Price, G. D., Badger, M. R., Woodger, F. J., and Long, B. M. (2008). Advances in understanding the cyanobacterial CO_2-concentrating-mechanism (CCM): Functional components, c_i transporters, diversity, genetic regulation and prospects for engineering into plants. *Journal of Experimental Botany, 59*(7), 1441-1461.

53. Steinhauser, D., Fernie, A. R., and Araújo, W. L. (2012). Unusual cyanobacterial TCA cycles: Not broken just different. *Trends in Plant Science, 17*(9), 503-509.

54. Lambert, D. H., and Stevens, S. E., Jr. (1986). Photoheterotrophic growth of *Agmenellum quadruplicatum* PR-6. *Journal of Bacteriology, 165*(2), 654-656.

55. Zhang, S., and Bryant, D. A. (2011). The tricarboxylic acid cycle in cyanobacteria. *Science (New York, N.Y.), 334*(6062), 1551-1553.

56. Munekage, Y., Hashimoto, M., Miyake, C., Tomizawa, K., Endo, T., Tasaka, M., and Shikanai, T. (2004). Cyclic electron flow around photosystem I is essential for photosynthesis. *Nature, 429*(6991), 579-582.

57. Cooley, J. W., and Vermaas, W. F. (2001). Succinate dehydrogenase and other respiratory pathways in thylakoid membranes of *Synechocystis* sp. strain PCC 6803: Capacity comparisons and physiological function. *Journal of Bacteriology, 183*(14), 4251-4258.

58. Cooley, J. W., Howitt, C. A., and Vermaas, W. F. (2000). Succinate: Quinol oxidoreductases in the cyanobacterium *Synechocystis* sp. strain PCC 6803: Presence

and function in metabolism and electron transport. *Journal of Bacteriology, 182*(3), 714-722.

59. Field, C., and Van Aalst, M. (2014). *Climate change 2014: Impacts, adaptation, and vulnerability* IPCC.

60. Singh, A., Nigam, P. S., and Murphy, J. D. (2011). Renewable fuels from algae: An answer to debatable land based fuels. *Bioresource Technology, 102*(1), 10-16.

61. Naik, S., Goud, V. V., Rout, P. K., and Dalai, A. K. (2010). Production of first and second generation biofuels: A comprehensive review. *Renewable and Sustainable Energy Reviews, 14*(2), 578-597.

62. Dismukes, G. C., Carrieri, D., Bennette, N., Ananyev, G. M., and Posewitz, M. C. (2008). Aquatic phototrophs: Efficient alternatives to land-based crops for biofuels. *Current Opinion in Biotechnology, 19*(3), 235-240.

63. Darzins, A., Pienkos, P., and Edye, L. (2010). Current status and potential for algal biofuels production. *A Report to IEA Bioenergy Task, 39.*

64. Yoo, S., Spalding, M. H., and Jane, J. (2002). Characterization of cyanobacterial glycogen isolated from the wild type and from a mutant lacking of branching enzyme. *Carbohydrate Research, 337*(21), 2195-2203.

65. Hu, Q., Sommerfeld, M., Jarvis, E., Ghirardi, M., Posewitz, M., Seibert, M., and Darzins, A. (2008). Microalgal triacylglycerols as feedstocks for biofuel production: Perspectives and advances. *The Plant Journal, 54*(4), 621-639.

66. Jiang, Q., Qin, S., and Wu, Q. Y. (2010). Genome-wide comparative analysis of metacaspases in unicellular and filamentous cyanobacteria. *BMC Genomics, 11*, 198-2164-11-198.

67. Xu, Y., Alvey, R. M., Byrne, P. O., Graham, J. E., Shen, G., and Bryant, D. A. (2011). Expression of genes in cyanobacteria: Adaptation of endogenous plasmids as platforms for high-level gene expression in *Synechococcus* sp. PCC 7002. *Photosynthesis research protocols* (pp. 273-293) Springer.

68. Bentley, F. K., and Melis, A. (2012). Diffusion based process for carbon dioxide uptake and isoprene emission in gaseous/aqueous two phase photobioreactors by photosynthetic microorganisms. *Biotechnology and Bioengineering, 109*(1), 100-109.

69. Hunter, W. N. (2007). The non-mevalonate pathway of isoprenoid precursor biosynthesis. *The Journal of Biological Chemistry, 282*(30), 21573-21577.

70. Chang, W., Song, H., Liu, H., and Liu, P. (2013). Current development in isoprenoid precursor biosynthesis and regulation. *Current Opinion in Chemical Biology, 17*(4), 571-579.

71. Ershov, Y. V., Gantt, R. R., Cunningham Jr, F. X., Jr, and Gantt, E. (2002). Isoprenoid biosynthesis in *Synechocystis* sp. strain PCC 6803 is stimulated by compounds of the pentose phosphate cycle but not by pyruvate or deoxyxylulose-5-phosphate. *Journal of Bacteriology, 184*(18), 5045-5051.

72. Peñuelas, J., and Munné-Bosch, S. (2005). Isoprenoids: An evolutionary pool for photoprotection. *Trends in Plant Science, 10*(4), 166-169.

73. Rohmer, M. (1999). The discovery of a mevalonate-independent pathway for isoprenoid biosynthesis in bacteria, algae and higher plants. *Natural Product Reports, 16*(5), 565-574.

74. Rodriguez-Concepcion, M., and Boronat, A. (2002). Elucidation of the methylerythritol phosphate pathway for isoprenoid biosynthesis in bacteria and plastids. A metabolic milestone achieved through genomics. *Plant Physiology, 130*(3), 1079-1089.

75. Rohdich, F., Kis, K., Bacher, A., and Eisenreich, W. (2001). The non-mevalonate pathway of isoprenoids: Genes, enzymes and intermediates. *Current Opinion in Chemical Biology, 5*(5), 535-540.

76. Rohmer, M. (2003). Mevalonate-independent methylerythritol phosphate pathway for isoprenoid biosynthesis. elucidation and distribution. *Pure and Applied Chemistry, 75*(2), 375-388.

77. Rohdich, F., Hecht, S., Gartner, K., Adam, P., Krieger, C., Amslinger, S., Arigoni, D., Bacher, A., Eisenreich, W. (2002). Studies on the nonmevalonate terpene biosynthetic pathway: Metabolic role of IspH (LytB) protein. *Proceedings of the National Academy of Sciences of the United States of America, 99*(3), 1158-1163.

78. Kaneda, K., Kuzuyama, T., Takagi, M., Hayakawa, Y., and Seto, H. (2001). An unusual isopentenyl diphosphate isomerase found in the mevalonate pathway gene cluster from *Streptomyces* sp. strain CL190. *Proceedings of the National Academy of Sciences of the United States of America, 98*(3), 932-937.

79. Steinbacher, S., Kaiser, J., Gerhardt, S., Eisenreich, W., Huber, R., Bacher, A., and Rohdich, F. (2003). Crystal structure of the type II isopentenyl diphosphate: Dimethylallyl diphosphate isomerase from *Bacillus subtilis*. *Journal of Molecular Biology, 329*(5), 973-982.

80. Berthelot, K., Estevez, Y., Deffieux, A., and Peruch, F. (2012). Isopentenyl diphosphate isomerase: A checkpoint to isoprenoid biosynthesis. *Biochimie, 94*(8), 1621-1634.

81. Hahn, F. M., Hurlburt, A. P., and Poulter, C. D. (1999). *Escherichia coli* open reading frame 696 is *idi*, a nonessential gene encoding isopentenyl diphosphate isomerase. *Journal of Bacteriology, 181*(15), 4499-4504.

82. Cordoba, E., Salmi, M., and Leon, P. (2009). Unravelling the regulatory mechanisms that modulate the MEP pathway in higher plants. *Journal of Experimental Botany, 60*(10), 2933-2943.

83. Wright, L. P., Rohwer, J. M., Ghirardo, A., Hammerbacher, A., Ortiz-Alcaide, M., Raguschke, B., Schnitzler, J., Gershenzon, J., and Phillips, M. A. (2014). Deoxyxylulose 5-phosphate synthase controls flux through the methylerythritol 4-phosphate pathway in *Arabidopsis*. *Plant Physiology, 165*(4), 1488-1504.

84. Han, M., Heppel, S. C., Su, T., Bogs, J., Zu, Y., An, Z., and Rausch, T. (2013). Enzyme inhibitor studies reveal complex control of methyl-D-erythritol 4-phosphate (MEP) pathway enzyme expression in *Catharanthus roseus*. *PloS One, 8*(5), e62467.

85. Banerjee, A., Wu, Y., Banerjee, R., Li, Y., Yan, H., and Sharkey, T. D. (2013). Feedback inhibition of deoxy-D-xylulose-5-phosphate synthase regulates the methylerythritol 4-phosphate pathway. *The Journal of Biological Chemistry, 288*(23), 16926-16936.

86. Estevez, J. M., Cantero, A., Reindl, A., Reichler, S., and Leon, P. (2001). 1-deoxy-D-xylulose-5-phosphate synthase, a limiting enzyme for plastidic isoprenoid biosynthesis in plants. *The Journal of Biological Chemistry, 276*(25), 22901-22909.

87. Carretero-Paulet, L., Cairó, A., Botella-Pavía, P., Besumbes, O., Campos, N., Boronat, A., and Rodríguez-Concepción, M. (2006). Enhanced flux through the methylerythritol 4-phosphate pathway in *Arabidopsis* plants overexpressing deoxyxylulose 5-phosphate reductoisomerase. *Plant Molecular Biology, 62*(4-5), 683-695.

88. BotellaPavía, P., Besumbes, O., Phillips, M. A., CarreteroPaulet, L., Boronat, A., and RodríguezConcepción, M. (2004). Regulation of carotenoid biosynthesis in plants:

Evidence for a key role of hydroxymethylbutenyl diphosphate reductase in controlling the supply of plastidial isoprenoid precursors. *The Plant Journal, 40*(2), 188-199.

89. Xu, Y., Guerra, L. T., Li, Z., Ludwig, M., Dismukes, G. C., and Bryant, D. A. (2013). Altered carbohydrate metabolism in glycogen synthase mutants of *Synechococcus* sp. strain PCC 7002: Cell factories for soluble sugars. *Metabolic Engineering, 16*, 56-67.

90. Aikawa, S., Izumi, Y., Matsuda, F., Hasunuma, T., Chang, J., and Kondo, A. (2012). Synergistic enhancement of glycogen production in *Arthrospira platensis* by optimization of light intensity and nitrate supply. *Bioresource Technology, 108*, 211-215.

91. Hickman, J. W., Kotovic, K. M., Miller, C., Warrener, P., Kaiser, B., Jurista, T., Budde, M., Cross, F., Roberts, J. M., and Carleton, M. (2013). Glycogen synthesis is a required component of the nitrogen stress response in *Synechococcus elongatus* PCC 7942. *Algal Research*, *2*(2), 98-106.

92. Osanai, T., Imamura, S., Asayama, M., Shirai, M., Suzuki, I., Murata, N., and Tanaka, K. (2006). Nitrogen induction of sugar catabolic gene expression in *Synechocystis* sp. PCC 6803. *DNA Research : An International Journal for Rapid Publication of Reports on Genes and Genomes, 13*(5), 185-195.

93. Hasunuma, T., Kikuyama, F., Matsuda, M., Aikawa, S., Izumi, Y., and Kondo, A. (2013). Dynamic metabolic profiling of cyanobacterial glycogen biosynthesis under conditions of nitrate depletion. *Journal of Experimental Botany, 64*(10), 2943-2954.

94. Grundel, M., Scheunemann, R., Lockau, W., and Zilliges, Y. (2012). Impaired glycogen synthesis causes metabolic overflow reactions and affects stress responses in the cyanobacterium *Synechocystis* sp. PCC 6803. *Microbiology (Reading, England), 158*(Pt 12), 3032-3043.

95. Latifi, A., Ruiz, M., and Zhang, C. (2009). Oxidative stress in cyanobacteria. *FEMS Microbiology Reviews, 33*(2), 258-278.

96. Glick, B. R. (1995). Metabolic load and heterologous gene expression. *Biotechnology Advances, 13*(2), 247-261.

97. Palomares, L. A., Estrada-Moncada, S., and Ramírez, O. T. (2004). Production of recombinant proteins. *Recombinant gene expression* (pp. 15-51) Springer.

98. Ho, K., K. (2005). Cytochrome c_6 genes in cyanobacteria and higher plants. In M. Pessarakli (Ed.), *Handbook of photosynthesis* (pp. 273-282). CRC Press.

99. Nomura, C. T. (2001). *Electron Transport Proteins of Synechococcus Sp.PCC 7002,* (Doctoral dissertation, The Pennsylvania State University).

100. Bialek, W., Nelson, M., Tamiola, K., Kallas, T., and Szczepaniak, A. (2008). Deeply branching c_6-like cytochromes of cyanobacteria. *Biochemistry, 47*(20), 5515-5522.

101. Ludwig, M., and Bryant, D. A. (2012). *Synechococcus* sp. strain PCC 7002 transcriptome: Acclimation to temperature, salinity, oxidative stress, and mixotrophic growth conditions. *Frontiers in Microbiology, 3.*

102. Frigaard, N., Sakuragi, Y., and Bryant, D. A. (2004). Gene inactivation in the cyanobacterium *Synechococcus* sp. PCC 7002 and the green sulfur bacterium *Chlorobium tepidum* using in vitro-made DNA constructs and natural transformation. *Photosynthesis research protocols* (pp. 325-340) Springer.

103. Miller, J. H. (1992). *A short course in bacterial genetics: Laboratory manual.* Cold Spring Harbor Laboratory Press.

104. Sambrook, J., & Fritsch, E., and Maniatis, T. (1989). Molecular cloning: A laboratory manual. *Cold Spring Harbor Laboratory Press, Cold Spring Harbor, NY, 11*, 18.

105. Berthold, D. A., Best, B. A., and Malkin, R. (1993). A rapid DNA preparation for PCR from *Chlamydomonas reinhardtii* and *Arabidopsis thaliana*. *Plant Molecular Biology Reporter, 11*(4), 338-344.

106. Gibson, D. G., Young, L., Chuang, R., Venter, J. C., Hutchison, C. A., and Smith, H. O. (2009). Enzymatic assembly of DNA molecules up to several hundred kilobases. *Nature Methods, 6*(5), 343-345.

107. Gibson, D. G. (2009). Synthesis of DNA fragments in yeast by one-step assembly of overlapping oligonucleotides. *Nucleic Acids Research, 37*(20), 6984-6990.

108. Mohamed, A., and Jansson, C. (1989). Influence of light on accumulation of photosynthesis-specific transcripts in the cyanobacterium *Synechocystis* 6803. *Plant Molecular Biology, 13*(6), 693-700.

109. Exton, D. A., Smith, D. J., McGenity, T. J., Steinke, M., Hills, A. J., and Suggett, D. J. (2010). Application of a Fast Isoprene Sensor (FIS) for measuring isoprene production from marine samples. *Limnology and Oceanography: Methods, 8*, 185-195.

110. Hagemann, M. (2011). Molecular biology of cyanobacterial salt acclimation. *FEMS Microbiology Reviews, 35*(1), 87-123.

111. Erdmann, N., Fulda, S., and Hagemann, M. (1992). Glucosylglycerol accumulation during salt acclimation of two unicellular cyanobacteria. *Journal of General Microbiology*, *138*(2), 363-368.

112. Hershkovitz, N., Oren, A., and Cohen, Y. (1991). Accumulation of trehalose and sucrose in cyanobacteria exposed to matric water stress. *Applied and Environmental Microbiology*, *57*(3), 645-648.

113. Ducat, D. C., Avelar-Rivas, J. A., Way, J. C., and Silver, P. A. (2012). Rerouting carbon flux to enhance photosynthetic productivity. *Applied and Environmental Microbiology*, *78*(8), 2660-2668.

114. Stevens, S. E., and Porter, R. D. (1980). Transformation in *Agmenellum quadruplicatum*. *Proceedings of the National Academy of Sciences of the United States of America, 77*(10), 6052-6056.

115. Mitschke, J., Georg, J., Scholz, I., Sharma, C. M., Dienst, D., Bantscheff, J., Voß, B., Steglich, C., Wilde, A., Vogel, J., and Hess, W. R. (2011). An experimentally anchored

map of transcriptional start sites in the model cyanobacterium *Synechocystis* sp. PCC 6803. *Proceedings of the National Academy of Sciences of the United States of America, 108*(5), 2124-2129.

116. Güven, G., Prodanovic, R., and Schwaneberg, U. (2010). Protein engineering–an option for enzymatic biofuel cell design. *Electroanalysis, 22*(7-8), 765-775.

117. Zhou, J., Zhang, H., Meng, H., Zhu, Y., Bao, G., Zhang, Y., Li, Y., and Ma, Y. (2014). Discovery of a super-strong promoter enables efficient production of heterologous proteins in cyanobacteria. *Scientific Reports, 4.*

118. Page, L. E., Liberton, M., and Pakrasi, H. B. (2012). Reduction of photoautotrophic productivity in the cyanobacterium *Synechocystis* sp. strain PCC 6803 by phycobilisome antenna truncation. *Applied and Environmental Microbiology, 78*(17), 6349-6351.

119. Kwon, J., Bernát, G., Wagner, H., Rögner, M., and Rexroth, S. (2013). Reduced light-harvesting antenna: Consequences on cyanobacterial metabolism and photosynthetic productivity. *Algal Research, 2*(3), 188-195.

120. Markou, G., Angelidaki, I., and Georgakakis, D. (2012). Microalgal carbohydrates: An overview of the factors influencing carbohydrates production, and of main bioconversion technologies for production of biofuels. *Applied Microbiology and Biotechnology, 96*(3), 631-645.

121. Lamers, P. P., van de Laak, Carlien CW, Kaasenbrood, P. S., Lorier, J., Janssen, M., De Vos, R. C., Bino, R. J., and Wijffels, R. H. (2010). Carotenoid and fatty acid metabolism in light stressed *Dunaliella salina*. *Biotechnology and Bioengineering*, *106*(4), 638-648.

122. Lamers, P. P., Janssen, M., De Vos, R. C., Bino, R. J., and Wijffels, R. H. (2012). Carotenoid and fatty acid metabolism in nitrogen-starved *Dunaliella salina*, a unicellular green microalga. *Journal of Biotechnology*, *162*(1), 21-27.

123. Boussiba, S., Bing, W., Yuan, J., Zarka, A., and Chen, F. (1999). Changes in pigments profile in the green alga *Haeamtococcus pluvialis* exposed to environmental stresses. *Biotechnology Letters, 21*(7), 601-604.

124. Domınguez-Bocanegra, A., Legarreta, I. G., Jeronimo, F. M., and Campocosio, A. T. (2004). Influence of environmental and nutritional factors in the production of astaxanthin from *Haematococcus pluvialis*. *Bioresource Technology*, *92*(2), 209-214.

125. Davies, F. K., Work, V. H., Beliaev, A. S., and Posewitz, M. C. (2014). Engineering limonene and bisabolene production in wild type and a glycogen-deficient mutant of *Synechococcus* sp. PCC 7002. *Frontiers in Bioengineering and Biotechnology, 2.*

126. Arnon, D. I., McSwain, B. D., Tsujimoto, H. Y., and Wada, K. (1974). Photochemical activity and components of membrane preparations from blue-green algae. I. coexistence of two photosystems in relation to chlorophyll a and removal of phycocyanin. *Biochimica Et Biophysica Acta (BBA)-Bioenergetics, 357*(2), 231-245.

127. Buzby, J. S., Porter, R. D., and Stevens, S. E.,Jr. (1985). Expression of the *Escherichia coli* lacZ gene on a plasmid vector in a cyanobacterium. *Science (New York, N.Y.), 230*(4727), 805-807.